Recalibration of the sunspot-number: status report

Clette, F. ORCID: https://orcid.org/0000-0002-3343-5153, Lefèvre, L. ORCID: https://orcid.org/0000-0003-1005-7353, Chatzistergos, T. ORCID: https://orcid.org/0000-0002-0335-9831, Hayakawa, H. ORCID: https://orcid.org/0000-0001-5370-3365, Carrasco, V. M. S. ORCID: https://orcid.org/0000-0001-9358-1219, Arlt, R., Cliver, E. W. ORCID: https://orcid.org/0000-0002-4342-6728, Dudok de Wit, T. ORCID: https://orcid.org/0000-0002-4401-0943, Friedli, T. K. ORCID: https://orcid.org/0000-0002-2086-7192, Karachik, N., Kopp, G., Lockwood, M. ORCID: https://orcid.org/0000-0002-7397-2172, Mathieu, S. ORCID: https://orcid.org/0000-0003-2105-9733, Muñoz-Jaramillo, A. ORCID: https://orcid.org/0000-0002-4716-0840, Owens, M. ORCID: https://orcid.org/0000-0003-2061-2453, Pesnell, D. ORCID: https://orcid.org/0000-0002-8306-2500, Pevtsov, A. ORCID: https://orcid.org/0000-0003-0489-0920, Svalgaard, L. ORCID: https://orcid.org/0000-0002-7375-7448, Usoskin, I. G. ORCID: https://orcid.org/0000-0001-8227-9081, van Driel-Gesztelyi, L. ORCID: https://orcid.org/0000-0002-2943-5978 and Vaquero, J. M. ORCID: https://orcid.org/0000-0002-8754-1509 (2023) Recalibration of the sunspot-number: status report. Solar Physics, 298 (3). 44. ISSN 1573-093X doi: 10.1007/s11207-023-02136-3 Available at

CentAUR

Central Archive at the University of Reading

Reading's research outputs online

REVIEW

Recalibration of the Sunspot-Number: Status Report

F. Clette[1] · L. Lefèvre[1] · T. Chatzistergos[2] · H. Hayakawa[3,4,5,6] ·
V.M.S. Carrasco[7] · R. Arlt[8] · E.W. Cliver[9] · T. Dudok de Wit[10,11] · T.K. Friedli[12] ·
N. Karachik[13] · G. Kopp[14] · M. Lockwood[15] · S. Mathieu[16] · A. Muñoz-Jaramillo[17] ·
M. Owens[15] · D. Pesnell[18] · A. Pevtsov[9] · L. Svalgaard[19] · I.G. Usoskin[20] ·
L. van Driel-Gesztelyi[21,22,23] · J.M. Vaquero[7]

Abstract

We report progress on the ongoing recalibration of the Wolf sunspot number (S_N) and group-sunspot number (G_N) following the release of version 2.0 of S_N in 2015. This report constitutes both an update of the efforts reported in the 2016 Topical Issue of Solar Physics and a summary of work by the International Space Science Institute (ISSI) International Team formed in 2017 to develop optimal S_N and G_N reconstruction methods while continuing to expand the historical sunspot-number database. Significant progress has been made on the database side while more work is needed to bring the various proposed S_N and (primarily) G_N reconstruction methods closer to maturity, after which the new reconstructions (or combinations thereof) can be compared with (a) "benchmark" expectations for any normalization scheme (e.g., a general increase in observer normalization factors going back in time), and (b) independent proxy data series such as F10.7 and the daily range of variations of Earth's undisturbed magnetic field. New versions of the underlying databases for S_N and G_N will shortly become available for years through 2022 and we anticipate the release of the next versions of these two time series in 2024.

1. Introduction

The sunspot number (S_N; Clette et al., 2014, 2015; Clette and Lefèvre, 2016) is a time series (1700 – present) that traces the 11-year cyclic and secular variation of solar activity and thus space weather, making S_N a critical parameter for our increasingly technological-based society (e.g., Baker et al., 2008; Cannon et al., 2013; Rozanov et al., 2019; Hapgood et al., 2021). While modern-day observations may provide better parameters for characterizing the space-weather effects, S_N is the oldest direct observation of solar activity, and thus, is an indispensable bridge linking past and present solar behavior. As such, the sunspot number is the primary input for reconstructions of total solar irradiance (TSI) for years before 1978 (Wang, Lean, and Sheeley, 2005; Krivova, Balmaceda, and Solanki, 2007; Kopp, 2016; Kopp et al., 2016; Wu et al., 2018a; Coddington et al., 2019; Wang and Lean, 2021; Chatzistergos et al., 2023).

Extended author information available on the last page of the article

The original formula of Rudolf Wolf (1816–1893; Friedli, 2016) for the daily sunspot number of a single observer is given by (Wolf, 1851, 1856)

$$S_N = k[(10 \times G) + S], \tag{1}$$

where G is the number of sunspot groups on the solar disk on a given day, S denotes the total number of individual spots within those groups, and k is a normalization factor that brings different observers to a common scale (k is the time-averaged ratio of the daily sunspot number S_N of the primary reference observer to that of a secondary observer). Because $S \approx 10G$ on average (Waldmeier, 1968; Clette et al., 2014), the two parameters have about equal weight in S_N.

G and S counts can vary between observers because of differences in telescopes, visual acuity, and environmental conditions. These factors are susceptible to both gradual (e.g., visual acuity) and abrupt (equipment-related) variations. Moreover, as we will see below, the working definitions of both G and S have changed over time. Obtaining the correct time-varying scaling relationships (k-coefficients) between multiple sets of overlapping observers over a time span of centuries − with frequent data gaps due to weather for individual observers and occasional periods of no overlap between any observers − is the daunting task of any reconstruction method. Finally, to add unavoidable noise to the process, there are differences between the daily G and S observations at different locations that are independent of instrumentation/environment/observer acuity and practice, reflecting only separation in universal time, either because of solar rotation (spots appearing at the Sun's east limb and/or disappearing at the west limb) as well as intrinsic solar changes, i.e., the evolution of spots and groups.

In order to illustrate the kinds of differences that may appear between two sunspot observations, Figures 1a, 1b show drawings made on the same day at two different stations. Figure 1a is a drawing from the Specola Solare Ticinese station in Locarno, Switzerland, showing the delineation of groups and counting of spots on 14 March 2000 near the maximum of Solar Cycle 23 (1996–2008). Figure 1b shows a sunspot drawing taken on the same date, about 7 hours later, at the US National Solar Observatory at Sacramento Peak in Sunspot, New Mexico (Carrasco et al., 2021f). While the drawings exhibit significant similarities, there are differences in the total number of sunspots and groups.

Although the difference in the number of groups between the two drawings is minimal (8 vs. 9), there are several other differences: e.g., groups 113 and 122 shown in Locarno observations are missing from Sacramento Peak drawings, and an unnumbered group to the northwest of AR 8910 that consists of a single pore is not present in the Locarno drawing. Just this single spot thus produces a difference of 11 in S_N. Groups 113 and 122 and the unnumbered group northwest of AR 8910 were all located close to solar limbs where visibility effects could be strongest. Such discrepancies can thus result from the difference in the time at which the observations were made, as a result of intrinsic changes on the Sun, viz., sunspot appearance or disappearance, growth or decay, as well as solar rotation. A study of the random noise in S_N (Dudok de Wit, Lefèvre, and Clette, 2016) shows that the random evolution of solar-active regions dominates over observing errors in the discrepancies between observations for the same date. Overall, in this case, S_N (Locarno; 14 Mar 2000) = 178 while S_N (Sacramento Peak; 14 Mar 2000) = 138.

Wolf modified the S_N time series several times before his death in 1893, but only for the years before 1848 when he began observing, i.e., for recovered data from early observers (see Section 2.1 in Clette et al., 2014). Wolfer, Wolf's successor as observatory director at Zürich, made a final revision to S_N in 1902 (for the 1802–1830 interval) based on the addition of new data from Kremsmünster. Thereafter, the S_N series, as maintained by the Zürich
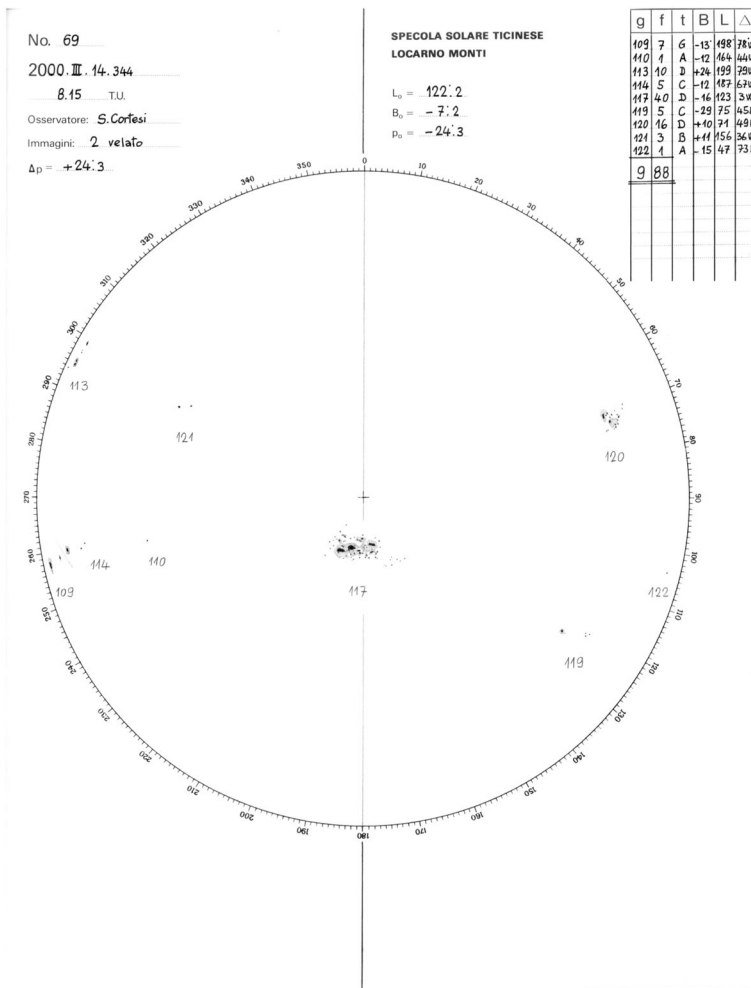
Figure 1a Sunspot drawing by Sergio Cortesi from Specola Solare Ticinese on 14 March 2000. Nine groups and 88 individual spots (in the table at the top-right corner marked as "flecken", which is "spots" in German) were observed to yield S_N (Locarno) = 178. (www.specola.ch/e/drawings.html)

Observatory until 1980 and subsequently by the Royal Observatory of Belgium (ROB), in Brussels, was left unchanged but continuously extended by appending new data to keep it up to date until the present.

S_N remained the only long-term time series directly retracing solar activity until 1998, when Hoyt and Schatten (1998a,b) developed a group-sunspot number (G_N)

$$G_N = k'G, \tag{2}$$

where k' is the station normalization factor. This simpler index does not include the count of individual spots, which characterizes the varying size of the sunspot groups but is often missing in early observations.

A key advantage of the G_N series was that Hoyt and Schatten (1998a,b) were able to reconstruct it back to the first telescopic observations of sunspots by Galileo and others
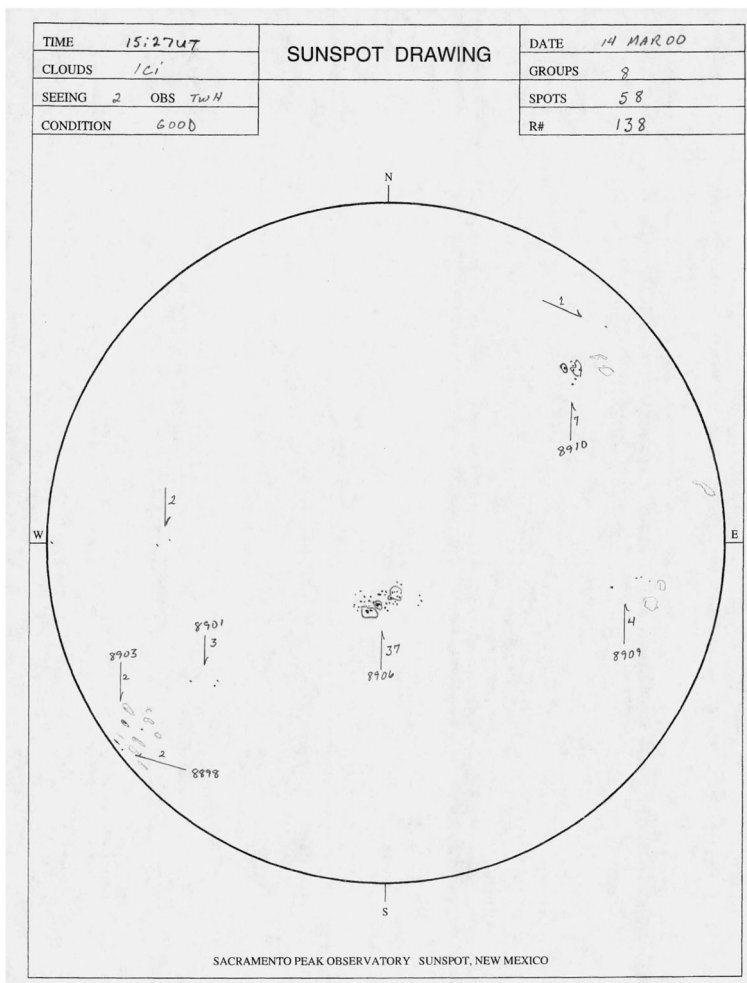
Figure 1b Sunspot drawing by Tim Henry from the US National Solar Observatory at Sacramento Peak on 14 March 2000, about 7 hours after the Locarno observation in Figure 1a. Eight groups and 58 sunspots were observed to yield S_N (Sacramento Peak) = 138. Fainter contours outline photospheric faculae, visible near the solar limb. (ngdc.noaa.gov/stp/space-weather/solar-data/solar-imagery/photosphere/sunspot-drawings/sac-peak/)

ca. 1610 vs. the initial year of 1700 for Wolf's S_N series. The new G_N thus encompassed the period of extremely weak sunspot activity from 1645 – 1715 known as the Maunder Minimum (Eddy, 1976; Spörer, 1887, 1889; Maunder, 1894, 1922). Until recently, another crucial advantage of G_N was the availability of all the raw source data in the form of an open digital database, while the S_N source data, forming a much larger collection (more than ~800 000 observations), were available in digital format only since 1981 (Brussels period). Older S_N data existed only in their original paper form or were even long considered as partly lost (see Section 2.1.1 below). The unavailability of those core data has so far prevented a full end-to-end reconstruction of the original S_N series from its base elements.

The S_N parameter defined by Wolf in Equation 1 requires more detailed observations than G_N because of the inclusion of the S (spot) component. However, early observations are often ambiguous, as many observers did not make a clear distinction between spots and groups, using the same name "sunspot" or "kernel" for both. Moreover, as can be seen in Figures 1a, 1b, large spots are enveloped in a penumbra that may contain one or several dark umbrae. Depending on the observer and epoch, each penumbra will either be counted as 1 in the S count, regardless of the number of embedded umbrae, or all umbrae will be counted separately, leading to a higher S value. Both the S and G counts are affected by the acuity threshold problem faced by each observer of distinguishing the smallest spots, in particular, for small groups consisting of a solitary spot (for which $G = 1$, $S = 1$, and $S_N = 11$) versus the absence of spots (G, S, and $S_N = 0$). Finally, the G variable presents its own difficulty: the separation of a cluster of magnetic dipoles into one or more distinct groups, depending on the cluster morphology and evolution. This splitting of groups depends on personal practices and on the scientific knowledge at different epochs, and becomes difficult mainly for a heavily spotted Sun, near the solar-cycle maximum.

1.1. Motivation for the ISSI International Team on Recalibration of the Sunspot Number

The series G_N and S_N[1] can be considered to be equivalent if one assumes that S is proportional to G, on average, with a constant of proportionality that does not change over time. In this case, differences between the form of the G_N and S_N time series would indicate calibration drifts in one or both time series. However, the possibility of a long-term change in solar behavior would mean that the ratio S/G could have varied and this would be a separate cause of deviations of G_N from S_N. A modulation of the S/G ratio by the solar cycle has actually been found by Clette et al. (2016b) and Svalgaard, Cagnotti, and Cortesi (2017), indicating a nonlinear relation between the two indices that seems to be stable in time. Therefore, where they overlap, S_N and G_N can be considered as close equivalents but with different detailed properties and calibrations.

While the original Zürich S_N (termed S_N (1) herein) and Hoyt and Schatten, 1998a,b; HoSc98) G_N series agreed reasonably well over their 1874–1976 normalization interval, HoSc98 was significantly lower for maxima before ∼1880 (see Figure 1(a) in Clette et al., 2015, and Figure 2 (below)). This situation was puzzling, if not unacceptable. What was the cause of the divergence? Could the two series be reconciled? Such questions have led to a decade-long effort by the solar community to construct more homogeneous and trustworthy S_N and G_N time series beginning with a sequence of four Sunspot Number Workshops from 2011–2014 (Cliver, Clette, and Svalgaard, 2013; Cliver et al., 2015). This effort produced major recalibrations of both S_N (1) by Clette and Lefèvre (2016) to yield S_N (2) and HoSc98 by Svalgaard and Schatten (2016) to yield SvSc16.

These recalibrations removed the marked divergence of S_N (1) and HoSc98 before ∼1880 (see Figure 1(b) in Clette et al., 2015) and reduced differences during the eighteenth century (Clette et al., 2015). However, questions were raised about the validity of the methods used (Usoskin et al., 2016; Lockwood et al., 2016) and new ideas for recalibration emerged. The revisions of the Wolf S_N series and the HoSc98 G_N series were accompanied by an independent revision/extension of S_N (Lockwood, Owens, and Barnard, 2014a,b; Lockwood et al., 2016; LEA14) and novel reconstructions of G_N by Usoskin et al. (2016; UEA16) and

---

[1]Throughout this update, we will use S_N and G_N generically for composite time series of sunspot numbers and group numbers irrespective of the calibration approach.
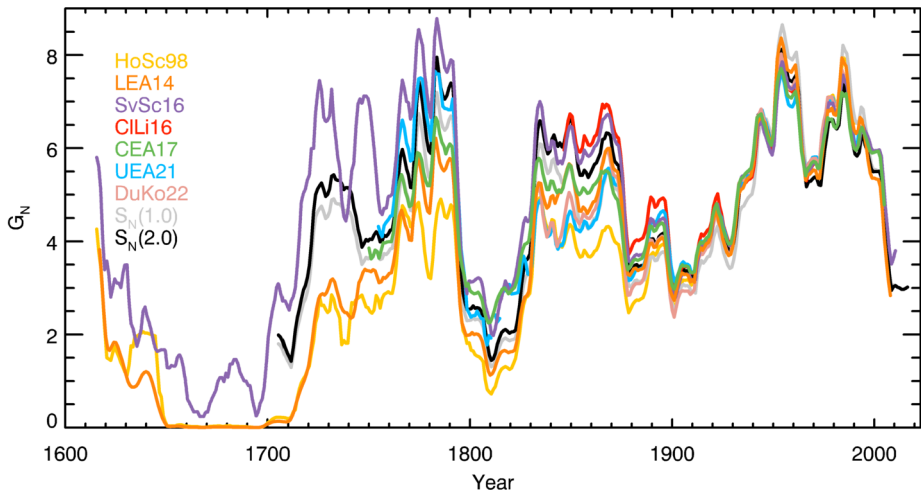
Figure 2 Eleven-year running means of 9 sunspot series: The original Wolf S_N ($S_N(1.0)$) series, the Hoyt and Schatten (1998a,b) G_N (HoSc98) series, the Lockwood, Owens, and Barnard (2014a, 2014b) S_N (LEA14) series, the Clette and Lefèvre (2016) corrected S_N ($S_N(2.0)$) series, the Svalgaard and Schatten (2016) reconstructed G_N (SvSc16) series, the Cliver and Ling (2016) G_N (ClLi16) series, the Chatzistergos et al. (2017) G_N (CEA17) series, the Usoskin, Kovaltsov, and Kiviaho (2021) G_N (UEA21) series, with predecessors given in Usoskin et al. (2016; UEA16) and Willamo, Usoskin, and Kovaltsov (2017; WEA17), and the newly constructed series based on tied ranking by Dudok de Wit and Kopp (DuKo22) which was developed within the framework of the ISSI team and is being prepared for publication (see Section 2.2.2 "Tied Ranking"). All series are scaled to the mean $S_N(2.0)$ series over 1920–1974. They agree closely over the twentieth century, but diverge significantly for earlier centuries. The latest moderate cycle (number 24) matches the amplitude of the solar cycles at the turn between the nineteenth and twentieth centuries, which are clearly higher than the Dalton minimum in the early nineteenth century and the Maunder minimum of the seventeenth century. The latter is covered only by the G_N reconstructions.

Chatzistergos et al. (2017; CEA17). Modifications to UEA16 were published by Willamo, Usoskin, and Kovaltsov (2017; WEA17) and WEA17 was subsequently modified by basing it on the new Vaquero et al. (2016; V16 herein; 16 for the year of release) database[2] rather than the original Hoyt and Schatten (1998a,b) database (Usoskin et al., 2021; UEA21). The resultant situation, documented in a Topical Issue of Solar Physics (Clette et al., 2016a), was similar to that which motivated the Sunspot Number Workshops, but writ larger (Cliver, 2017; Cliver and Herbst, 2018): several independently constructed series that diverged before ∼1880 (Figure 2) – largely bounded by those of SvSc16 and HoSc98. This state of affairs prompted a successful International Space Science Institute (ISSI) Team proposal in 2017 entitled "Recalibration of the Sunspot Number Series" by Matt Owens and Frédéric Clette. Team meetings were held in Bern in January 2018 and August 2019. The ultimate goal, yet to be met, of the proposal was to provide consensus "best-method" reconstructions of S_N and G_N including quantitative time-dependent uncertainties, for use by the scientific community. Here, we report the results of this effort and provide an update of the 2016 Topical Issue.

In Section 2, for S_N and G_N, in turn, we present highlights of the data-recovery effort and discuss work on sunspot-number reconstruction methodologies. In Section 3, we dis-

---

[2]Both the Vaquero et al. (2016; V16) database for G_N reconstruction and the original Hoyt and Schatten (1998a,b) observer database can be found at www.sidc.be/silso/groupnumberv3.

cuss two "benchmarks" for sunspot-number recalibration (quasi-constancy of spot-to-group ratios over time and an increase, as one goes back in time, of k- and k'-values). In Section 4, we review associated work on independent long-term measures of solar activity. Such proxies as quiet-Sun solar radio emission, solar-induced geomagnetic variability, and cosmogenic radionuclide concentrations, can be used as correlates/checks on new versions of S_N and G_N. We stress, however, that, thus far, the sunspot and group number back to 1610 remain fully independent of these proxies. In Section 7, we discuss efforts to connect primary observers Schwabe and Staudacher across the data-sparse interval from $1800 - 1825$ and the challenges of the first ~ 140 years of S_N and G_N time series ($1610 - 1748$). Sections 6 and 7 contain a summary of ISSI Team results and a perspective/prospectus for the ongoing recalibration effort, respectively.

2. Solar Physics Topical Issue Update / ISSI Team Report

2.1. Wolf Sunspot Number (S_N)

2.1.1. Data Recovery: The Sunspot-Number Database

Data recovery is a never-ending task, and future revisions of sunspot series will occur intermittently as part of a continuous upgrading process. The last few years have witnessed significant advances in recovery and digitization of data underlying the S_N time series, particularly in the context of the ISSI Team collaboration over $2019 - 2021$. The focus in this section is on sunspot observations that were either made at Zürich and later at Locarno and Brussels for the creation of S_N, or collected and archived from external observatories by the Directors of the Zürich Observatory, and since 1981 by the World Data Center for Sunspot Index and Long-term Solar Observations (WDC-SILSO) in Brussels, for this purpose.

The Zürich sunspot number produced by Wolf and his successors from $1700 - 1980$ is based on three types of data: (1) the raw counts from the Zürich observers (the director and the assistants) from $1848 - 1980$, (2) corresponding counts sent to the Observatory of Zürich by external auxiliary observers, and (3) historical observations for years before 1849 collected mainly by Wolf but also by Wolfer, his successor. Much of this material was published over the years in the bulletins of the Zürich Observatory, the Mittheilungen der Eidgenössischen Sternwarte Zürich (hereafter, the Mittheilungen). This is a fundamental resource for any future recomputation of S_N.

Until recently, this large collection of printed data was completely inaccessible in digital form. During $2018 - 2019$, a full encoding of the Mittheilungen data tables, from the printed originals, was undertaken at WDC-SILSO in Brussels, constituting the initial segment of the sunspot-number database. This includes all data published between 1849 and 1944 (black curve in Figure 3) when Max Waldmeier, the last Director of the Zürich Observatory decided to cease publishing raw data. This database now contains 205 000 individual daily sunspot counts (Clette et al., 2021): it currently includes data from the Zürich and auxiliary observers between 1849 and 1944, and all long data series in the early historical part, from 1749 to 1849, that were found and collected by Wolf in his epoch. (NB: Isolated observations, randomly scattered over time, are less exploitable and will be added later.) In addition to daily counts of spots and groups, the database includes metadata – in particular, changes of observers or instruments.

Although the published data were globally comprehensive, some parts are missing. The Mittheilungen provide the full set of observations from the Zürich team itself only from

1871 onwards, when Wolf started to publish separate tables for himself and his assistants as well as data received from external observers (Friedli, 2016). Before 1871, Wolf published only a single yearly table, with all his own observations, and data from external observers or assistants were only included to fill the remaining random missing days. Later, after World War I (WW I), Alfred Wolfer added many external observers, creating a truly international network. However, given the strong increase in the amount of collected data, for financial reasons, he greatly reduced the published raw data, limiting them to those from Zürich observers and ∼10 external observers. When William O. Brunner succeeded Wolfer as director of the Zürich Observatory in 1926, he stopped publishing data from external observers. Only observations from the Zürich Observatory itself and from Karl Rapp (Locarno, Switzerland) were published after that year. Then in 1945, when Max Waldmeier became the new Director, the publication of source data ceased completely, and only a list of contributing stations was provided for each year.

All those unpublished data, collected during the Zürich era, were stored in paper archives at the Zürich Observatory, which were supposed to include the whole collection, though in a less directly accessible manner. Unfortunately, following the closing of the Observatory of Zürich in 1980, when the curatorship of the sunspot number was transferred to ROB, those unpublished archives went missing. Figure 3 (brown and blue curves) shows the resulting major ∼60-year shortfall (1919 – 1979) in the preserved raw data. The absence of a large portion of the 1919 – 1979 sunspot data constituted a critical missing link between the early Zürich epoch and the modern international sunspot number produced in Brussels since 1981, for which all data are preserved in a digital database.[3] In particular, this period spans one of the main scale discontinuities identified in the Zürich series, the "Waldmeier jump" in 1947 (Clette et al., 2014; Lockwood, Owens, and Barnard, 2014a; Clette and Lefèvre, 2016; Svalgaard, Cagnotti, and Cortesi, 2017).

In a key development, the amount of missing data from 1919 – 1980 was greatly reduced in late 2018 and early 2019 when a serendipitous find by the staff of the Specola Solare Ticinese Observatory in Locarno, followed by subsequent searches in Zürich and Brussels, resulted in the recovery of the entire Waldmeier data archive (1945 – 1979) (Clette et al., 2021). The recovered Waldmeier data archive includes the last 35 years of the Zürich era, up to the transition with WDC-SILSO in Brussels, in the form of yearly handwritten tables. They thus bring the essential missing link between the entire past Zürich series and the current SILSO S_N production and its complete input-data archive. The recovered paper originals have now been converted to digital images by the ETH Zürich University Archives (ETH catalog entry: Hs1304.8) and are accessible online on the Swiss e-manuscripta portal (www.e-manuscripta.ch).

This recovery already delivered key explanations regarding the main discontinuity formerly found in 1947 in the S_N series (Clette et al., 2021; see below), but the time-consuming digitization of the huge set of observations (more than 300 000 daily numbers) to expand the S_N database will require more resources and time. Simultaneously, efforts are continuing to

---

[3]1980 was a disturbed closing year at the Zürich Observatory. The standard yearly tables of source data were not produced by the Zürich staff, and the resulting sunspot numbers were published as crude typewritten pages instead of the normal printed edition of the Mittheilungen. However, the original reports sent to Zürich by all auxiliary stations were recovered and were transferred in 2007 to the World Data Center SILSO in Brussels. Those original reports were exploited for the production of the revised series S_N V2.0 in 2015, as an important link to join the Zürich series and the international sunspot number across the 1980 – 1981 transfer from Zürich to Brussels. As a consequence of this disorganization in 1980, the collection of standard Zürich source tables thus ends in 1979. All internal data from Zürich observers for 1980 as well as the documentation about the monthly S_N processing were provided to the new team in Brussels by the assistants of the Zürich observatory at the occasion of personal visits in Zürich and Brussels.
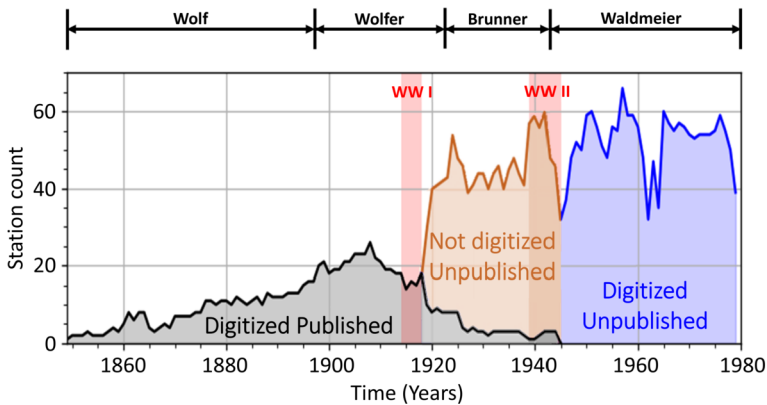
Figure 3 Evolution of the number of contributing stations collected by Zürich for each year. The raw source data published in the Mittheilungen of the Zürich Observatory (gray curve) have now been digitized into a new database. After 1918, the number of external stations grew significantly, but the Zürich Observatory did not publish all its source data any longer, and even ceased completely after 1945. Those unpublished data, stored in handwritten archives, but missing until recently, are shown by the brown and blue-shaded curves. In 2019, the archives for the period 1945–1979 were finally recovered (blue part), and the original sheets were scanned, but the values still need to be extracted to fill the database. The archived source data from 1919–1944 (brown part) are still missing, and are the target of further searches. The two vertical shaded bands mark the two World Wars, both of which left a clear imprint on the Zürich data set. Tenures of the Zürich Observatory Directors are indicated at the top of the panel. (Figure adapted from Clette et al., 2021).

recover the last missing data from the auxiliary stations between 1919 and 1944. Figure 3 shows that the recently digitized data from the unpublished source data of the Mittheilungen constitutes only about half of the observations taken and collected from external sources by the Zürich Observatory from the end of WW I until 1980.

Finally, two important source documents also bring essential information regarding the early part of Wolf's period, between 1849 and 1877: Wolf's handwritten source books and the collection of input-data tables maintained first by Wolf and then by Wolfer until 1908 (Friedli, 2020). Both documents are preserved at the ETH Zürich University Archives, and have now been entirely scanned and made accessible online. Wolf's source book provides yearly tables and contains invaluable information about the calculation of each daily sunspot number, which was never published in the Mittheilungen: e.g., the distinction between Wolf and Schwabe's daily numbers, where they overlapped between 1849 and 1868, and yearly k coefficients for each external observer. The source tables are more comprehensive and list all raw counts from all observers, back to 1610, including data that were never used for production of the sunspot number. So far, part of the source book has been encoded (1849–1877) by the Rudolph Wolf Society, and is accessible online (Friedli, 2016; www. wolfinstitute.ch). Those original data complement the published tables in the Mittheilungen, and will prove essential to better understand the multiple methodological changes introduced by Wolf during his long career – in particular, the scale transfers between Schwabe and Wolf over 1849–1868 and between Wolf and Wolfer over 1877–1893 (Friedli, 2020, see below; Bhattacharya et al., 2023).

2.1.2. Reconstruction Methodology for S_N

The New S_N(2.0) Series Two primary S_N time series have been constructed thus far: the original series S_N (version 1.0; 1700–2014) constructed by Wolf (1851, 1856) and its first

Table 1 S_N time series.

Ref.	Abbrev.	Years	Cadence	Source	Calibration Stitching
1	$S_N(1.0)$[*]	1818 – 2015	daily	Zürich/SILSO	pilot observer (single station), linear scaling, daisy chain and external index before 1848
2	$S_N(2.0)$	1818 – 2020	daily	Zürich/SILSO	pilot observer (single and multistation), linear scaling
3	LEA14[**]	1818 – 2014	daily	Lockwood, Owens, and Barnard (2014a; as supporting information)	linear scaling, external indices provisional[***]
4	$F(S_N(1.0)_{COR})$	1877 – 1893	monthly	Friedli (2020; their Table 2)	linear scaling of Wolf to Wolfer, time-limited correction to $S_N(1.0)$

References: 1 = (Wolf, 1851, 1856; see Section 2.1 in Clette et al. (2014) for Wolf's subsequent development of $S_N(1.0)$), Wolfer (1902), Waldmeier (1961), McKinnon (1987)); 2 = Clette and Lefèvre (2016); 3 = Lockwood, Owens, and Barnard (2014a,b); 4 = Friedli (2016, 2020).

[*]For the 1849 – 1980 period when the Wolf sunspot-number series was produced at Zürich, it was variously referred to as R_W (for Wolf) or R_Z (for Zürich), where the R denotes a relative rather than absolute scale. After 1980, the Wolf series was commonly referred to as R_i (for international). The S_N (version) notation used generically in this status report for the Wolf sunspot-number series was introduced in Clette and Lefèvre (2016), when releasing the first recalibrated series $S_N(2.0)$.

[**]Here and in Table 2, Figures 2, 13, 14, 19, and 20, EA = et al.

[***]Provisional in nature and not intended as a prescription or method for reconstructions of S_N.

revised version $S_N(2.0; 1700 – \text{present})$ (Clette and Lefèvre, 2016). $S_N(1.0)$ and $S_N(2.0)$ give daily values starting in 1818, monthly values starting in 1749 and yearly averages starting in 1700. Both series are available at www.sidc.be/silso/. In addition, Lockwood, Owens, and Barnard (2014a,b) constructed a S_N series (LEA14; 1610 – 2012) by appending a scaled-up Hoyt and Schatten (1998a,b) G_N series for years prior to 1749 to $S_N(1.0)$ with corrections applied ca. 1850 and 1950, using geomagnetic indices as an external reference. Friedli (2016, 2020; $F(S_N(1.0)_{COR})$ reconstructed the 1877 – 1893 segment of $S_N(1.0)$ for which Wolf and Wolfer overlapped. Specifics of these four series are summarized in Table 1.

Version 2.0 of the S_N time series (Clette and Lefèvre, 2016; $S_N(2.0)$) included three corrections applied to different time intervals. In reverse time order, these were: (1) the Locarno drift correction (1981 – 2015), (2) the Waldmeier jump (1947 – 1980), and (3) the "Schwabe–Wolf" correction (1849 – 1863). Those three corrections were based on the three largest anomalies diagnosed in the series.

In addition, a new conventional scale was adopted, taking Wolfer as reference observer instead of Wolf. This removed the 0.6 scale factor applied so far by heritage to all modern data after 1893, and it brought $S_N(2.0)$ in line with what is actually observed on the Sun with modern instruments. As this 0.6 downscaling factor uses partly undocumented early observations as a reference, and as it rests on assumptions and interpretations that may be questioned in the future (see next section), its application to data posterior to this less documented early period was inappropriate. In $S_N(2.0)$, the scale of all data since 1894 is now left unchanged, and instead, the inverse factor $1/0.6 (= 1.667)$ is applied to the early part

of the series, before 1894, which is effectively the part for which the counts are incomplete and require a compensating factor.

Of the three above-mentioned corrections in $S_N(2.0)$, only the first one led to a full recalculation of the S_N, based on the raw input data, which are fully archived in digital form by SILSO since 1981 (Clette et al., 2016a, 2016b). The other two corrections consisted in the application of a correction factor to the original $S_N(1.0)$ Zürich series over the time interval affected by each diagnosed inhomogeneity (Clette and Lefèvre, 2016). Indeed, in the Zürich system before 1981, most of the daily sunspot numbers, as published in the Mittheilungen and in Waldmeier (1961), were simply the raw Wolf numbers (k coefficient fixed at unity) from the primary observer at the Zürich observatory, without any kind of statistical processing (Clette et al., 2014; Friedli, 2016, 2020). In this scheme, the numbers from external auxiliary stations were only used on days when the Sun could not be observed in Zürich (on average, less than 20% of all days), and thus played a secondary role. This approach thus rested entirely on the personal life-long stability of individual reference observers, and on the assumed equivalence "by construction" of successive observers observing from the same place with mostly the same instrument. Any correction thus implies the use of alternate observers. Unfortunately, as described in the previous section, until recently, the Zürich source data were not available in digital form and part of the archives were even missing, which prevented any reconstruction from a wide base of source data from multiple alternate observers.

Reconstructing a sunspot database for the entire Zürich period before 1980 will thus be a key step for any future upgrade of the S_N series. This focused the efforts over the last few years, as described in the previous section and also in Section 2.2.1. Although the database is still incomplete at this time and a full end-to-end reconstruction cannot be undertaken yet, the data gathered thus far already allowed to clarify two primary scale transitions in the S_N series.

The Wolf–Wolfer Scale Transfer The Wolfer to Wolf conversion factor of 0.6, embedded in the $S_N(1.0)$ time series, was introduced because Wolfer, Wolf's successor, counted more groups and spots than Wolf in simultaneous observations spanning 17 years (1877–1893). Those higher counts resulted from two simultaneous causes. First, Wolfer used the standard telescope of Zürich Observatory (Aperture: 83 mm; magnification 64x), while Wolf was only using a much smaller portable telescope during that part of his observing career (Aperture: 40 mm, Magnification: 20x). This enabled Wolfer to see and count single small pores (small sunspots without penumbra and area from $0.5 – 4$ millionths of a solar hemisphere (μsh); Tlatov, Riehokainen, and Tlatova, 2019) that were undetectable in Wolf's small telescope. In addition, as Clette et al. (2007) wrote: "*In 1882, A. Wolfer . . . introduced an important change in the counting method (Hossfield, 2002 [see also Wolf, 1857; Wolfer, 1895; Kopecký, Růžičková-Topolová, and Kuklin, 1980]). While Wolf had decided not to count the smallest sunspots visible only in good conditions and also not to take into account multiple umbrae in complex extended penumbrae, in order to better match his counts with the earlier historical observations, the new index included all small sunspots and multiple umbrae.* [Figures 1a, 1b illustrate how small groups with low spot counts balance the effect of large groups with many spots in S_N.] By removing factors of personal subjectivity, this led to a much more robust definition of the S_N that formed the baseline for all published counts after 1882. To complete this transition, A. Wolfer determined the scaling ratio between the new count and the Wolf S_N series over the 16-year Wolf–Wolfer overlap period (1877–1892). This led to the constant Zürich reduction coefficient ($K_Z = 0.6$) [that was used] to scale . . . [$S_N(1.0)$] to the pre-1882 Wolf sunspot counts.*" (This change does not,
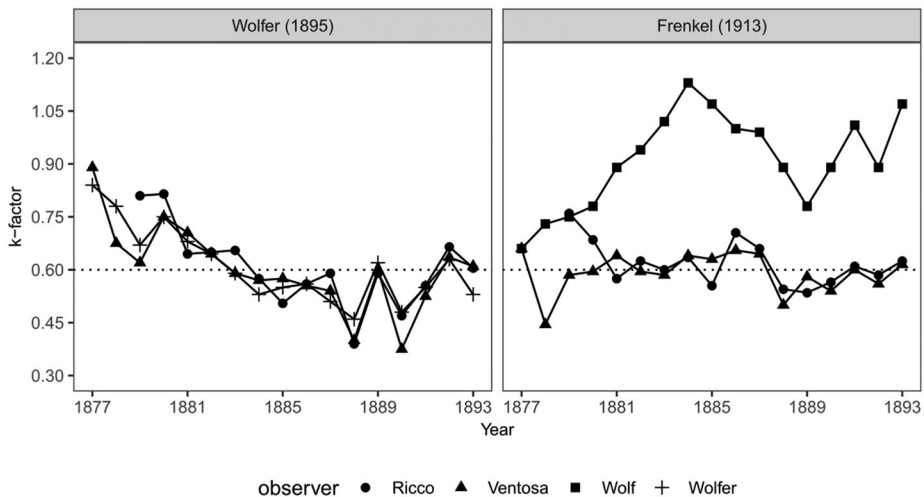
Figure 4 Left panel: yearly k-factors of Riccó, Ventosa, and Wolfer relative to Wolf as given by Wolfer (1895), showing a clear drift before 1884. Right panel: yearly k-factors of Riccó, Ventosa, and Wolf as given by Frenkel (1913) using Wolfer as reference. The k factors are stable over the whole time interval, indicating that all observers are stable. By contrast, the yearly k-factor of Rudolf Wolf, with the small portable refractor relative to the numbers from Wolfer using the 83-mm standard Zürich refractor (squares), shows the same trend between 1877 and 1884, but also a modulation that follows the solar cycle (minima in 1879 and 1890, maxima in 1884 and 1894) (from Friedli, 2020).

however, affect the G_N where multiple umbrae within the same penumbra do not alter the number of groups.) However, already in Wolfer's original study (Wolfer, 1895), the yearly mean Wolf–Wolfer ratio shows a clear drift over the interval 1877 – 1883, followed by a stabilization (Figure 4, left panel), which sheds doubts on the accuracy of this mean 0.6 factor and indicates that it should be redetermined. Earlier studies confirmed the specificity of this transition (Svalgaard, 2013; Cliver and Ling, 2016; Cliver, 2017; Bhattacharya et al., 2021, 2023).

Recently, in the framework of the ISSI Team, Friedli (2020) revisited this important transition, by using unpublished source data tables compiled by Wolfer (1912) in the framework of a PhD thesis by his student Elsa Frenkel (1913; with Albert Einstein as supervisor). Those tables include data from multiple observers over the same time interval, allowing to retrace any drift in Wolf's or Wolfer's data (Figure 4, right panel). Friedli concludes that Wolfer was stable over this interval of overlap, while Wolf's series changed relative to all other observers, probably due to a slow degradation of his eyesight associated with aging. In particular, he found that the mean factor should be lowered to 0.55, which means that the maxima of Cycle 12 (1884) and Cycle 13 (1893), which are framed by the 1877 – 1893 interval, should be ∼10% higher than in the original Wolf series, as also suggested by Cliver and Ling (2016), implying a similar correction for $S_N(2.0)$.

Moreover, in the early part of the interval, between 1877 and 1883, the scale factor is lower than in the final part, after 1890, by up to a factor of 0.76. This would suggest that all S_N values before 1877 were scaled too high by up to 25% relative to all S_N values after 1894. However, the first years of this interval fall in the minimum between Solar Cycles 11 and 12. The uncertainty in the ratios between observers is thus very high, due to the low sunspot counts during that period. Moreover, Friedli's analysis shows that the comparison between observers with widely different personal k coefficients shows a significant modulation with

the solar cycle, which could be the consequence of a nonlinear relation between the counts of two observers with very different instruments. This is precisely the case for Wolf, who used only his small portable telescope, by contrast with all other observers who had much larger instruments, with an aperture of 80 mm or more. Therefore, Wolf's drift diagnosed here with a linear model may include, at least partly, a spurious solar cycle variation (Figure 4, right panel). In that case, the drift found in the rising part of Cycle 12 (1877 – 1883) may actually reverse and vanish before 1877, when solar activity reached higher levels in Cycle 11, as well as in the other cycles before it. Such possible effects were not analyzed yet, and Friedli (2020) rightly concludes: "*Before 1877, the scale transfer from the 40/700 mm Parisian refractor as used by Rudolf Wolf to the 83/1320 mm Fraunhofer refractor as used by Alfred Wolfer will need to be analyzed further*."

The 1947 Jump and the Sunspot Weighting Effect By a comparison with data from the Madrid and Greenwich observatories, Svalgaard (2012, 2013) identified a sharp upward jump in the Zürich sunspot number, occurring around 1945 – 1947. A likely cause for this jump was quickly identified: the introduction in the observing practice of Zürich observers of a weighting of the sunspot counts according to the size of the spots (Svalgaard, 2013; Clette et al., 2014; Svalgaard, Cagnotti, and Cortesi, 2017). The effects of this weighting can be seen in Figure 1a for spot groups 114 (3 spots observed; 5 listed) and 121 (2 observed; 3 listed). In order to validate the weighting hypothesis, a systematic double-counting project was initiated at the Specola Solare Ticinese observatory in Locarno, which, as a former auxiliary station of the Zürich Observatory since 1957, continues nowadays to use this weighted counting method, providing a living memory of how Zürich observers worked back in 1945 (Cortesi et al., 2016; Ramelli et al., 2018). Based on simultaneous weighted and normal counts (Wolf's original formula), Svalgaard, Cagnotti, and Cortesi (2017) found that the weighting method produced a mean inflation of about 17% on average over the studied interval (2012 – 2014). The amplitude of this effect closely matches the magnitude of the 1947 jump, thus giving a strong indication that the introduction of this weighting led to an overestimate of the $S_N(1.0)$ over the whole period after 1945, up to the present, as the Specola Observatory kept the role of pilot station after the move of the sunspot production from Zürich to Brussels in 1981.

However, the magnitude of the 1947 jump, initially estimated at 20% (Svalgaard, 2012, 2013), was quickly questioned. Lockwood, Owens, and Barnard (2014a) compared the mean ratios between the $S_N(1.0)$ and independent series (Greenwich sunspot areas and group counts, interdiurnal variability (IDV) geomagnetic index) and found a much smaller jump amplitude of 11.5% between the mean ratios over two long intervals, 1875 – 1945 and 1946 – 2012. This discrepancy was clarified by Clette and Lefèvre (2016). First, uncorrected inhomogeneities were present before 1900 in the original Greenwich group counts used as one of the references, and the choice of 1945 as the separating year (time of a cycle minimum) did not match the actual time of the jump present in the series. By just correcting those two flaws, the same analysis leads to a larger jump of about 16%. Moreover, by a finer analysis of the double counts conducted at the Specola Observatory, Clette and Lefèvre (2016) and subsequently Svalgaard, Cagnotti, and Cortesi (2017) found that the inflation factor varies with the level of solar activity, starting near 1 at low activity, then increasing to an asymptotic plateau that is reached around $S_N = 50$. Above this limit, the inflation factor levels out near a mean value of 1.177. A slight upward dependency may persist for very high S_N, which could explain even larger values closer to 1.2, as found by Svalgaard (2013), for the maxima of very strong solar cycles, considering that this analysis was applied to Cycle 24, which was weaker by a factor two than the cycles of the mid-twentieth century. Likewise, the dependency of the inflation factor on solar activity, and thus the resulting variation
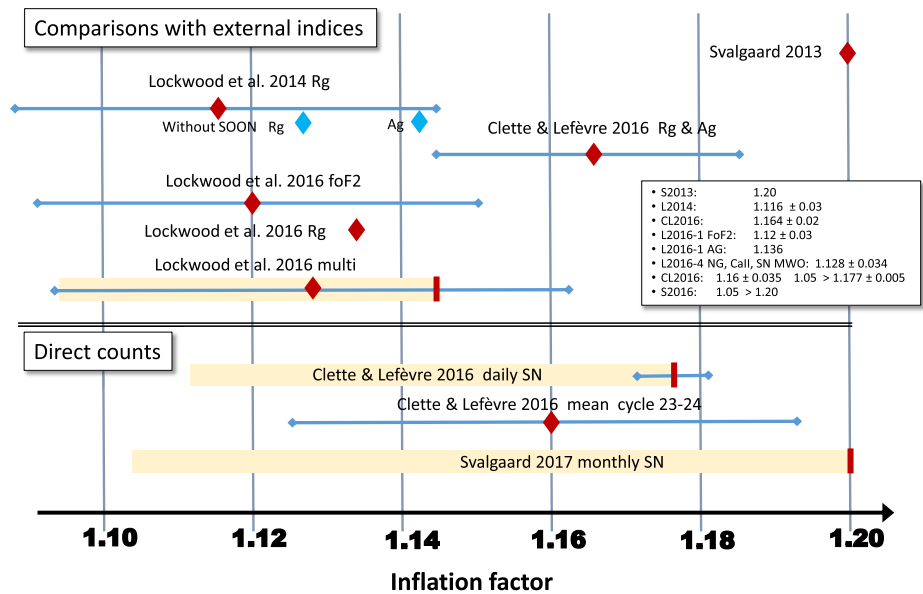
Figure 5 Summary of published determinations of the amplitude of the 1947 jump (upper part) and of the inflation factor derived from simultaneous weighted and unweighted direct counts (lower part). Red and blue diamonds indicate mean values, with the uncertainty ranges shown as blue arrows. Yellow bands indicate the range of values, when the factor is found to be variable. Vertical red bars are the upper limits, typically found near solar cycle maxima. R_g = relative group-sunspot number (G_N) and A_g = group area.

over a range from 1 to 1.177 in the course of each solar cycle, also explains why lower mean inflation values of about 1.15 are obtained when averaging over a full solar cycle or multiple solar cycles, like in the analysis by Lockwood, Owens, and Barnard (2014a). A synthesis of those elements by the ISSI Team thus allowed us to conclude that the issue of the amplitude is now largely settled. A graphic summary of the various determinations of the amplitude of the discontinuity in S_N ca. 1947 is given in Figure 5.

The date of this jump also raised another issue; the assumption that the Zürich weighting method is truly the primary cause of the jump. Indeed, different pieces of evidence indicate that the weighting method was implemented in the early twentieth century, decades before 1947 (Cortesi et al., 2016; Svalgaard, Cagnotti, and Cortesi, 2017). Mentions in the Mittheilungen and in the Zürich archives indicate that this method was introduced by Wolfer for the Zürich assistants, apparently to help them to obtain counts matching more closely his own (unweighted) counts, as the primary observer. The use of the weighting in the first half of the twentieth century was also verified by consulting original sunspot drawings from the Zürich Observatory. However, surprisingly, no significant inflation is found in the counts of Broger and Brunner, the main assistant and the successor of Wolfer, who both used the weighting, except for low S_N numbers below 25 (Svalgaard, Cagnotti, and Cortesi, 2017; their Figure 19). This very long delay before the putative effect of the preexisting weighting became effective thus required an explanation. Moreover, the sharp scale jump finally occurred in 1947, as found in the data, while Waldmeier had become Director of the Zürich Observatory and primary observer in 1945, two years earlier. Therefore, this prominent change in the history of the Zürich S_N construction does not even match the exact time
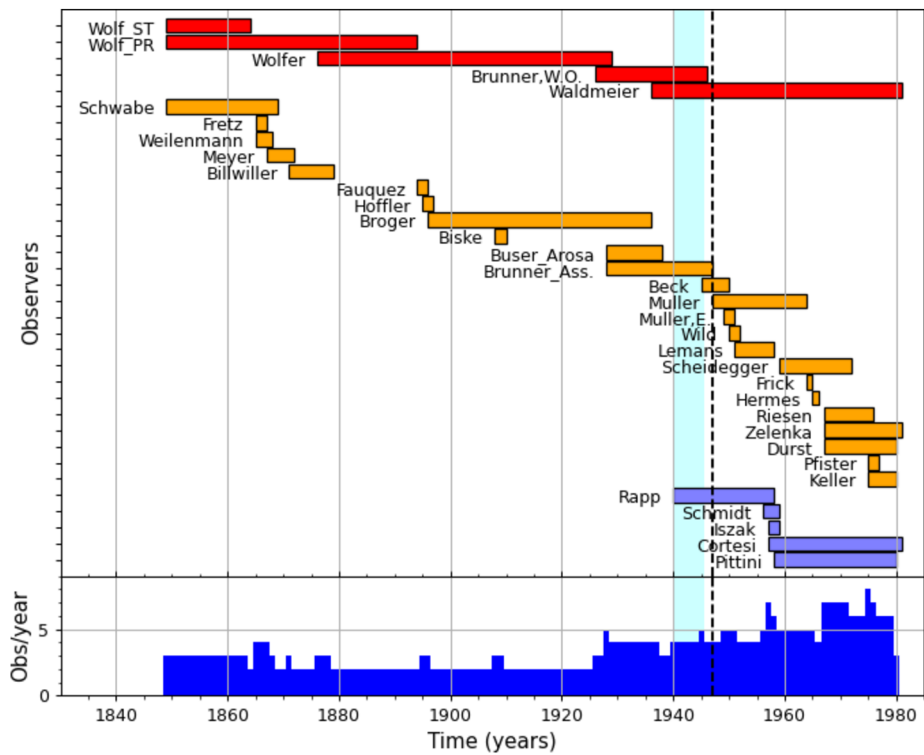
Figure 6 Timelines of the active observing periods of all Zürich observers. In red (top group), the primary observers and in orange (bottom group), the assistants. In purple, the observers of the auxiliary station in Locarno, who were considered as members of the Zürich core team. The vertical shaded band marks World War II and the vertical dashed line indicates the time when the 1947 scale jump occurs in the original S_N series. The bottom plot gives the number of active Zürich observers for each year (from Clette et al., 2021).

of this anomaly. The case for a role of the weighting thus also required additional evidence of another key transition in the Zürich system.

Following the creation of the S_N database and the recent recovery of all source data for the period 1945 – 1980, Clette et al. (2021) conducted a full survey of contributing stations since Wolf started recruiting assistants and auxiliary observers, up to the Waldmeier period that concludes the Zürich era of the S_N, with its extended worldwide network of auxiliary stations (cf. Section 2.1.1). The resulting timelines revealed two unique disruptions in the history of the Zürich sunspot number that occurred almost simultaneously, immediately after the end of WW II. Due to the war, the former set of contributing stations was replaced by an entirely new and larger international network of auxiliary stations in the years following 1945. At the same time, in Zürich, Brunner and his primary long-term assistant continued to observe until the end of 1946, and were then replaced by Waldmeier and by new assistants, among whom the first ones only stayed at the Observatory for a short time (Figure 6). Both factors produced a break in the continuity of the Zürich system, as almost all new internal and external participants never contributed before or worked in parallel with former observers. This unique event corresponds to a sudden loss of past memory of the Zürich system. This can be quantified by counting the cumulative number of past observing years for all observers active on a given year. This amount plotted as a function of time is marked
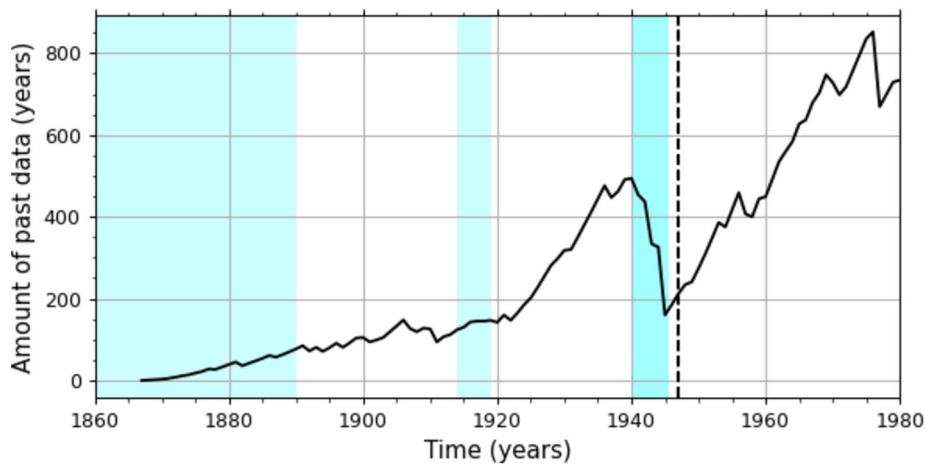
Figure 7 Plot of the total number of preceding observed years by all external stations contributing to the Zürich S_N and active in each year. This count is a global measure of the amount of past information on which the S_N calibration could rest for any given year. After an almost continuous increase, a sharp drop by more than a factor 2 occurred just after the onset of WWII. The shaded vertical bands mark the early Wolf period and the first and second world wars. The vertical dashed line marks the location of the 1947 jump, accompanying the last observations from Brunner (from Clette et al., 2021).

by a large abrupt drop in 1947 (Figure 7), a sharp transition that is unique over the whole 1849–1980 interval. Clette et al. (2021) now show that this abrupt transition coincides with the departure of the Brunner team, which had been observing since 1926, and that it falls in 1947, precisely when the jump is diagnosed in the original S_N series. This finally gives a clear historical base for the occurrence of this jump and its timing.

2.1.3. Orientations for Future Progress

The potential recovery of the complete Zürich set of observations, including those from 1919–1944, will make it possible to fully construct a $S_N(3.0)$ time series independently of the direct use of $S_N(1.0)$, only rescaled over certain epochs, as was done to produce $S_N(2.0)$. The methodology of constructing the $S_N(3.0)$ series has not been selected, but several options are possible, given the recent advances in methods acquired over the last few years.

Such a reconstruction could, for example, be based on the k-based method implemented at the WDC-SILSO since 1981. Nonlinear probability distribution functions (Usoskin et al., 2016; Chatzistergos et al., 2017), developed so far for the group number (described in Section 2.2.2), could also be applied after adapting them to the sunspot number. Another obvious improvement would consist in replacing the single preselected pilot observer by a set of reference stations, selected on the base of systematic statistical quality criteria (Clette and Lefèvre, 2016). The elements of such a method are now developed and trained on actual data from the SILSO network. This new state-of-the-art approach, presented by ISSI team members (Mathieu et al., 2019, 2023), uses advanced statistical techniques to derive a nonparametric measure of the short- and long-term stability of each individual observer or observatory team, and it also introduces a proper nonnormal distribution of uncertainties, in particular in the special case when the S_N is close to zero, with the constraint of nonnegativity. In addition to creating a new time series, such tools can form the basis for a permanent

quality-monitoring process, applicable both to the past reconstruction and to the current and future production of the S_N at the WDC-SILSO.

However, gathering enough base data remains the essential prerequisite for any progress. This will thus require recovering more historical and revising the existing data series, which were often inherited indirectly through past data searches, sometimes a long time ago. For the twentieth century, except for the remaining lost Zürich archives between 1919 and 1944, we now have reasonable data coverage. Still, even for this more recent period, new data series that were not known or not collected by the Zürich observatory can help in completing the S_N database, either with entirely new series from other observers or by extending and revising original series partly collected in Zürich. For instance, we can cite the sunspot catalog of the Madrid Observatory (Aparicio et al., 2018) and sunspot-count series from dedicated Japanese observers like Hisako Koyama (Hayakawa et al., 2020a), Hitoshi Takuma (Hayakawa et al., 2022b) or Katsue Misawa (active over 1921 – 1934).

As nicely illustrated by Muñoz-Jaramillo and Vaquero (2019), the main challenge resides in the sparse data of the first decades of the nineteenth century and in the eighteenth century. For the nineteenth century, we can incorporate recounts of Schwabe's daily sunspot numbers based on examination of his drawings (Arlt et al., 2013) to better bridge the gap corresponding to the sunspot dearth in the Dalton minimum and to shed light on the validity of the 1849 – 1863 "Schwabe–Wolf" scale transfer. In the mid-nineteenth century, although Wolf produced the only long and continuous series, his method went through several meaningful changes between 1861 (introduction of k-coefficients) and 1877 (start of the Wolfer contribution), as summarized by Friedli (2016, 2020). Therefore, a full understanding of the scale stability before the Wolf–Wolfer transition described above (Section 2.1.2) requires a revision and extension of known data series, like the recent recounting of sunspots from the original high-quality synoptic maps by Richard Carrington over 1853 – 1861 (Bhattacharya et al., 2021). One important goal is to fix the scale transfer between Schwabe, the last link of historical observations, and Wolfer, the first modern long-duration sunspot observer.

In the eighteenth century, the data-recovery effort largely merges with the one for the group number (see Section 2.2.1 below) with the extra requirement that for the S_N we need the spot counts in addition to the group counts that were already collected in the G_N database (Vaquero et al., 2016). As many early observers did not provide such detailed counts or often did not make the distinction between sunspots and sunspot groups, progress during this era will require consultation of original sources, in particular sunspot drawings, following the example of the recounting of Staudacher's drawings by Svalgaard (2017). Such a recounting is currently in preparation for the drawing series from De Plantade (which was considered lost; Hoyt and Schatten, 1998a,b) as a result of Hisashi Hayakawa's manuscript recovery. De Plantade's manuscript covers the first decades of the eighteenth century (1705 – 1726), and thus the critical period when the solar cycle restarted at the end of the Maunder Minimum.

2.2. Group Sunspot Number (G_N)

2.2.1. Data Recovery and Revision

For the ∼400-year span of the G_N series, Muñoz-Jaramillo and Vaquero (2019) define two qualitatively different periods. The first corresponds roughly to the first two centuries of telescopic sunspot observations (1610 – 1825) for which the number of observations is low, and directly overlapping temporal comparisons between observers are difficult to make. The second period spans from ∼1825 to the present, when the temporal coverage is better and there is a clear network of related and comparable observers.

Historical sunspot drawings are taking on an increasingly important role in space-climate studies (e.g., Muñoz-Jaramillo and Vaquero, 2019) because they constitute ground-truth raw data – with a direct picture of the shape, size, and distribution of spots and groups on the solar disc. They also give finer diagnostics to understand how the observations were made and their resulting quality. For modern times, annotated drawings indicate how group splitting was accomplished. The recovery of sunspot observations, and sunspot drawings in particular, is now essential as the current revision efforts shift from correction of existing time series to full reconstruction from raw data.

The development by Hoyt, Schatten, and Nesme-Ribes (1994) and Hoyt and Schatten (1998a,b) of the group-number time series was accompanied by the creation of a G_N database that was revised and updated by Vaquero et al. (2016). The open-source V16 data makes it possible to apply different methodologies to compose G_N time series. As a related development, within the past decade, the Historical Archive of Sunspot Observations (HASO; haso.unex.es/) was established at Extremadura University by José M. Vaquero (Clette et al., 2014; Cliver et al., 2015; Vaquero et al., 2016). The objective of HASO is "*to collect and preserve all documents in any format* (*original, photocopy, photography, microfilm, digital copy, etc.*) *with sunspot observations that can be used to calculate the sunspot number in the historical period or related documents.*" For a comprehensive review of historical sunspot records and the recent improvements available, see Arlt and Vaquero (2020).

Since 2016, more than 30 papers have been published on sunspot data recovery with ISSI Team members as principal or coauthors. Here, we review some key results of these studies, focusing on the recovery/revision of group counts, which have been incorporated into V16. Many of the data sets that have been recently uncovered and analyzed (e.g., Carrasco et al. (2018b; for Hallaschka), Arlt (2018; for Wargentin), Nogales et al. (2020; for Oriani), Hayakawa et al. (2021e; for Johann Christoph Müller)) provide information (counts and/or drawings) for both S and G and thus can be applied to revisions of S_N as well as to G_N. As a manifestation of the increasing focus on recovery and archival of sunspot drawings, several recent works have constructed butterfly diagrams for historical observers (e.g., Leussu et al., 2017; Neuhäuser, Arlt, and Richter, 2018; Hayakawa, Besser, and Iju, 2020; Hayakawa et al., 2022a; Vokhmyanin, Arlt, and Zolotova, 2021; see Figure 9 below).

(*a*) *The earliest sunspot observations: 1610 – 1645*

Thomas Harriot recorded the earliest sunspot drawing that was based on telescopic observation in 1610. Vokhmyanin, Arlt, and Zolotova (2020) revised Harriot's sunspot-group number and reconstructed butterfly diagrams on the basis of copies of his original manuscript. Shortly afterward, in 1611, Galilei and Scheiner started their sunspot observations. Galilei's data quality greatly improved after Benedetto Castelli invented a method to project a solar disk on a white paper. This method update has been detected in the comparison of Galilei's data with Harriot's data (Carrasco, Gallego, and Vaquero, 2020). Sunspot data by Galilei and his contemporaries have been comprehensively analyzed in Vokhmyanin, Arlt, and Zolotova (2021).

Christoph Scheiner was the most active observer before the Maunder Minimum. He published his sunspot observations in 'Rosa Ursina' and 'Prodomus' (Scheiner, 1830, 1851). On their basis, Arlt et al. (2016) derived the sunspot positions and areas from his sunspot observations for the period 1611 – 1630. Carrasco et al. (2022b) have studied Scheiner's sunspot-group number in comparison with V16 and Arlt et al. (2016) and obtained two important results: (i) the shape of the second solar cycle of the telescopic era is similar to a standard Schwabe cycle, and (ii) the amplitude of this solar cycle (according to raw data)

is significantly lower than the previous one. This last result supports a gradual transition between normal solar activity and deep solar activity in the Maunder Minimum (see, for example Vaquero et al., 2011).

Charles Malapert was a key sunspot observer ca. 1618 – 1626. He is the only observer in the V16 G_N database for ∼60% of his 185 observation days. From an examination of Malapert's reports from 1620 and 1633, Carrasco et al. (2019c, 2019a) increased the net number of Malapert's daily observations to 251. Moreover, they determined that while Malapert sometimes drew only a single group in his drawings, he sometimes observed several groups. Therefore, Malapert's group counts, taken from the drawings, are now known to be lower limits.

Jean Tardé and Jan Smogulecz recorded sunspot observations in 1615 – 1617 and 1621 – 1625. Their results had been recorded in their books for sunspots as sunspot drawings and textual descriptions (Arlt and Vaquero, 2020). These records permit derivations and comparisons with other observers of sunspot-group number and sunspot positions for these periods (Carrasco et al., 2021c).

Daniel Mögling was another key sunspot observer in 1626 – 1629. Hayakawa et al. (2021c) exploited his original manuscript in the Universitäts- und Landesbibliothek Darmstadt and confirmed his sunspot observations for 134 days. This study revised Mögling's sunspot-group number as well as those of Hortensius and Schickard. It also derived Mögling's sunspot positions to construct a butterfly diagram. These results filled the data gap in the declining phase of Solar Cycle -12 showing the decay of the sunspot-group number and equatorward migration of the reported groups.

Pierre Gassendi conducted sunspot observations in 1631 – 1638. Vokhmyanin and Zolotova (2018) have analyzed his publications to revise the sunspot-group number and derive sunspot positions.

Hevelius (1647) carried out the last known systematic sunspot records made by any astronomer before the Maunder Minimum for the period 1642 – 1645. Carrasco et al. (2019b) revised the sunspot drawings included in this documentary source as well as the textual reports, showing the good quality of the sunspot records made by Hevelius. Carrasco et al. (2019b) determined that the solar-activity level calculated from the active-day fraction (annual percentage of days with at least one sunspot on the Sun) just before the Maunder Minimum was significantly greater than that during the Maunder Minimum. Moreover, Carrasco et al. (2019b) confirmed Hevelius's observations of sunspot groups in both solar hemispheres in contrast with those of the Maunder Minimum that exhibited significant hemispheric asymmetry (Ribes and Nesme-Ribes, 1993).

(*b*) *The Maunder Minimum: 1645 – 1715*

The Maunder minimum (1645 – 1715) was an exceptional period in the recent history. Sunspot activity remained extraordinarily low during several solar cycles and the spots that did appear had a strong hemispheric asymmetry, with preference for the southern solar hemisphere (Eddy, 1976; Ribes and Nesme-Ribes, 1993; Usoskin et al., 2015; Riley et al., 2015). In recent years, a great effort has been made to improve our understanding of solar activity during this remarkable period. For example, the umbra–penumbra area ratio was computed by Carrasco et al. (2018a) for sunspots recorded during the Maunder Minimum. This ratio is similar to that calculated from modern data and, therefore, the absence of sunspots in the Maunder Minimum cannot be explained by changes in this parameter. On the other hand, comparisons with contemporary eclipse drawings have revealed that significant coronal streamers were apparently missing during the Maunder Minimum, unlike those of the modern solar cycles (Hayakawa et al., 2021f), substantiating a conjecture by Eddy (1976).

The combined observing intervals in the Hoyt and Schatten (1998a,b) G_N database of Martin Fogelius and Heinrich Siverus, both from Hamburg, spanned the years 1661–1690, approximately half of the 1645–1700 core of the Maunder Minimum (Vaquero and Trigo, 2015). Even after removal from the Hoyt and Schatten database of several full years of continuous reported spotless days for Fogelius and Siverus (implausible because of local weather conditions at Hamburg), the two observers were the 13th and 7th most active observers (from 1661–1671 (with 318 observations) and 1671–1690 (1040), respectively) from 1610 to 1715 in V16. Hayakawa et al. (2021d) consulted Ettmüller (1693) and compared it with the correspondence of Fogelius in the Royal Society archives, leading to the following proposed changes to the V16 database: (1) a reduction of the number of active days for Fogelius from 26 to 3 and a corresponding (net) reduction for Siverus from 20 to 15; (2) conversion of the dates of several observations from the Julian to the Gregorian calendar; and (3) removal of all "ghost" spotless days (days with no explicit sunspot observations interpreted as spotless days) for both observers, representing 98–99% of their observations.

Sunspot records from the Eimmart Observatory of Nürnberg have been analyzed by Hayakawa et al. (2021e), based in part on Chiaki Kuroyanagi's archival investigations. The original logbooks from this observatory have been preserved in the Eimmart Archives in the National Library of Russia (St. Petersburg; fond 998). Analysis of these manuscripts removed ghost spotless days and reduced their daily patrol coverage in contrast with V16. Hayakawa et al. (2021e) revised the sunspot-group number from the Eimmart Observatory for 78 days, that from the Altdorf Observatory for 4 days, and those of Johann Heinrich Hoffmann and Johann Bernhard Wideburg for 22 days and for 25 days, respectively. Among the Eimmart Archives, Johann Heinrich Müller's logbook recorded explicit spotless days and allowed us to derive robust active-day fractions and a reliable S_N for him in 1709 to confirm its significantly lower level of solar activity than in other small solar cycles such as cycles 14 and 24 and even those of the Dalton Minimum (Carrasco et al., 2018b; Hayakawa, Besser, and Iju, 2020; Carrasco et al., 2021d). These records also allowed Hayakawa et al. (2021f) to derive sunspot positions and confirmed significant hemispheric asymmetry in the southern solar hemisphere.

William Derham recorded sunspot observations at the end of the Maunder Minimum. Derham (1710) listed his observations from 1703 to 1707 in a table where he only recorded one group for each day except on 15 November 1707 when he recorded two groups. Carrasco et al. (2019c) pointed out those could not be the real numbers of groups observed by Derham in that period, showing a sunspot drawing made by an anonymous observer between 30 November and 2 December 1706 recording three groups. (Note that the quality of the Derham's drawings is better than the one of the anonymous drawing.) Therefore, the group counts assigned to Derham in V16 should be used with caution and Derham's counts should be revised accordingly on the basis of his original records.

Carrasco, Vaquero, and Gallego (2021) present and analyze two sunspots recorded by Gallet in the middle of the Maunder Minimum. In addition to the sunspot observed by Gallet from 9 to 15 April 1677 (recorded by other astronomers), Gallet reported a spot group from 1 to 6 October in the same year for which there is no record of observations by others. The latitude of this sunspot was $\sim 10°$ S, comparable to most of the sunspots observed during the second half of the Maunder Minimum.

(*c*) *Solar Cycles in the eighteenth Century: 1715–1795*

Solar Cycle -3 ($\sim$1711–$\sim$1723) is considered as the first solar cycle after the Maunder Minimum. Hayakawa et al. (2021b) examined the sunspot drawings of Johann Christoph
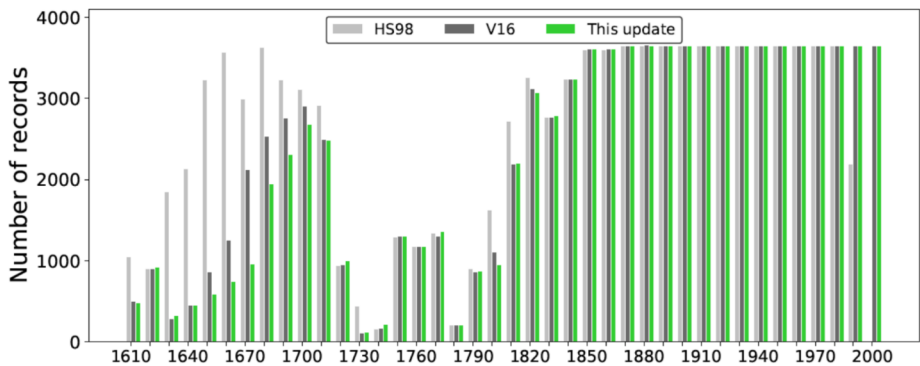
Figure 8 Number of days with records per decade in the Hoyt and Schatten (1998a,b) (gray columns) database and in its revision by Vaquero et al. (2016) (black columns). The green columns reflect subsequent modifications to the V16 database up to the current time. The smaller numbers of records in the V16 database for decades before 1830 are due to the removal of spurious records of days with no sunspots from the Hoyt and Schatten (1998a,b) database. (Adapted from Vaquero et al., 2016).

Müller during this cycle to revise his sunspot-group numbers (G) and derive individual sunspot numbers (S). His sunspot-group numbers are significantly different from the contemporary observations of Rost. For example, on 15 June 1719, Johann Christoph Müller recorded 3 sunspot groups (Hayakawa et al., 2021b), whereas Rost's report gave 30 "sunspot groups" according to V16. Comparative analyses have revealed that Rost's data most probably described not the sunspot-group number (G) but individual sunspot number (S). This manuscript also allowed Hayakawa et al. (2021b) to derive sunspot positions in both solar hemispheres. This result contrasts sunspot activities in 1719 – 1720 with those of the Maunder Minimum during which spots were predominantly in the southern hemisphere (Ribes and Nesme-Ribes, 1993; Hayakawa et al., 2021f). Another important observer, François de Plantade (1670 – 1741), also recorded sunspots quite systematically during the exit from the Maunder minimum, from 1705 to 1726, and will be the subject of an upcoming study.

Few sunspot records are available for the 1721 – 1748 interval, as shown in Figure 8 (adapted from Vaquero et al., 2016). This is the weakest link in the entire sunspot-number time series. Recently, several relatively short-duration observers during this interval have been identified and documented. Johann Beyer's sunspot records in 1729 – 1730 have been examined and revised in Hayakawa et al. (2018a). Pehr Wargentin is the only observer given for 1747 in V16, with group counts reported for 17 days for which drawings are available. Arlt (2018) documented an additional 32 days with group (and individual spot) counts (but without drawings) by this observer.

Including those data, Hayakawa et al. (2022a) have comprehensively reviewed and revised the sunspot observations in 1727 – 1748. Hayakawa et al. (2022a) revised the group counts of known observers, such as Krafft in 1729 and Winthrop and Muzano in 1739 – 1742, and added previously unknown data, such as those of Van Coesfeld in 1728 – 1729, Duclos in 1736, and Martin in 1738. These results have improved the morphology of Solar Cycles –2 (∼1723 – 1733), –1 (1733 – 1743), and 0 (1743 – 1755) confirming the existence of regular cycles from 1727 – 1748. Hayakawa et al. (2022a) derived sunspot positions from the contemporary records and filled the data gap of the existing butterfly diagrams during this interval, confirming the occurrence of sunspots in both solar hemispheres and their equatorward migrations over each solar cycle.
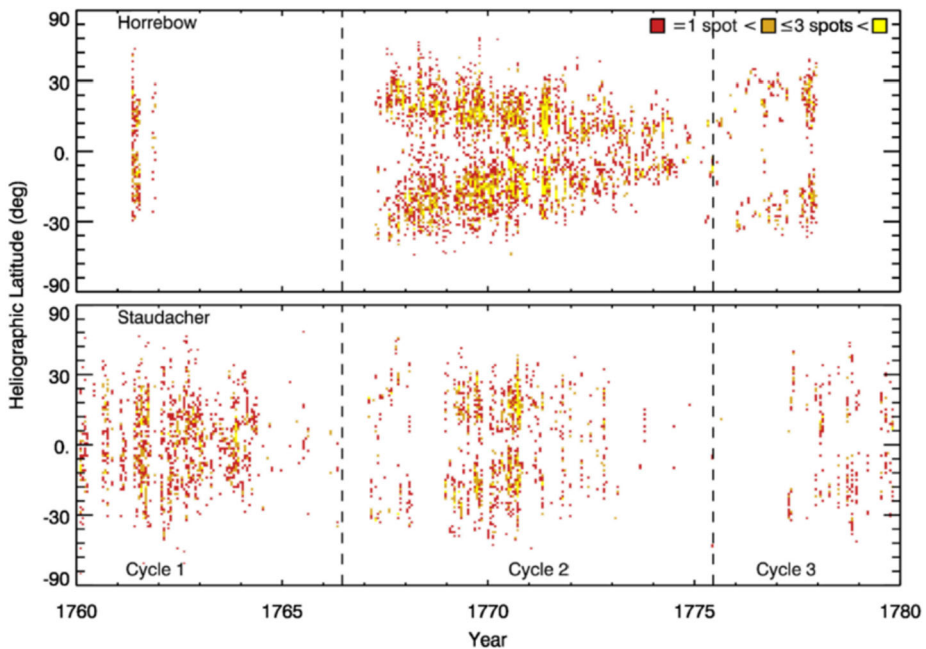
Figure 9 Top panel: Butterfly diagram constructed from Horrebow's sunspot observations. Bottom panel: Butterfly diagram constructed from the observations of Staudacher, Horrebow's contemporary, for the same interval. The dashed lines indicate times of solar minima. (From Karoff et al., 2019).

Additional data have been acquired from East Asia. Hayakawa et al. (2018c,b) reported on Japanese astronomers at Fushimi and Edo (current Tokyo) who conducted sunspot observations for 1 day in 1793 and 15 days in 1749 – 1750, respectively. These data fill data gaps around the neighborhood of the "lost cycle" conjectured to have occurred during the decline of Solar Cycle 4 in 1784 – 1798 (Usoskin et al., 2009; see also Karoff et al., 2015; cf., Zolotova and Ponyavin, 2011; Owens et al., 2015) and the maximum of Solar Cycle 0 (1743 – 1755).

Barnaba Oriani conducted sunspot observations in 1778 – 1779 at the Brera Observatory (Milan, Italy). Nogales et al. (2020) uncovered 52 daily sunspot observations made by Oriani for the near-maximum year of 1779 (peak in 1778) that are not included in V16. Only three other observers reported group counts for 1779, for a combined total of 19 active days. Of the 19 days, only 8 overlapped with those of Oriani, who thus accounts for 44 of 63 active days yet known for 1779. In addition, Nogales et al. determined that Oriani's group counts should be revised upward by 80% on average for his 97 daily observations for 1778 included in V16. A total of 117 active days were observed for 1878 and on 91 of these days, Oriani supplied the only observation.

Christian Horrebow's original logbooks of sunspot records are located in the Aarhus University. These records are particularly important, as his team observed sunspots from 1761 – 1776 and anticipated Schwabe's discovery of the sunspot cycle (Jørgensen et al., 2019). Horrebow's butterfly diagram, constructed by Karoff et al. (2019), in Figure 9 (top panel) has the characteristic structure first shown by Carrington (1858) and more definitively by Maunder (1904) for later cycles. The bottom panel in Figure 9 gives the butterfly diagram constructed from Staudacher's observations for the same interval (Arlt, 2008).

(*d*) *Reanalysis of a key observer improves G_N records during the Dalton Minimum (1798 – 1833)*

The Dalton Minimum is a period of relatively low solar activity from 1798 – 1833, which has been named after John Dalton, who noticed a significant reduction of the auroral frequency during this time (Silverman and Hayakawa, 2021). The Dalton Minimum is similar to (though with even lower cycle peak sunspot numbers) sunspot minima that began ca. 1900 and 2010 (Feynman and Ruzmaikin, 2011). These three secular ebbs of sunspot activity, termed centennial or Gleissberg variations (after Gleissberg, 1965), are punctuated by longer periods of enhanced activity centered near ∼1855 and ∼1970 (Figure 2). These secular ebbs and flows of sunspot activity are less marked than the severe sunspot drought of the Maunder Minimum (Usoskin et al., 2015) and the prolonged sequence of strong solar cycles from ∼1945 – 2008 known as the Modern Grand Maximum (Solanki et al., 2004; Clette et al., 2014; Usoskin, 2017).

The sunspot observations from 1802 to 1824 of Thaddäus Derfflinger, Director of the Kremsmünster Observatory, span the deepest part of the Dalton Minimum. From analysis of Derfflinger's drawings and associated metadata, Hayakawa, Besser, and Iju (2020) concluded that the spot drawings were a secondary and therefore optional aspect of measurements of the solar elevation angle. As a result, they eliminated observations of spotless days attributed to Derfflinger, reducing the number of his daily records from 789 to 487. In addition, the butterfly diagram (Carrington, 1858; Spörer, 1880; Maunder, 1904) showing the latitudinal variation of sunspots over the solar cycle constructed by Hayakawa, Besser, and Iju (2020) from Derfflinger's observations was more or less symmetric about the solar equator during this period, in contrast to the deep Maunder Minimum, where spot formation occurred primarily in the southern hemisphere (Ribes and Nesme-Ribes, 1993). These results have been confirmed with Stephan Prantner's sunspot drawings for 1804 – 1844 from Wilten Monastery (Hayakawa et al., 2021g). Sunspots occurred preferentially in the northern hemisphere right before the Dalton minimum (Usoskin et al., 2009). These results require further investigations on the Dalton Minimum and the hypothesized 'lost cycle' at its beginning (Usoskin et al., 2009; Karoff et al., 2015; cf., Krivova, Solanki, and Beer, 2002; Zolotova and Ponyavin, 2011; Owens et al., 2015).

(*e*) *Solar Cycles in the nineteenth century*

Starting with the nineteenth century and even more in the twentieth century, sunspot data are typically providing clearly separated counts of groups and individual spots. Therefore, those data are as relevant to the S_N as to the G_N reconstruction, and all the following data sets are thus contributing to the S_N database described in Section 2.1.1.

After the end of the Dalton Minimum, Toubei Kunitomo conducted sunspot observations for 157 days in 1835 – 1836. While his sunspot records had been known in the existing datasets (Hoyt and Schatten, 1998a,b; Vaquero et al., 2016), preliminary analyses on the original documents have uncovered 17 additional days with Kunitomo observations in 1835 and one such day in 1836. Kunitomo's sunspot-group number has been revised and the area has been measured by Fujiyama et al. (2019). These records have filled a data gap in the existing datasets and are consistent with other sunspot observers' data, such as those of Schwabe (Fujiyama et al., 2019).

New records were recovered from Antonio Colla, a meteorologist and astronomer at the Meteorological Observatory of the Parma University (Italy). Colla's records cover the period from 1830 to 1843, just after the Dalton Minimum (Carrasco et al., 2020a). Colla recorded

a similar number of sunspot groups as his contemporary sunspot observers regarding common observation days. However, as is the case for Hallaschka, sunspot positions and areas recorded by Colla seem unrealistic and should not be used for scientific purposes.

William Cranch Bond was the director of the Harvard College Observatory in the mid-nineteenth century. Bond recorded sunspot drawings from 1847 to 1849. According to V16, Bond is the observer with the highest daily number of sunspot groups observed in Solar Cycle 9 (18 groups on 26 December 1848). However, Carrasco et al. (2020b) detected mistakes in these counts. These errors are due to the use of sunspot position tables instead of the solar drawings. This new revision indicates that solar activity for Solar Cycle 9 was previously overestimated according to raw data, and Schmidt would be the observer with the highest daily group number (16 groups on 14 February 1849). A comparison between sunspot observations made by Bond, Wolf, and Schwabe (using the common observation days) shows that (i) the number of groups recorded by Bond and Wolf are similar, and (ii) Schwabe recorded more groups than Bond because he was able to observe smaller groups.

Richard Carrington made sunspot observations at Redhill Observatory in the United Kingdom, which he published in the form of a catalog (Carrington, 1863). An observer from the current WDC-SILSO network (T.H. Teague, UK) has reanalyzed his observations (Bhattacharya et al., 2021) by recounting the groups and individual sunspots from Carrington's original drawings. Bhattacharya et al. (2021) compared Carrington's own counts (Carrington, 1863; Lepshokov, Tlatov, and Vasil'eva, 2012; Casas and Vaquero, 2014) with contemporary observations, Rudolf Wolf's own observations, and Carrington's tabulations both from the Mittheilungen. They conclude that Carrington's counting methods (Carrington, 1863) for the groups were comparable to modern methods but those for individual sunspots produced significant undercounts. On the other hand, Wolf's own counts and his recounting of Carrington's drawings show numbers very similar to modern methods. The key here, is that Carrington's catalog was, in fact, a position catalog, thus it recorded only the biggest spots and groups, while his drawings were more precise and, when counted by Wolf in the 1860s or Teague 160 years later, give results comparable to modern observations.

Angelo Secchi observed sunspots and prominences from 1871–1875. Carrasco et al. (2021e) have constructed machine-readable tables from Secchi's book "Le Soleil" (Secchi, 1875). Secchi's original drawings indicate that he had begun sunspot observations as early as 1858 (Hayakawa et al., 2019; Ermolli and Ferrucci, 2021). These results encouraged further investigations of Secchi's original notebooks containing sunspot records in the Rome Observatory and will be the focus of an upcoming study.

(f) Modern long-term observers

Although the number of observers increased strongly during the twentieth century, in particular after World War II, many series have a rather short duration and some series from professional observatories suffer from inhomogeneities due to change of instruments or observers. Therefore, the recovery of new long-duration series that were never collected and exploited, or only partly so, can help to refine the stability of the most recent part of the S_N and G_N records (e.g., the Zürich 1947 discontinuity found by Clette et al., 2021), and connecting it seamlessly to contemporary observations.

In this regard, sunspot observations for more recent long-term institutional and individual observers not currently included in V16 continue to be processed and digitized. The Astronomical Observatory of the Coimbra University published a catalog with sunspot observations (including G and S) from 1929 to 1941 (Lourenço et al., 2019). In addition, a dataset of sunspot drawings made at the Sacramento Peak Observatory (SPO) from 1947–2004 has

Table 2 List of studies that produced a Group Sunspot Number time series

Ref.[*]	Abbrev.[**]	Years	Cadence	Database	Calibration Stitching
1	HoSc98[a]	1610 – 2013	Daily	HoSc98	Daisy chain, limited backbone, linear scaling
2	SvSc16[a]	1610 – 2015	Annual	V16(1.0)	Daisy chain, backbone, linear scaling
3	ClLi16[a]	1841 – 1976	Daily	HoSc98	Daisy chain, backbone, linear scaling[***]
4	UEA16[a]	1749 – 1995	Daily	HoSc98	Active days, synthetic reference, nonlinear
5	CEA17[b]	1739 – 2010	Daily	V16(1.12)	Daisy chain, backbone, nonlinear
6	WEA17[c]	1749 – 1996	Monthly	HoSc98	Active days, synthetic reference, nonlinear
7	UEA21[d]	1749 – 1996	Monthly	V16(1.21)	Active days, synthetic reference, nonlinear
8	DuKo22[e]	1825 – 1995	Daily	V16(1.21)	Tied ranking, linear

[*]References: (1) Hoyt and Schatten (1998a,b); (2) Svalgaard and Schatten (2016); (3) Cliver and Ling (2016); (4) Usoskin et al. (2016); (5) Chatzistergos et al. (2017); (6) Willamo, Usoskin, and Kovaltsov (2017); (7) Usoskin, Kovaltsov, and Kiviaho (2021); (8) Preliminary. See Section 2.2.2 "Tied Ranking".

[**]Time series available at:

[a]www.sidc.be/silso/groupnumberv3.

[b]cdsarc.u-strasbg.fr/viz-bin/qcat?J/A+A/601/A109.

[c]www.aanda.org/articles/aa/full_html/2017/05/aa29839-16/T2.html.

[d]link.springer.com/article/10.1007/s11207-020-01750-9#Sec9.

[e]Pending publication.

[***]Provisional in nature and not intended as a prescription or method for reconstruction of G_N; based on the Hoyt and Schatten (1998a,b) G_N construction method but used an adjusted RGO time series from 1874 – 1915 and Schmidt (scaled to adjusted RGO) for years before 1874 as primary observers.

been recently digitized by Carrasco et al. (2021f). This work is the first step for the publication of the complete SPO sunspot catalog that will include information on sunspot positions and areas. Carrasco et al. (2018c) digitized this catalog and reconstructed the corresponding total and hemispheric S_N series from Coimbra data.

The published sunspot counts of Hisako Koyama (Koyama, 1985; Knipp, Liu, and Hayakawa, 2017), a staff member at the Tokyo Science Museum (later renamed the National Museum of Nature and Science (NMNS)) from 1947 – 1985, have been used for one of the backbones of the group-number reconstruction of Svalgaard and Schatten (2016). Recent surveys of the archives of the NMNS in Tsukuba have located Koyama's sunspot drawings and logbooks from 1945 to 1996 (Hayakawa et al., 2020a). Hayakawa et al. (2020a) described and analyzed a full digital database (encoded by Toshihiro Horaguchi and Takashi Nakajima) of Koyama's sunspot observations and diagnosed a previously undetected inhomogeneity in the resulting sunspot counts affecting the later part of the series, after 1983. Hayakawa et al. (2022b) have analyzed Hitoshi Takuma's sunspot drawings from 1972 – 2013 in the Kawaguchi Museum. Comparisons with the contemporary records have shown Takuma's observations to be one of the most stable data sets over this ∼40-year time period.

2.2.2. Reconstruction Methodologies for G_N

Several G_N time series have been generated since the first such series of Hoyt and Schatten (1998a,b). These series, including that of Hoyt and Schatten (1998a,b), are listed in Table 2. The G_N series listed in Table 2 are based on four basic methods:

Table 3 Summary of Sunspot Time-Series Reconstruction Methods.

Method	Requires overlap of observers	Inherently computes uncertainties	Requires parametrization assumptions	Maturity regarding sunspot series
Daisy Chaining	Yes	No	Yes	High
Active-Day Fraction	No	No	No	Low
Probability Distribution Function	Yes	Yes	No	Medium
Tied Ranking	Yes	Yes	No	Low

1. Linear Daisy Chaining: Linear scaling of successive overlapping observers (daisy chaining) or "backbones of observers" (Hoyt and Schatten, 1998a,b; Svalgaard and Schatten, 2016; Cliver and Ling, 2016).

2. Active-Day Fractions: Independent scaling of all observers relative to a "perfect" observer (based on the RGO catalog). A synthesized imperfect observer is created on a daily basis by means of a quality factor or threshold (S_S; analogous to k' in Equation 2) determined by the fraction of days on which spots were observed (active-day fraction) (Usoskin et al., 2016; Willamo, Usoskin, and Kovaltsov, 2017; Usoskin, Kovaltsov, and Kiviaho, 2021) relative to the "perfect" observer. Moreover, the scaling is also based on a cross-correlation matrix, i.e., the probability distribution function (PDF) between the "perfect" observer and the synthesized observer, giving a nonparametric conversion.

3. Probability Distribution Function: Nonlinear nonparametric scaling of successive overlapping observers via a correlation matrix (Usoskin et al., 2016), using primary (backbone) observers, on a daily basis (Chatzistergos et al., 2017).

4. Tied Ranking: Dudok de Wit and Kopp constructed a series based on the tied-ranking method using the rank ordering (Kendall, 1945) of group counts for a given day rather than their actual values (DuKo22 in Figure 2).

In the following subsections, we describe each of these methods in more detail, including their advantages and shortcomings, which are summarized in Table 3.

Linear Daisy Chaining This method, used by Hoyt and Schatten (1998a,b) followed the normalization approach first used by Wolf to relate his observations to those of external (to Zürich) observers before 1848. Rather than using Wolf or any other Zürich director as a primary observer, Hoyt and Schatten used the photography-based Royal Greenwich Observatory (RGO) 1874–1976 series of group numbers (Willis et al., 2013a,b; Erwin et al., 2013) as their primary reference. For observers who began observing before 1874, however, they employed "daisy chains" of individual observers in their normalization scheme, sometimes multiple chains, making it difficult, if not impossible, to replicate k'-factors for such observers (Cliver and Ling, 2016; Cliver, 2017). Hoyt and Schatten (1998a,b) were the first to use "backbones" (Svalgaard and Schatten, 2016), albeit in a limited fashion, with RGO from 1874–1976, Horrebow designated as primary observer from 1730–1800 and Galileo filling this role for the earliest observers in the seventeenth century. Svalgaard and Schatten (2016) used linear scaling of contiguous "backbones" for four primary observers.

Because the possibility for error increases with the number of contiguous links in a chain, Svalgaard and Schatten (2016) reduced the number of links in daisy chains by linking separate (mostly nonoverlapping) "backbones" of observers, each scaled to a single common reference observer within a limited time interval, rather than series (single or multiple) of
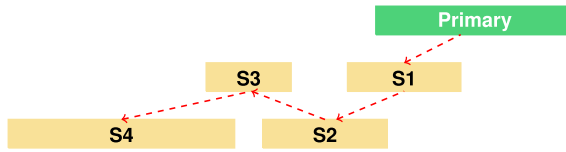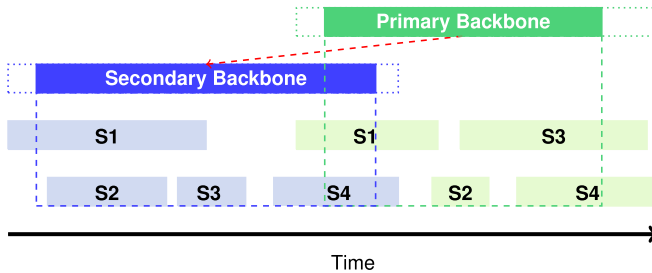
Figure 10 Schematic showing the difference between daisy-chaining and backbone methodologies. In daisy chaining, primary (green) and secondary observers (tan) are scaled sequentially to each other based on their interval of overlap. In the backbone method (Svalgaard and Schatten, 2016), several secondary observers (light-green and light-blue) are scaled to multiple backbone observers based on their interval of overlap and then the contiguous backbone series tied to each primary observer are scaled to each other. While both daisy chaining (e.g., Hoyt and Schatten, 1998a,b) and the backbone method employ daisy chaining, the advantage of the backbone method is the reduction of the number of links in the chain, reducing the accumulation of errors. See text for differences in the backbone approach employed by Svalgaard and Schatten (2016) and Chatzistergos et al. (2017). (Adapted from Chatzistergos, 2017).

individual observers as Hoyt and Schatten (1998a,b) did prior to 1874. Moreover, they only used visual observers as primary references, instead of the photographic RGO group numbers. Svalgaard and Schatten (2016) used correlations of yearly averages of observer and primary counts over the interval of overlap to determine their k' factors (rather than ratios of summed daily counts for common observation days with one or more groups as used by Hoyt and Schatten, 1998a,b), forcing the fits through zero for strict proportionality. Figure 10, adapted from Chatzistergos (2017), illustrates the difference between daisy chaining and the backbone method.

The general criticisms of the daisy-chain method are the following:

1. subjective initial selection of backbone observers, whose choice can significantly impact the outcome, introducing bias;
2. the method does not exploit all possible periods of overlap and in this sense is not optimal;
3. the final result is affected by the order in which the records are stitched together;
4. errors accumulate monotonically at each stitch (Lockwood et al., 2016), although the method does not inherently determine time-dependent uncertainties;
5. the method cannot temporally span data gaps (applies to all methods except Usoskin et al., 2016).

In the Svalgaard and Schatten (2016) backbone approach, three of the four backbone links have no overlap of the primary observers vs. four of nine such links for Chatzistergos et al. (2017). For the nonoverlapping cases, the cross calibration is based completely

on the overlap of the dotted-line extensions of the backbones (Figure 10). An example of nonoverlapping backbone observers in the Svalgaard and Schatten (2016) reconstruction is that of Schwabe (backbone length: 1794 – 1883) and Wolfer (1841 – 1944); Schwabe ceased observing after 1867 while Wolfer's first observations (in Svalgaard and Schatten, 2016) began in 1878. The advantage of this method is that it permits long intervals of overlap with fewer backbones, but in doing so it is relying on the more uncertain parts of the extended backbone series for crosscalibration. Another difference between the backbone methodologies of Svalgaard and Schatten (2016) and Chatzistergos et al. (2017) was that secondary observers in the SvSc16 series could be scaled to both backbones, e.g., the light green S1 observer in Figure 10, but not in CEA17.

In addition, the application of a 7% reduction of the group count due to a suspected change in group-splitting technique at Zürich applied for years after 1940 in the Svalgaard and Schatten (2016) series needs to be verified independently.

A third key difference between SvSc16 and CEA17 – discussed in Section 2.2.3 – is the scaling procedure: linear scaling of yearly averages vs. a nonparametric mapping of daily values of a pair of observers. The latter allows for nonlinear relations between counts of a pair of observers, and avoids side effects of temporal averaging (the different distributions of observing dates within a year, the linearization effect of temporal averages). While the two series agree reasonably well after ∼1880, they diverge beforehand (Figure 2).

Recently, Velasco Herrera et al. (2022) announced a reconstruction of the G_N series using wavelet and machine-learning techniques that supports the validity of the original HoSc98 series. However, rather than recalibrating the G_N series or exploiting the recent revised G_N database (Vaquero et al., 2016), they just produce a harmonic model of the original HoSc98 series, which essentially replicates the characteristics of this input series, based on a limited set of variable periodic components. Such approaches also suffer from the stochastic nature of solar activity (e.g., Cameron and Schüssler, 2019; Charbonneau, 2020; Petrovay, 2020). This technique may help in interpolating intervals with scarce data or predominantly spotless days, on the base of periodicity assumptions, but it cannot provide diagnostics of possible flaws in the original series. On the other hand, this paper does not address any of the above issues identified in the daisy-chaining principle, as well as the homogeneity issue in the early part of the RGO photographic catalog. For the above reasons and the fact that the Velasco Herrera et al. (2022) G_N series is not a recalibration of actual data, but rather a model, we will not further consider this series here.

Individual Nonlinear Scaling, Based on the Active-Day Fraction, Relative to a Degraded "Perfect" Observer Usoskin et al. (2016; see also Willamo, Usoskin, and Kovaltsov, 2017, and Usoskin, Kovaltsov, and Kiviaho, 2021) introduced a normalization procedure with several novel aspects. Instead of working directly with group counts, they considered the systematic statistical relation between the relative group counts of individual observers and the number of days over which they reported spots (active days) as a fraction of the total number of days on which they observed (including spotless days), i.e., the so-called active-day fraction (ADF). By using this individual indicator, the scale of each observer can then be determined independently of other observers, thus avoiding any kind of daisy chaining. A key potential advantage of this approach is that it does not rely on overlapping observations in relating any two observers, so can span large time ranges (and even gaps in observations) just as accurately as short ones. The method does rely, however, on consistency in solar activity on multicentennial timescales because of the relatively limited duration of the RGO universal observer (1900 – 1976; Willamo, Usoskin, and Kovaltsov, 2017).

In order to derive this scale across multiple observers, the ADF statistics must be referred to a "perfect" reference observer, assumed to be capable of seeing all groups down to the size

Figure 11 Cumulative probability distribution $P(A, S_S)$ for the reference data set (for different values of the threshold observed area (S_S) and complete data coverage ($f = 1$)). $S_S = 0$ corresponds to the full RGO data set. (From Usoskin et al., 2016).
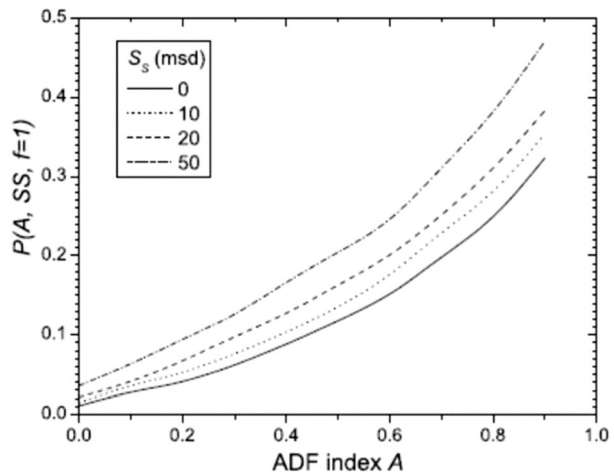
of the smallest pore. For this purpose, it was assumed that the RGO photographic catalog from $1900 - 1976$ provided a universal reference against which any other observer could be compared regardless of whether they observed over the $1900 - 1976$ time range of RGO data. As a scaling factor to the universal RGO observer, they determined a quality factor S_S that is in fact an acuity threshold (the spot-area threshold over which the individual observers starts seeing spots/groups) for each observer by matching its individual ADF statistics with the ADF obtained by synthetically degrading the universal (presumed "perfect") RGO observer.

This was done by assuming that counts by imperfect observers are lowered due to their limited acuity, i.e., their inability to detect the smallest spots. This was simulated by eliminating from RGO data all sunspot groups with an area below a certain threshold S_S in millionths of a solar disk (μsd). The threshold value S_S that provided the best match between the thresholded RGO data and the actual ADF, A, of an observer is derived via a set of cumulative probability distribution functions (PDFs) $P(A, S_S)$ of the ADF for RGO degraded at different levels (Figure 11). Once this ADF-based S_S value is determined, the correction to the group numbers themselves for the target observer is derived from the relation between the group numbers for the degraded RGO data set corresponding to this S_S, and the reference group number for the full RGO data set, representing the "perfect" observer, via their cross-probability density distribution. In this final step, instead of regressing a mathematical model, this correction was implemented in a nonparametric way, by remapping directly the raw daily group numbers for the corresponding observer, via the RGO cross-PDF, delivering the corrected group number (peak of the PDF at the given raw G_N value), with uncertainties (width of the PDF at this G_N value).

Difficulties/shortcomings with the ADF-based universal observer method as developed thus far include:

(1) The possibility of unreported spotless days during periods of low solar activity, resulting in an overestimation of the ADF and to underestimated corrections for some observers (Svalgaard and Schatten, 2017).

(2) Variations in the definition of a spot group (evolving group-splitting rules) used by observers from different epochs, which are not considered as another personal factor, next to the acuity of an observer. This factor can play an important or perhaps even a dominant role near a solar-cycle maximum, when activity is high and many groups are packed on the solar disk, and the fraction of big sunspot groups becomes large compared to tiny groups

(i.e., the ones for which acuity is important). This applies to all series involving the group counts, thus both G_N and S_N.

(3) Relative insensitivity of observer group counts to S_S factors (Cliver, 2016; Svalgaard and Schatten, 2017).

(4) Applicability of the ADF approach only when the ADF is <0.8, thus only during the low part of the solar cycles. The corrected G_N values for the maxima of the cycles are thus obtained by an extrapolation, outside of the range over which the ADF is calibrated for an observer.

(5) Differential sensitivity of the S_S threshold to the level of activity (Usoskin, Kovaltsov, and Chatzistergos, 2016), i.e., S_S may be over- or underestimated if the overall level of activity is different for the epoch of the target observer and for the epoch of the reference RGO data. (Solar-activity consistency is assumed.) As a result, the method works well for moderate activity but tends to slightly (<10%) underestimate high-activity levels and strongly (∼30%) overestimate the low-activity levels, overall leading to a slight overestimate of the activity for the nineteenth century, given a larger occurrence of weaker cycles compared to the base time interval of the RGO data set in the twentieth century (Willamo, Usoskin, and Kovaltsov, 2018). This differential effect is probably a consequence of the extrapolation of cycle maxima mentioned in point (4) above.

(6) The observation window is different between RGO and the observer (a simple ratio of the number of days for which groups were reported to the total number of days on which observations were made is not sufficiently representative).

(7) The reference observer, in this case the RGO catalog, is obviously not "perfect". A simple analysis reproducing the same method as in Usoskin et al. (2016) but with different parts of the RGO catalog (by selecting different long-term time periods) shows that the obtained S_S are not consistent with the error bars reported in Usoskin et al. (2016) (private communication, L. Lefèvre).

The above-described limitations (1 – 4, 6, and 7) to the applicability and accuracy of the ADF method were not addressed in Usoskin et al. (2016), Willamo, Usoskin, and Kovaltsov (2017), or Usoskin, Kovaltsov, and Kiviaho (2021). Factor (5) in the above list was quantified by Willamo, Usoskin, and Kovaltsov (2018) and Usoskin, Kovaltsov, and Kiviaho (2021), but factors 1 – 3 may lead to larger errors and biases.

At the ISSI workshops, Muñoz-Jaramillo introduced a segmented-ADF method in order to improve the method published by Usoskin et al. (2016). The general idea of this new method is to determine the threshold in the same way, but to compensate for points (5 – 7) by applying a temporal window based on the data coverage of the imperfect observer and to make it move (in time) with regard to the reference dataset to account for the level of activity within the "imperfect observer" data. Then, this threshold is applied to the reference data to count groups. Here, the actual group numbers play again a role, next to the ADF itself. Note also, that the reference dataset is slightly modified to account for possible drifts in the first years. Like the original ADF methodology for G_N reconstruction, this refined segmented-ADF approach remains to be fully developed and still requires an end-to-end validation.

Willamo, Usoskin, and Kovaltsov (2017) also point out that the ADF principle is inapplicable during periods of grand minima. As is the case for daisy chaining, this approach also breaks down during intervals with sparse data. However, while the daisy-chaining methods cannot cross such data gaps, and thus reach a dead end at the first sparse-data link in the early nineteenth century, the ADF has the potential (as yet undemonstrated) to provide a calibrated tie-point to any "more populated" interval between such gaps, e.g., in the eighteenth century, as shown in Carrasco et al. (2021d). Thus, a hybrid approach of using the
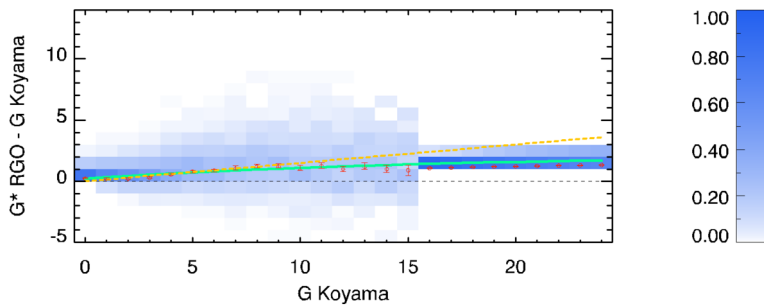
Figure 12 Calibration matrix showing the probability distribution of the residual difference between RGO (primary observer G^*) and Koyama (secondary observer, G) as a function of G over 1947 – 1976. To compensate for the small number of data points in the upper range, columns for $G > 15$ have been filled with the results of a Monte Carlo simulation. The red circles with error bars depict the mean G^* values for each G column and their 1σ uncertainty. The dashed yellow line shows the k'-factor from Hoyt and Schatten (1998a,b), and the green line is an exponential fit, showing a slight nonlinearity. (See similar figures in Chatzistergos et al., 2017).

ADF method to span data gaps and daisy chaining for contiguous-observing periods is a possible strategy for creating time series over longer periods than daisy chaining alone.

Backbones with Nonlinear Scaling via Nonparametric Probability Distribution Functions
Chatzistergos et al. (2017) followed Svalgaard and Schatten (2016) by reconstructing G_N using a sequence of primary "backbone" observers, but improved the original concept in several respects, to avoid some of the weaknesses attributed to the initial version:

1. Use of daily values instead of yearly means.

2. Adding more primary observers, in order to have a direct temporal overlap between all of them, instead of using secondary observers to bridge temporal gaps between disconnected primary observers (although the probability of error accumulation increases with each link).

3. Using a nonparametric mapping based on probability distribution functions (PDFs) of the respective values of a pair of observers, allowing for nonlinear corrections, in place of least-square fitting a purely linear relation (the nonparametric mapping method was first introduced in Usoskin et al., 2016, as part of the ADF method described in the previous section). Linear scaling has bias to overestimate strong cycles, while the nonparametric approach tends to overestimate minima and slightly underestimate maxima.

4. The ability to inherently estimate uncertainties in the reconstruction. In this nonparametric approach, they scaled the group counts G of secondary observers to those (G^*) of primary observers through PDFs of G^* for each G value. An example of a calibration matrix, for a high-quality secondary observer, Koyama, and primary observer RGO, is shown in Figure 12. This procedure makes no assumption about the type of relationship between G and G^* (e.g., linearity) and the error estimate is straightforward. For each backbone, Chatzistergos et al. (2017) constructed a composite series by averaging all the PDFs of all the available observations for every day, to obtain a distribution based on all available observers. When there are few data points, as in the upper range of G_N values, uncertainties can be estimated by applying Monte Carlo techniques to the PDFs of paired observers when creating time series.

While this PDF approach using daily observations allows a more robust error analysis than the backbone-based method of Svalgaard and Schatten (2016; see Section 2.2.2), it suffers from other limitations, including limited accuracy in the PDF for high group counts

due to lower statistics than for low group counts, which is especially important to calibrate the maxima of solar cycles.

Tied Ranking Tied ranking (Kendall, 1945) is a new approach to sunspot-number recalibration that is not based on the G_N values themselves, but instead on their distribution as measured by observer pairs. Tied ranking replaces the G_N variable for a given observer by its order ("ranking") relative to all the other values of that variable. By working with ranked values rather than with original ones, one bypasses the need for correcting individual observers for their nonlinear response, which is one of the main difficulties faced by all methods in the merging process. However, ranked records can be meaningfully compared only if they span the same time interval. To fill data gaps, the expectation maximization method (Dempster, Laird, and Rubin, 1977; Rubin, 1996; Little and Rubin, 2002) is used. This method is a powerful generalization of the backbone and daisy-chain methods in the sense that it uses all possible overlaps to fill the data gaps, avoiding the subjective choice of periods of overlap and backbones. The final composite is an average of all the available rankings on a specific day (excluding interpolated values), and then the combined ranking is turned back into group counts using a specific observer. The absolute scale of G_N series could be given by a complementary approach, e.g., ADF (Usoskin et al., 2016).

Possible limitations of the tied-ranking method include: (1) Calibration is dependent on the time interval (phase of the solar cycle, level of activity in the interval covered by the data); and (2) the method cannot account for a trend in an observer. (This latter limitation is common to all methods.) In this method, several mathematical techniques are used in succession, and the way in which the output of each step may influence the subsequent ones and the final results must still be fully understood. This will require the separate analysis of intermediate steps, by creating synthetic "benchmarking" input data sets with known characteristics and imperfections. Substantial work is thus still needed for a full validation of this fully innovative approach that emerged from the work of the ISSI team.

2.2.3. Conclusions on the Reconstruction Methods

Ideally, the reconstruction problem should be separated into two parts: a scientific choice (What is the best approach for converting the different pieces of information in numbers that can be processed?), and a statistical or analytical choice (What is the best method for merging these numbers into a single composite, given their uncertainties?). The reason for decoupling the two is that the production of the composite should not influence how the raw data are interpreted and assembled into source-data series.

One of the lessons learned from the ISSI team is that such a decoupling is very difficult to achieve at this stage because all these problems are so much interrelated. The general framework that is most appropriate for dealing with such problems is a probabilistic one, in which the sunspot data record from each observer is considered as a conditional distribution that depends on the different observed or unobserved parameters. These parameters may, for example, be the number of spots on a given day (given the resolution of the telescope, the visual acuity of the observer, etc.) or knowing that the observer did not report anything because they probably saw no spots during that week. The central goal then is to determine the probability to have a true sunspot number of a given value, given the various observed or unobserved parameters: $p(\text{data}|\text{parameters})$.

Such a probabilistic approach naturally leads to Bayesian inference [Gelman et al., 2013] that offers a natural way for estimating such probabilities, with, for example, a pathway for eliminating unobserved variables by integrating them out. Bayesian thinking also offers a

natural way for updating the results when new evidence comes in. Although Bayesian inference has been found to be highly effective for building composites (e.g., Tingley et al., 2012), there still is a long way to go before the sunspot estimation and reconstruction problem can be expressed in terms of conditional probability distributions. However, even if this is not feasible without making approximations, it forces us to express observations that are of very different types into a common and rigorous framework for which well-established methods are available.

3. Benchmarks for Sunspot-Number Time-Series Constructions

Benchmarks are rules of thumb or expectations that serve as checks, or points that need to be considered, for any sunspot-based reconstruction of solar activity. They differ from proxies in that they are based solely on sunspot data.

3.1. Expectation (1): Similarity of the S_N and G_N Time Series

The ongoing sunspot-number recalibration effort was motivated by the expectation that the Wolf S_N(1.0) and Hoyt and Schatten (1998a,b) G_N time series, which closely tracked each other through a broad range of solar activity during the twentieth century, should do so throughout their common time interval, rather than abruptly diverging as they did ca. 1880 (See Figure 1 in Clette et al., 2014, and Figure 1(a) in Clette et al., 2015). This same expectation holds for the current sets of G_N time series, which agree reasonably well with S_N series during the twentieth century but exhibit a broad spread in reconstructions of yearly values before $\sim$1880 (Figure 2). At present, the most likely explanation for a separation of G_N and S_N series at this time lies in Wolfer's decision (when he became an assistant at Zürich in 1876) to count individual small pores as groups (see Section 2.1.2). The alternative – a change in the internal workings of the Sun resulting in a difference in the relative number of spots and groups at solar maxima – seems less plausible. It is clear that the years ca. 1880, based on the marked dispersion in values of the various series in Figure 2 starting near this time, present a challenge for sunspot-number reconstructions.

Figure 13 shows the ratios of S_N(2.0) to the various G_N series, after an 11-year running window smoothing, scaled to a value of 1.0 over 1920–1974. We find the S_N/G_N ratio for all sunspot series to be roughly constant over the twentieth century (in agreement with Svalgaard, 2020), while the various series show divergence prior to 1900. Given the broad range of activity during the $\sim$100-year interval $\sim$1900–2010, we would expect S_N/G_N for any G_N series to remain quasiconstant also before $\sim$1900 − as is the case for the CEA17 and SvSc16 series. We note that when computing the ratios, we excluded years with $S_N < 11$. The choice of thresholds influences the computed ratios, with increasing threshold leading to higher S_N/G_N ratios for all series except HoSc98, while the ratio for the series by SvSc16 gets closer to unity. We note that a nonlinear relation between group and sunspot numbers has been reported, hinting at a slight dependence of the relationship between groups and sunspots to the level of activity (Clette et al., 2016b).

3.2. Expectation (2): Observers Should Improve, and Correction Factors Should Decrease, over Time

Cliver (2016) defined a "correction factor" time series [CF_i] for a given G_N time series (Equation 3), obtained by dividing the annual group count [G_{Ni}] by the corresponding yearly
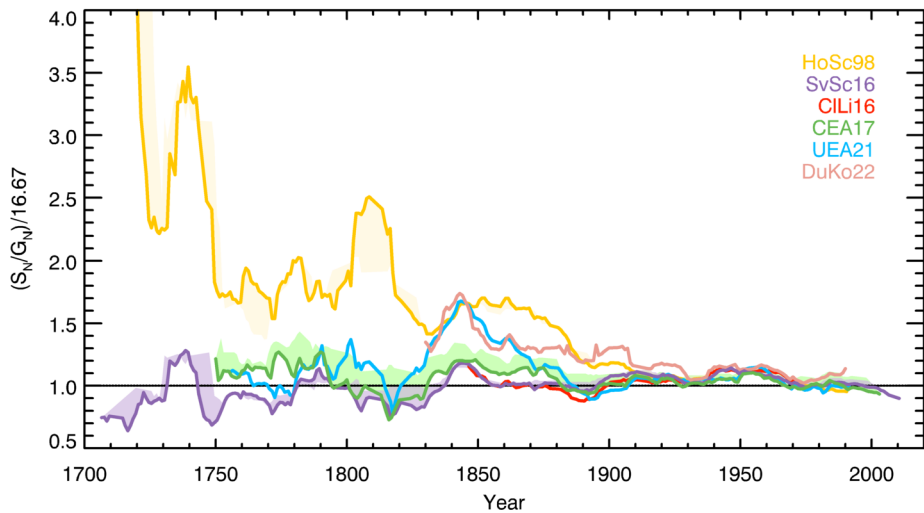
Figure 13 Ratios of the various G_N series to $S_N(2.0)$ after an 11-year running window smoothing, scaled to a value of 1.0 over 1920–1974. Years with $S_N < 11$ were ignored when computing the ratios. To illustrate the effect of the S_N threshold on the ratios we also show as shaded surfaces (only for SvSc16, HoSc98, and CEA17) the case when years with S_N less than 50 are ignored.

average of raw group counts for all observers [G_{Nraw}], that can be used to assess the reliability of new G_N and S_N reconstructions. G_{Nraw} thus represents a fully uncorrected group number, without any compensation of the global improvement of observing techniques.

$$CF_i = G_{Ni}/G_{Nraw}. \tag{3}$$

[G_{Nraw}] in Cliver (2016) was produced from all observers in the V16 database and applied in Equation 3 to various G_N series regardless of which database (Hoyt and Schatten, 1998a,b or Vaquero et al., 2016) (and/or which observers within these databases) they were constructed from. Here, we produced correction factors (in essence, ensemble-averaged k- and k'-factors of observers for a given year) by considering the data used by each series and the corresponding database of raw counts. Specifically, we consulted the tables of observers listed by Cliver and Ling (2016), Chatzistergos et al. (2017), Usoskin et al. (2021), and DuKo22 (in preparation), and produced a [G_{Nraw}] series by averaging the raw counts of those specific observers from the database used in each case. For HoSc98 we used all available observers in the Hoyt and Schatten (1998a,b) database, while for SvSc16 we used all observers in the V16 database, but in all cases we excluded the time series from Mt Wilson derived from just the center of the solar disk.

We would expect that in general CF values for all series would increase more or less monotonically from values ∼1 in the twentieth century to higher values ≳ 2 when moving back to the early nineteenth century and before (see Section 5.1) because of (1) inferior telescope technology for earlier centuries, and (2) the change in sunspot counting procedure from Wolf to Wolfer (see Section 2.1.2). Both of these changes will result in higher counts for a given level of solar activity in the modern era and a corresponding increase in CF going back in time – as can be seen for nearly all time series in Figure 14. Most G_N series show to various degrees the expected decreasing trend, but it is very limited for the original HoSc98 series, which is thus incompatible with the known progress of the observations.
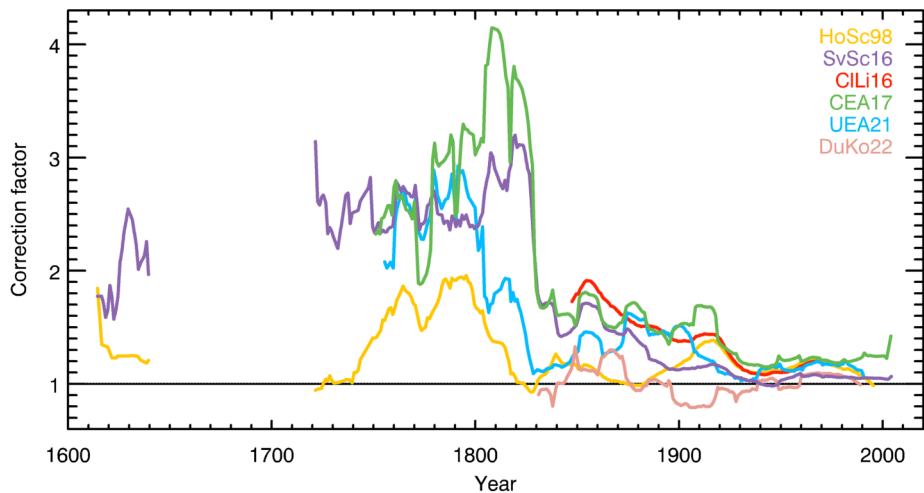
Figure 14 11-year running averages of correction factor time series from $1600-2010$ for the various sunspot series denoted in the legend.

Another kind of test can be based on determination of the threshold area of small spots missed by imperfect observations, using contemporary data. In this respect, the difference in the definitions of G and S between Wolf and Wolfer had an underlying instrumental cause that extended beyond Wolf's desire to maintain fidelity with earlier observers. After 1860, Wolf primarily used two small-aperture (40 mm/700 mm (focal length) and 42 mm/800 mm) portable telescopes while, beginning in 1876, Wolfer used the standard 83 mm/1320 mm telescope at the Zürich Observatory (Friedli, 2016, 2020). As shown by Karachik, Pevtsov, and Nagovitsyn (2019) who degraded numerically high-resolution photospheric images from the Heliospheric and Magnetic Imager (HMI; Scherrer et al., 2012) instrument on board the Solar Dynamics Observatory (SDO; Pesnell, Thompson, and Chamberlin, 2012) spacecraft as shown in Figure 15, telescopes with aperture < 80 mm do not resolve a significant number of small pores, and thus, likely underestimate the group number. Telescopes with apertures larger than 80 mm, resolve the smallest pores sufficiently well, and provide a better representation of G. This is in line with the idea of quantifying the observer's quality via the acuity threshold, as discussed in Section 2.2.2, rather than a constant scaling factor.

Karachik, Pevtsov, and Nagovitsyn (2019) also draw attention to nonsolar-induced variability of the spot-to-group ratio (see Section 3.1), writing, "*Our results indicate that there is an effect of telescope aperture on the S_N/G_N ratio, which should be kept in mind while comparing modern ratios with the early observations made with small aperture instruments and using human eye as the detector.*" The high values of S/G for raw (uncorrected) G_N series during the eighteenth century are due to the inability to see small groups, i.e., groups of one or two small spots (see Section 7), due to small (<80 mm) or imperfect objective lenses.

4. Proxies: Independent Long-Term Time Series as Crosschecks on S_N and G_N

Different methods of sunspot-number calibration include complex assumptions that may or may not be correct, and it is important to compare them to other measures of solar activity,
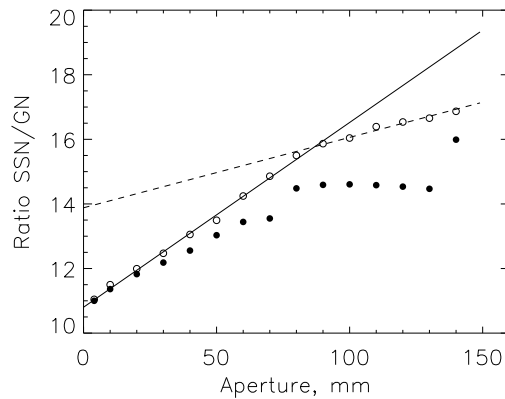
Figure 15 Dependence of the ratio S_N/G_N on telescope aperture derived from numerically degraded images from SDO/HMI. Open circles – without scattered light; filled circles – with added 5% scattered light; solid line – fitted linear function for the ratio corresponding to apertures lower than 80 mm; dashed line – fitted linear function for the ratio corresponding to apertures more than 80 mm. The step-wise change in the solid circles from 130 – 140 mm is an artifact related to the clear aperture of 140 mm for SDO/HMI. (Based on Karachik, Pevtsov, and Nagovitsyn, 2019).

either direct (such as solar radio emission, e.g., F10.7, or chromospheric indices, such as Ca II plage areas) or indirect (e.g., cosmogenic nuclides and geomagnetic responses). Because of large uncertainties of S_N and G_N in the nineteenth century and earlier, the use of proxy datasets can be used to corroborate sunspot estimates in the past.

Proxy data sets provide a measure of solar magnetic variability through its effects on the terrestrial environment, viz., the ionosphere via UV solar irradiance, the magnetosphere via the solar wind, or the atmosphere via the flux of cosmic rays modulated by the interplanetary magnetic field. These proxies are not affected by sunspots themselves but they are all different manifestations of the same process of solar-surface magnetic activity produced by the solar dynamo in the convection zone (Charbonneau, 2020). We would expect the physical relationships of the sunspot number to such parameters to be relatively constant over time (Svalgaard, 2016; Cliver, 2017), particularly in annual averages, which remove diurnal and seasonal variations. Recent studies, however, have shown that the true relationship may be convolutive (Preminger and Walton, 2006; Dudok de Wit et al., 2018; Yeo, Solanki, and Krivova, 2020; Krivova et al., 2021), i.e., one cannot transform one solar index/proxy into another simply by assuming an instantaneous linear (or nonlinear) relationship. Indeed, solar proxies may be a delayed, cumulative, or differential response to the primary solar input. This can be explained by the fact that solar indices based on chromospheric or coronal emission also include a large contribution from the extended decay of active regions, while sunspots are much more directly tied to the initial flux emergence. Time averages of at least three months are thus expected to improve the comparisons.

Proxy data should only be used as a last resort in the construction of sunspot-number time series, viz., when methods to bridge gaps in the sunspot record based on sunspot observations are unreliable, or for intervals before 1610 for which proxy S_Ns have been based on cosmogenic nuclide data (e.g., Usoskin et al., 2021). In general, proxy data can be used both to corroborate S_N and G_N time series and to raise questions about their validity, particularly when abrupt discontinuities separating two extended stable periods (jumps) are observed between sunspot-number time series and those for proxy parameters. The diagnostic gains
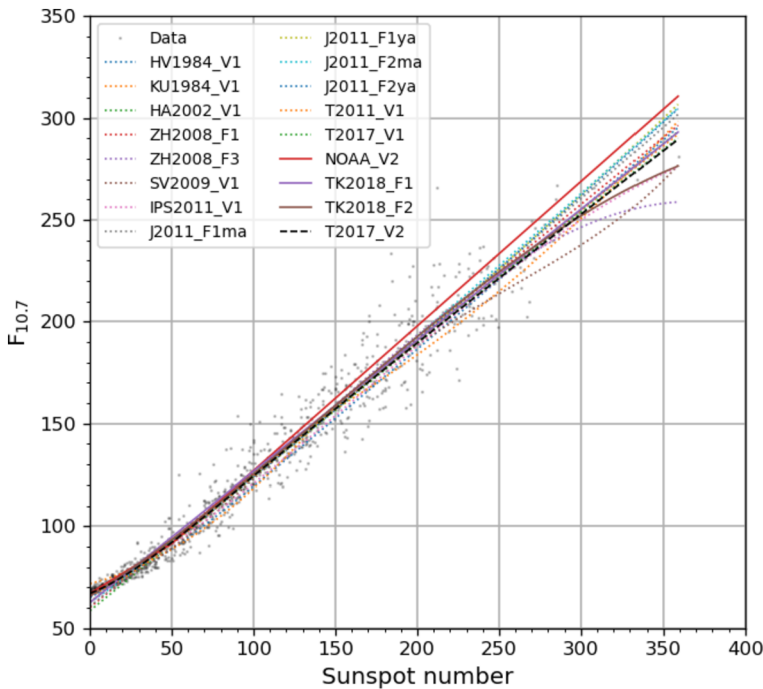
Figure 16 Plots of F10.7 vs S_N (2.0) for various studies from 1984–2018. (From Clette, 2021.). The gray dots correspond to monthly means of all original S_N and F10.7 data since 1947.

in robustness if the same offset is found in comparisons of the same sunspot-data series with multiple unrelated proxies or benchmarks.

4.1. 2.8 GHz Solar Radio Emission (F10.7)

Shortly after the first reported detection of solar radio waves (Southworth, 1945; Hey, 1946), it was found that the Sun's daily background 2.8 GHz emission (labeled F10.7 for the wavelength in cm) was related to sunspot activity (Pawsey, Payne-Scott, and McCready, 1946; Covington, 1947). Covington and Medd (1954) reported that F10.7 tracked the sunspot number – a close correlation that has been examined and confirmed many times since (Figure 16), most recently by Clette (2021). This good correlation can be explained by the presence at 10.7 cm of a significant contribution from gyrosynchrotron emission arising from the lower corona above sunspots. The near 75-year span of the carefully calibrated F10.7 record beginning from 1947 (Tapping, 2013) provides a straightforward check of S_N and G_N series for the modern epoch. The agreement between F10.7 and sunspot-number time series vouches for the physical significance of S_N and G_N.

Yeo, Solanki, and Krivova (2020) compared various facular indices, including F10.7, to sunspot data and found a power-law function with a finite impulse response to represent the data best. In a recent indepth study of the relation between the sunspot number and F10.7, Clette (2021) concludes that the relation between the two indices is fully linear over the whole range of values for the raw daily values. The long-known nonlinearity found in the low range for $S_N < 30$ when working with monthly or yearly averages can be fully accounted for by the combined effect of temporal averaging with the nonzero minimum
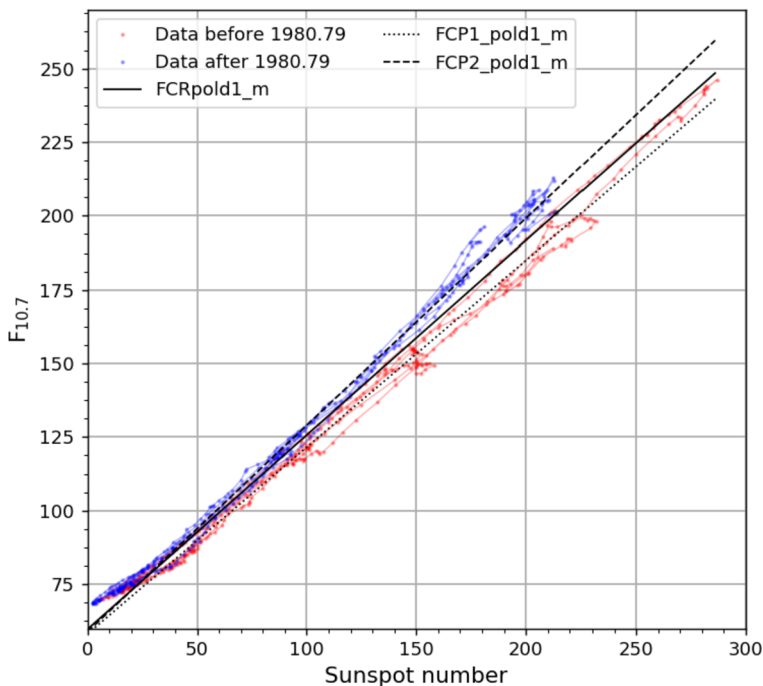
Figure 17 Plot of the 12-month smoothed monthly mean values of F10.7 versus S_N (2.0). By smoothing the monthly data shown in Figure 16 and linking the successive points, the temporal evolution appears more clearly, with solar cycles tracing very narrow loops stretching along the diagonal. This plot shows the largely linear relation between the two indices, and also the different slopes (F10.7/S_N ratio) before 1981 (red) and after this transition (blue). The corresponding linear fits (black dotted and dashed lines) indicate a higher ratio after 1981, by 10.5%. The black line shows a global fit over the whole 70-year long series (figure from Clette, 2021).

F10.7 background flux for a fully quiet Sun (67 sfu) and the $0 - 11$ jump for the first sunspot in the definition of S_N.

This all-quiet background F10.7 flux was, by itself, the subject of various studies leading to a range of disagreeing determinations. Clette (2021) found that this lowest value is actually a function of the duration of the spotless period, increasing from 67 sfu for the longest observed intervals (30 days) up to 74 sfu for single spotless days, thereby explaining the apparently contradictory values published previously.

Moreover, by tracking the temporal evolution of the S_N/F10.7 relation, this study shows that the relation was fully stable over the entire 70-year interval, except for a 10.5% jump in 1981 (Figure 17). Several tests support the determination that this scale jump is due to an inhomogeneity in the F10.7 series, and that it coincides with the only major historical transition in the operational production of this radio index (unique succession between the two main scientists in charge of this index, and simultaneous transition from the original manual processing to the current computerized production).

The Clette (2021) analysis supports the homogeneity of S_N version 2.0 (Clette and Lefèvre, 2016). This homogeneity is also confirmed by comparisons with individual long-term sunspot observers, including some extra observers who were not included in the 2015 compilation of the S_N version 2.0 (Clette, 2021; Hayakawa et al., 2022b). Equivalent comparisons of F10.7 with the original S_N version 1 series and with version 2 show that the

agreement between the two series is particularly improved after 1981, i.e., for the part of S_N version 2.0 that resulted from a full reconstruction. Several deviations reported earlier (Yeo, Solanki, and Krivova, 2020; Clette et al., 2021) have been largely eliminated. The larger residuals before 1981 indicate that larger errors and temporary deviations remain in the Zürich part of the series and that the accuracy of that part of the series could still be significantly improved in future versions.

4.2. Ca II K Plage Areas

Plage-area is another facular parameter with a connection to sunspot-number series. Plage areas are determined from full-disc Ca II K (393.367 nm) observations (Chatzistergos et al., 2022b). Such observations exist since 1892 and continue to be performed from many sites around the world (Chatzistergos et al., 2022b), thus being one of the longest direct solar datasets. Various studies compared sunspot-number series to plage areas (e.g., Kuriyan, Muralidharan, and Sampath, 1982; Foukal, 1996; Fligge and Solanki, 1998). Recently, Chatzistergos et al., 2022a compared plage-area series from 38 archives as well as a composite series of plage areas from all available data (Chatzistergos et al., 2020) to $S_N(1.0)$, $S_N(2.0)$, SvSc16, and CEA17 sunspot series. A power-law relation between plage areas and sunspot-number series was found to represent the data best, while a slight dependence of the relationship on the activity level was also reported. A better agreement between plage areas and $S_N(2.0)$ compared to $S_N(1.0)$ was also found, lending further support to the corrections applied to $S_N(1.0)$.

4.3. Geomagnetic Proxies

4.3.1. Interdiurnal Variation of Geomagnetic Activity (IDV)

The level of energization of the Earth's magnetosphere by the near-Earth solar wind is determined by (in approximate order of importance): heliospheric magnetic-field orientation and intensity, the solar-wind speed, and the solar-wind mass density (Vasyliunas et al., 1982; Pulkkinen, 2007). Thus, geomagnetic indices, quantitative indicators of global magnetospheric disturbance based on prescribed sets of ground-based magnetometers, can be used to reconstruct near-Earth solar-wind conditions (Feynman and Crooker, 1978). Given varying geometric effects associated with Earth orbit and axial inclination relative to the Sun, reconstructions are typically limited to the annual time scale, on which such effects average out (Lockwood, 2013; Lockwood et al., 2013). Different geomagnetic indices have different dependencies on the near-Earth solar-wind conditions. Thus, pairs of indices can be used to disentangle specific solar-wind parameters and estimate both the near-Earth magnetic-field intensity (B) and speed (V), and the open solar flux (OSF) (Svalgaard, Cliver, and Le Sager, 2003; Lockwood, Owens, and Barnard, 2014b). Of particular value in this regard is the interdiurnal variation (IDV) index (Svalgaard and Cliver, 2005, 2010), which is highly correlated with B and relatively insensitive to V. Using IDV, B reconstructions can be extended back to 1845 with reasonable confidence. Fair agreement between the geomagnetic B estimates (red line) and direct in situ spacecraft observations (black) is shown in Figure 18.

In order to compare the geomagnetic estimates with S_N, it is necessary to convert S_N to either B or open solar flux (OSF). Owens et al. (2016) considered two approaches. The first uses an empirical relationship between B and $S_N^{1/2}$ (Wang and Sheeley, 2003; Wang, Lean, and Sheeley, 2005; Svalgaard and Cliver, 2005). The second uses a physically constrained model of OSF (Owens and Lockwood, 2012), which assumes sunspots are a proxy
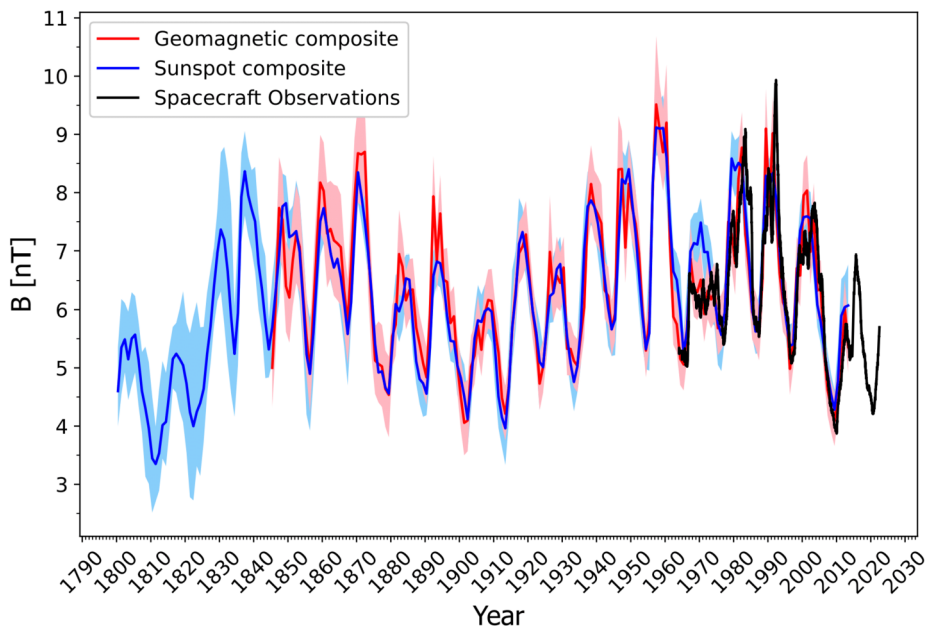
Figure 18 Time series of near-Earth heliospheric magnetic-field intensity, B, estimated from different methods. All data are annual means. Direct observations of B, which have been made by in situ spacecraft back to 1964, are shown in black. A composite of weighted geomagnetic estimates of B are shown in red. A composite of weighted sunspot-based estimates, using a range of S_N and G_N time series (Clette and Lefèvre, 2016; (S_N(2.0)); Lockwood, Owens, and Barnard, 2014a,b; LEA14); Svalgaard and Schatten (2016; SvSc16), and Usoskin et al. (2016; UEA16), and two methods for converting the sunspot number to B, is shown in blue. The shaded regions show the 1σ uncertainty ranges. (Figure adapted from Owens et al., 2016).

for OSF production (Solanki, Schüssler, and Fligge, 2000, 2002, 2007). By assuming a constant solar-wind speed, the resulting S_N-based OSF estimate can subsequently be converted to B.

Both methods were applied by Owens et al. (2016) to a range of S_N and G_N records (S_N(2.0), LEA14, SvSc16, UEA16). The resulting composite series is shown in blue in Figure 18. The general agreement with the geomagnetic series is strong, with the most notable deviations being an overestimate of the magnitude of B during Solar Cycle 20 (around 1970) and a persistent underestimate (within uncertainties) before 1900. All the individual sunspot series overestimate Solar Cycle 20 (1964 – 1976), suggesting that the difference could result from measuring global solar activity from sunspots versus the inherently local, near-Earth, measure from geomagnetic and spacecraft observations. Conversely, the higher values of B inferred from geomagnetic records before 1900 are in better agreement with the "high" S_N and G_N records in Figure 2 and less consistent with the original "low" sunspot records, namely HoSc98, LEA14 and UEA16.

4.3.2. Daily Range of Geomagnetic Activity (rY)

The daily variation of Earth's magnetic field was first linked to the quasi-decadal variation of sunspot activity (Schwabe, 1844) in 1852 (Wolf, 1852; Gautier, 1852). During the second half of the nineteenth century, this correlation provided the strongest evidence that the magnetic field at the Earth's surface was affected by the Sun (Ellis, 1880, 1898).

Svalgaard ([2016](#)) described the physical link between the Sun's spottedness and the daily variation of the geomagnetic field as follows, "*Solar magnetism (as directly observed and as derived from its proxy the sunspot number) gives rise to an ... extreme ultraviolet (EUV) excess over that expected from solar blackbody radiation ... Solar radiation into the Earth's atmosphere is controlled by the zenith angle and causes thermal winds, which, in conjunction with solar (and lunar) tides, move the atmosphere across geomagnetic-field lines. Radiation with a short-enough wavelength ionizes atmospheric constituents (primarily molecular oxygen), and there is a balance between ion formation and subsequent rapid recombination establishing an ... ionospheric conducting layer of electrons and ions [the E-layer of the ionosphere] that due to collisions moves with the winds of the neutral atmosphere across the ... geomagnetic field. The resulting inductive dynamo maintains an electric current whose magnetic effect is observable on the ground (Svalgaard, Cliver, and Le Sager, 2004; Nusinov, 2006). The day-night cycle imposes a ... diurnal variation of the magnetic effect, which has been observed for several centuries. ... The output of the entire process is the ... total daily range of the magnetic variation, which can be readily observed over a wide range of latitude.*"

The annual diurnal variation, parameterized by the daily range of the (nonstorm) east-component [rY] of Earth's magnetic field, has been reconstructed and tabulated by Svalgaard ([2016](#)) back to 1840. It should be noted that measurements of this diurnal variation exist before 1840, but the accuracy of the resulting rY index is probably insufficient for reliable comparisons with G_N and S_N. Indeed, as shown in Yamazaki and Maute ([2017](#)), rY has a sensitivity to seasonal effects when source data are incomplete (as is the case before 1840), because rY involves averages over whole years and over longitude.

Figure [19](#) shows the variation of the ratios of various scaled S_N and G_N series to the rY index over the interval $1840 - 2010$. Over the twentieth century, the gradual rise of the 11-year smoothed ratios from $\sim$1900 to $\sim$1975 tracks the general increase in S_N and G_N reconstructions during this interval, as well as the sharp drop after $\sim$2000. This modulation of the ratio by the amplitude of the solar cycle may indicate a nonlinear relation that is not fully accounted for. Nevertheless, as this relation is expected to be the same at all times, this rough agreement over $1900 - 2000$ should hold outside of this interval. Of the nine S_N and G_N time series considered in the figure, CEA17 is the one for which the value of the G_N/rY time series is most internally consistent for corresponding extremes of solar activity in different epochs, viz., the peaks in the eighteenth and nineteenth and the troughs at the beginning of the twentieth and twenty-first centuries. It gives a ratio that remains closest to unity. On the other hand, low reconstructions, like HoSc98 or DuKo22, strongly deviate to low ratios before 1900, thus giving the worst agreement.

4.4. Cosmogenic Radionuclides

Cosmogenic nuclides are radioactive isotopes that are not normally expected to exist in the terrestrial system as a result of the natural radioactivity of the solid Earth, nor to survive from the time of the planetary system formation. The only (or dominant) source of such isotopes is related to energetic cosmic-ray particles continuously impinging on Earth, that initiate a nucleonic-electromagnetic-muon cascade in the atmosphere. As a subproduct of the cascade, some specific radionuclides can be produced in traceable amounts and stored in natural dateable archives, such as tree trunks, ice sheets or lake/marine sediments.

The most used cosmogenic isotopes for solar-terrestrial studies are ^{14}C (radiocarbon) and ^{10}Be (Beer, McCracken, and von Steiger, [2012](#); Usoskin, [2017](#)). The concentration of ^{14}C in dendrochronologically dated tree rings and ^{10}Be in glaciologically dated polar (Antarctic and Greenland) ice cores serve as measures of the abundance of these isotopes in the
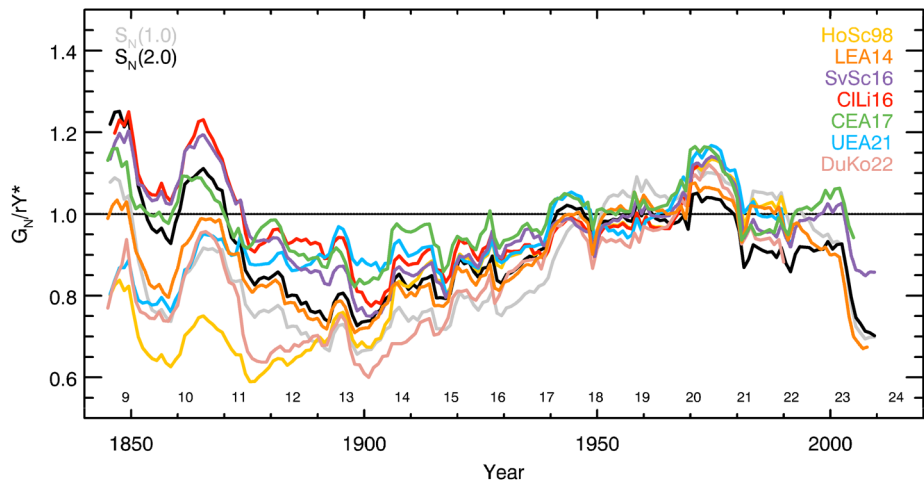
Figure 19 Ratios between the annual mean group-sunspot number and annual mean range rY in nT smoothed with an 11-year running window. The sunspot-number series were normalized to $S_N(2.0)$ over the period $1920-1974$. rY was linearly scaled to CEA17 G_N series to render the ratio (G_N/rY*) around 1. The numbers at the lower part of the panel denote the conventional solar cycle numbering and are shown roughly at the time of cycle maximum.

troposphere in the past. The flux of galactic cosmic rays near Earth is modulated by solar magnetic activity (Potgieter, 2013; Cliver, Richardson, and Ling, 2013) that is often quantified via the modulation potential of the solar wind and heliospheric magnetic field (Caballero-Lopez and Moraal, 2004; Usoskin et al., 2005), after accounting for the effect of Earth's slowly changing geomagnetic field, which provides additional shielding from cosmic rays (Usoskin, Solanki, and Korte, 2006; Snowball and Muscheler, 2007). Production tables for individual isotopes have been computed by Webber and Higbie (2003), Usoskin and Kovaltsov (2008), Webber, Higbie, and McCracken (2007), and Kovaltsov, Mishev, and Usoskin (2012). The most recent and accurate computational set was provided by Poluianov et al. (2016), which agrees well with the measurements, also in absolute terms (Asvestari and Usoskin, 2016). The first physics-based solar-activity reconstruction based on cosmogenic-isotope data was made ∼20 years ago (Usoskin et al., 2003; Solanki et al., 2004), and the most recent one is based on a Bayesian multiproxy approach (Wu et al., 2018b), covering the last ten millennia of the Holocene. Such reconstructions have increasing uncertainties beyond that time because the transport and deposition patterns of isotopes in the atmosphere are less well known for ice-age conditions.

Deconvolving the cosmogenic nuclide data to infer a solar modulation potential and ultimately a proxy sunspot number for years prior to 1610 is a formidable, but necessary, task as cosmogenic isotopes provide the only quantitative information on solar activity before the telescopic era (Beer, McCracken, and von Steiger, 2012; Usoskin, 2017). One of the goals of the sunspot-number workshops (Cliver, Clette, and Svalgaard, 2013; Cliver et al., 2015) that initiated the present sunspot-number reconstruction effort was to provide a robust ∼400-year sunspot series that could set the level of a cosmogenic-based sunspot number for the 10 millennia preceding 1610. As Cliver et al. (2015) wrote: "*Calibration of such a time series is complex, however, owing to variations of cosmogenic-nuclide concentrations caused by Earth's magnetic field, terrestrial climate, and possibly volcanic activity* [*as well as the high noise level of the raw data*]. *Thus it is necessary to have as long and as accu-*

rate a record of solar activity as possible to characterize the effect of these other variables on a long-term cosmogenic-nuclide-based [*sunspot number*]." While the cosmogenic record works reasonably well for characterizing the relative overall level of solar activity and can distinguish between features such as the Modern Grand Maximum (Usoskin et al., 2003; Solanki et al., 2004; Usoskin, 2017) and the Maunder and Spörer Grand Minima (Eddy, 1976; Usoskin, Solanki, and Korte, 2006; Usoskin, 2017; Asvestari et al., 2017), its use as a reliable arbiter of the smaller differences that characterize discontinuities between newly developed S_N and G_N times remains to be demonstrated.

Until recently, the quality/time-resolution of the cosmogenic-isotope data was insufficient to reliably reconstruct sunspot cycles before 1600 AD (Muscheler et al., 2016). In 2021, Brehm et al. (2021) reported high-precision measurements of ^{14}C concentration in an oak tree archive for years after 970 AD. This new dataset together with an improved semiempirical model describing the evolution of the Sun's global total and open magnetic flux (Krivova et al., 2021) made the first high-resolution millennium-long (970 – 1900) sunspot-cycle reconstruction possible (Usoskin et al., 2021). Figure 20 compares the ^{14}C-based sunspot number of Usoskin et al. (2021) from 1610 – 1900 (gray shading indicates 67% confidence intervals) with the S_N(2.0), HoSc98, SvSc16, CEA17, and UEA21 time series. Overall, it best matches intermediate sunspot series, like CEA17. Discrepancies between the amplitudes and timings of the sunspot and ^{14}C-based time series increase as one goes back in time, making the comparison less reliable. Note the high minimum in the ^{14}C-based S_N record ca. 1780. Although the properties of individual solar cycles cannot be reliably established by this method during grand minima of activity (Usoskin et al., 2021), the averaged ^{14}C-based S_N level is consistent with zero, implying very low S_N during the Maunder minimum (see also Carrasco et al., 2021d).

Another cosmogenic-nuclide that can be used to trace the evolution of long-term solar activity is the ^{44}Ti isotope measured in meteorites that have fallen through the ages (Taricco et al., 2006, 2016). This isotope agrees most closely with the lowest G_N series (HoSc98) and argues against the highest series over the nineteenth century, within the estimated uncertainties. However, it is less precise than the terrestrial isotopes and does not provide a firm diagnostic over the eighteenth and nineteenth centuries. It can only indicate reliably a relatively high cosmic-ray level (respectively, low solar activity) during the Maunder minimum (Asvestari et al., 2017).

Overall, the different kinds of diagnostics described above can be summarized as follows, regarding the amplitude of the reconstructed solar cycles in the nineteenth century (Table 4). Most of those tests, except the cosmogenic radionuclides, fully exclude the lowest reconstructions, which includes the original G_N series (HoSc98). The intermediate reconstructions are the only ones compatible with most of those external criteria, although the agreement is not optimal in most cases (generally on the lower limit of the acceptable range). Only the radionuclide proxies currently exclude the highest reconstructions, but their limited accuracy makes detailed diagnostics difficult except for large deviations like grand minima.

Therefore, the overall answer provided by those comparisons remains partly ambiguous. As all those external tests and proxies do not fully agree yet among themselves, further progress is definitely needed to improve those indirect solar tracers of solar activity, and to elucidate the remaining disagreements, before they can deliver a fully robust and independent benchmark for the S_N and G_N series.
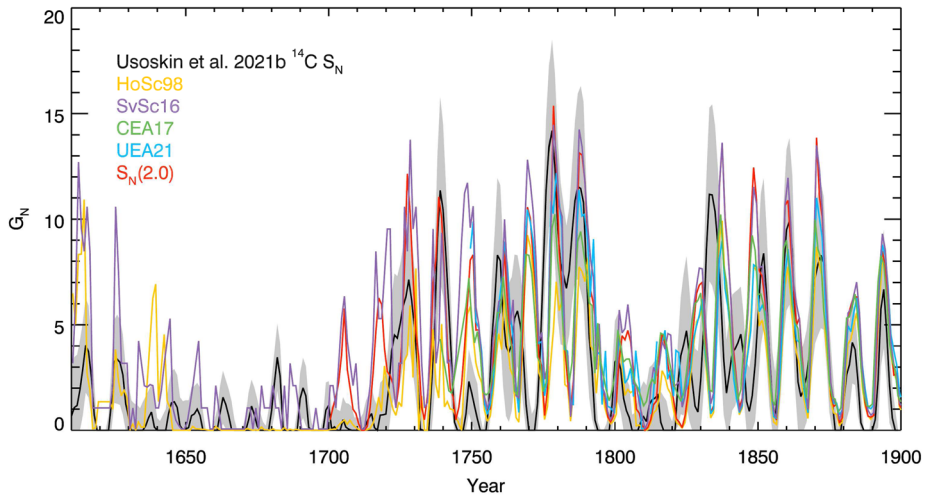
Figure 20   Comparison of ^{14}C-based sunspot number (black curve with $\pm 1\sigma$ grey-shaded uncertainties) with $S_N(2.0)$ (red), HoSc98 (yellow), SvSc16 (purple), CEA17 (green), and UEA21 (light blue) time series for the 1610 – 1900 interval. Shown are annual values, while $S_N(2.0)$ and ^{14}C-based sunspot number were divided by 16.67 to bring them roughly to the same scale as the GSN series. All series, except the ^{14}C-based sunspot number, were scaled to match over the period 1920 – 1974. (Adapted from Usoskin et al., 2021).

Table 4   Summary of the diagnostics derived from the benchmarks and proxies described in Sections 3 and 4. The three categories (horizontally: low, medium, high) globally divide the total range of G_N and S_N reconstructions over the nineteenth century in three equal bins. The second column lists the reconstructed series that fall in those broad categories (S_N series in italics). "BEST" indicates the closest match, while "NO" corresponds to a full incompatibility. When there is a "FAIR" agreement, the reconstructions are compatible with the corresponding proxy (columns) within the uncertainties provided for it, but can be either too low or too high relative to the proxy, as indicated between brackets.

	G_N and S_N series	Observer correction factor (Figure 14)	$S_N(2.0)/G_N$ (Figure 13)	Geomagnetic IDV index (Figure 18)	Diurnal rY modulation (Figure 19)	Isotopes ^{14}C, ^{10}Be (Figure 20)
HIGH	SvSc16 ClLI16 *S_N V2.0*	BEST	BEST	BEST	BEST	NO
MEDIUM	CEA17 DuKo22 UEA21 *S_N V1.0* LEA14	FAIR (low)	FAIR (low)	FAIR (low)	FAIR (low)	BEST
LOW	HoSc98	NO	NO	NO	NO	FAIR (low)
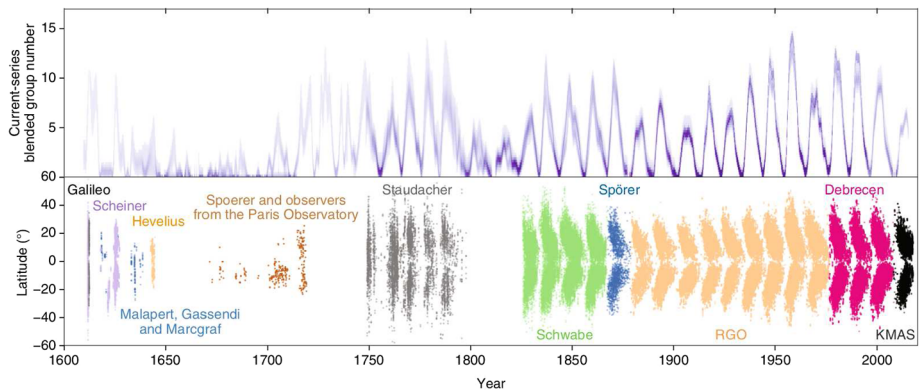
Figure 21 (Top) Composite of various G_N times series. (Bottom) Composite butterfly diagram showing the separation of sunspot-coverage epochs into intervals before and after Schwabe began his patrol. (Adapted from Muñoz-Jaramillo and Vaquero, 2019.)

5. Fault Lines in the G_N and S_N Data Series

5.1. Traversing the Dalton Minimum: Staudacher to Schwabe (1798 – 1833)

As Muñoz-Jaramillo and Vaquero (2019) point out, there is a marked drop-off in both the quality and quantity of sunspot data before 1825 (Figure 8 and Figure 21). Bridging the data-sparse period of the Dalton Minimum to scale Staudacher, who counted spots from 1749 – 1799, to Schwabe (1826 – 1867) is a key challenge for any sunspot-number series. Recently recovered datasets for the Dalton Minimum will help to address this problem (Hayakawa, Besser, and Iju, 2020; Hayakawa et al., 2021g). In general, the relative performance/accuracy of the various reconstruction methods in sparse data environments needs to be examined/assessed (e.g., Usoskin, Mursula, and Kovaltsov, 2003).

Amateur astronomer Johann Casper Staudaucher made 1146 drawings of the spotted solar disk from 1749 – 1799. Quoting from Svalgaard (2020): "*Haase* (1869) ... *reviewed the Staudach[4] material and reports that a 4-foot telescope was used, but that it was not of particular good quality and especially seemed not to have been achromatic, because he quotes Staudach himself remarking on his observation of the Venus transit in 1761 that 'for the size and color of the planet there was no sharp edge, instead it faded from the same black-brown color at the inner core to a still dark brown light red, changing into light blue, then into the high green and then to yellow'. So we may assume that the telescope suffered from spherical and chromatic aberration. We can build replicas with the same optical flaws as telescopes available and affordable to amateurs in the 18th century. On Jan. 16, 2016 we started observations of sunspots with such replicas. Three observers (expert members of "The Antique Telescope Society", webari.com/oldscope/) have made drawings of the solar disk by projecting the sun onto a sheet of paper. We count the number of individual spots as well as the number of groups they form. Comparing our counts with what modern observers report for the same days we find that the sunspot number calculated from the count by modern observers is three times larger as what our intrepid observers see ... and that the number of groups is 2.5 times as large. This suggests that we can calibrate the 18th*

---

[4]In the literature, this observer is referred to as both Staudacher and Staudach. Here, we generally refer to Staudacher (e.g., Figures 9 and 21) except when directly quoting Svalgaard.

century observations in terms of the modern level of solar activity by using the above factors. [$S_N(2.0)$] *divided by 3 . . . is a reasonable match to the sunspot number calculated from Staudach's drawings* (Svalgaard, 2017), *thus roughly validating the revised SILSO values and not compatible with the low values of the* [*Hoyt and Schatten, 1998a,b*] *reconstruction . . .*."

Svalgaard and Schatten (2016) had earlier used a factor of ∼2.5 (obtained through what they described as an *"innovative* (*and some would say perhaps slightly dubious*) *analysis"* involving a comparison of "high count" and "low count" observers from ∼1750 to ∼1850 to scale Staudacher's observations to those of Wolfer in their G_N series. The study based on antique telescopes (Svalgaard, 2020) puts this factor on a firmer footing. We also note that this 2.5 value matches the correction factors found for two other G_N reconstructions before the nineteenth century (Figure 14).

Telescope aperture and optical quality are not the only factors that affect sunspot-group count. Group splitting also plays a role. Before Hale's (1908) discovery of sunspot magnetism, closely spaced groups were generally lumped together into very large groups, sometimes spanning more than 40° in longitude, as the bipolarity of sunspot groups and the maximum possible size of an active region (∼25°) were then unknown. This tendency to form overly large groups was probably also favored by the lower magnification and smaller drawing size used in early observations. In the mid-twentieth century, Waldmeier (1938) introduced a group-classification system that took the temporal evolution of bipoles in a cluster of sunspots into account, abandoning proximity as the sole, or primary, criterion for identifying groups (Friedli, 2009; Svalgaard and Schatten, 2016). As a result, clusters of sunspots that previously had been counted as a single group could now be divided (split) into two or more groups (see Figure 1b for an example of such splitting), thus raising the group counts.

Arlt (2008; Arlt and Vaquero, 2020) suggested that Staudacher, with his eighteenth-century telescope, missed all of the small A- and B-type spot groups (according to the Waldmeier classification) that make up 30–50% of all groups seen today (Clette et al., 2014). These reductions in group counts would imply a Staudacher k'-factor (Equation 2) ranging from ∼1.4 to 2.0. From an analysis of Staudacher's sunspot drawings, Svalgaard (2017) found that Waldmeier's classification system would increase Staudacher's group counts in V16 by 25%. Combining the instrumental correction factor (1.43–2.0) with that for group splitting (1.25) yields a group scaling factor (k') range for Staudacher (to Wolfer) from of ∼1.8 to 2.5, in good agreement with the above reconstitution using replicas of historical telescopes.

5.2. Galileo to Staudacher: Encompassing the Maunder Minimum

Figure 8 shows that the 1730s and 1740s are the weakest link in the sunspot-number time series. Substantial attention has been focused on this data-poor interval (Section 2.2.1(c)) by Hayakawa et al. (2022a) which is critical to connect Staudacher to the Maunder Minimum (Section 2.2.1(b); the low end of the lever arm for TSI reconstruction and climate-change studies; Solanki et al., 2013) and all preceding years, including those for which the sunspot record must be inferred from cosmogenic radionuclides.

The degree of difficulty of getting the first ∼140 years of a sunspot-number series correct is underscored by the fact that there are only two systematic reconstructions of such a series that extend to 1610: (1) the Hoyt and Schatten (1998a,b) G_N series that assigned an average k-factor of 1.255 (slightly higher than the average correction factor for observers during the second half of the twentieth century; Figure 14) to 78 of 171 pre-1749 observers that did not

have any common days of observation with other observers, with a median value of 1.002 for the remaining 93 observers (vs. 1.000 for RGO); and (2) the Svalgaard and Schatten (2016) G_N series for which the pre-Schwabe years are based in large part on the high-count/low-count observer comparison scheme used to scale Staudacher to Schwabe (Section 5.1) and a somewhat related "brightest star" method based on the highest daily group count recorded in a given year by any observer. Such speculative methods and reliance on proxies for corroboration will likely be required to obtain yearly values from 1610 – 1748. The active-day fraction (Kovaltsov, Usoskin, and Mursula, 2004; Vaquero et al., 2015; Usoskin, 2017) has been used to estimate the general level of activity during the Maunder Minimum (Carrasco et al., 2021d, 2022a), which was relatively well observed (Figure 8), and may be useful to firm up estimates elsewhere in the early series, pending the recovery of more historical data.

6. Summary of Progress

The main achievement of the ISSI Sunspot Number Recalibration Team was the data-recovery effort headed by Arlt, Carrasco, Clette, Friedli, Hayakawa, and Vaquero, with an emphasis on the identification, digitization, and analysis of primary records, images in particular. Such data can play a key role to bridge gaps between early (pre-Schwabe) segments of the sunspot record. (Sections 2.1.1 and 2.2.1)

A prime focus of the team meetings was the presentation/probing of novel G_N reconstruction methods by Chatzistergos, Dudok de Wit, Kopp, Lefèvre, Mathieu, Muñoz-Jaramillo, Svalgaard, and Usoskin, with an emphasis on the application of modern statistical methods and determination of uncertainties (e.g., Mathieu et al., 2019, 2023) as summarized in Tables 2 and 3.

Less progress was made during the team meetings on proxy time series, although considerable progress had been made beforehand by Svalgaard, Usoskin, Lockwood, Owens, and others on long-term geomagnetic and cosmogenic-nuclide-based time series, and Clette has carried out a thorough comparison of F10.7 and $S_N(2.0)$ as a follow up of discussions in the Team meetings. These proxies can be used to corroborate as well as to identify potential weaknesses in new time series (Section 4).

During the ISSI Team meetings, Clette introduced the concept of benchmarks for the reconstruction project, e.g., the concept that because of improvements in telescope technology and changes in the definitions of spots (reduced minimum size) and groups (from lumping to splitting), one would expect modern observers to count more spots than those preceding Wolfer (leading to smaller normalization or correction factors over time for a given level of sunspot activity), an expectation that the Hoyt and Schatten G_N series failed to meet (Section 3).

"Reverse engineering" experiments based on old (Svalgaard) and new (Karachik, Pevtsov, and Nagovitsyn, 2019) telescopes helped to assess the effect of improvements in telescope technology on the observability of sunspots over time. These studies are relevant for the scaling of Staudacher, the key observer for the second half of the eighteenth century, to Schwabe, the principal observer for the first half of the eighteenth century (Sections 3.2 and 5.1).

At the team meetings, Pesnell represented the space-forecasting community, Van Driel-Gesztelyi served as rapporteur, and Kopp reviewed the "triad" results (see below) and mapped the path forward. This also led to considerations about the broader implications of the current upgrades of the long-term sunspot series, which go beyond the domain of solar physics (e.g., Chatzistergos, 2022).

Perhaps the most important marker of progress during the ISSI Team meetings was the joining of key stakeholders to argue/debate/discuss the reconstruction of the S_N and G_N number time series, with commitment to the goal of producing the optimal series with the data at hand and current best practice methodology. As Clette and Lefèvre (2016), wrote, the present focus on the sunspot number "marks a fundamental transition between the earlier unalterable and unquestioned data series to a genuine measurement series, like any other physical data series. As for any other measurement, it is natural to revise it as new data sources and new analysis methods become available."

7. Perspective and Prospect

The sunspot number has been called the longest running experiment in science (Owens, 2013). The renewed emphasis on this time series reflects the Sun's impact on our increasingly technology-based society and the need to better quantify the time-varying solar input to the terrestrial climate.

The end goal of the present effort that began in 2011 and continued through the Topical Issue in 2016 and the ISSI Team meetings of 2018 and 2019 to the present day remain the same: to produce a community-vetted series (Cliver, Clette, and Svalgaard, 2013) with quantified time-dependent uncertainties (e.g., Dudok de Wit, Lefèvre, and Clette, 2016) for the last ∼400 years. Such a base reference can be used to anchor a millennial-scale cosmogenic-nuclide-based time series of solar variability dating back to the last glacial period and to test and validate physical models of the coupling between the past solar input and the observed response of the Earth system.

The last decade has shown that this process of acquiring consensus via applications and discussions of multiple approaches followed by reviews of their results cannot be rushed. The Hoyt and Schatten (1998a,b) time series, valuable both for the introduction of a G_N series that could be extended to 1610 and for the creation of the first publicly available digitized database, taught the lesson of the necessity for due diligence regarding modifications/revisions of the S_N. The now-apparent issues with the Hoyt and Schatten G_N time series were not independently examined for more than a decade (Cliver and Ling, 2016), during which time it became entrenched as an alternative to S_N, in part because of its extension to the Maunder Minimum. In Appendix 1 of Hoyt and Schatten (1998a,b), the k'-factors for Wolf (1.117) and Wolfer (1.094) are within 2% of each other, despite the fact that Wolfer counted 65% more groups than Wolf (Svalgaard, 2013; Cliver, Clette, and Svalgaard, 2013). Had this peculiarity been noticed when the Hoyt and Schatten (1998a,b) series was introduced, it is unlikely that their then new G_N series would have gained the traction/usage that it retains at some level to this day (e.g., Coddington et al., 2019; Wang and Lean, 2021; Krivova et al., 2021). To ensure that all new S_N and G_N time series were subjected to scrutiny, the ISSI Team formation was preceded by an informal reexamination of each new sunspot-number time series by separate "triads" consisting of an advocate, critic, and mediator. This format had the advantages of having former competitors working together – fostering both critical analysis and team building in anticipation of the ISSI effort.

What is then the way forward? The interactions between the members of the ISSI team have shown that the reconstruction of the sunspot number is a multifaceted and highly multidisciplinary problem. At a more conceptual level, this problem consists in collecting information of various types and origins, which are linked in different ways to the main observable of interest, which is the number of sunspots or sunspot groups. Ideally, one should decompose such a problem into two parts: a scientific choice and a statistical or analytical

choice (Section 2.2.3). One of the main benefits of this exercise is that it makes us think in a probabilistic way, i.e., never separate an observation and its uncertainty.

Keeping this in mind, the expanded ISSI Sunspot Team of observers, analysts, and modelers will remain electronically connected (with the welcome prospect of actual meetings in time), with the immediate goals of refining the methodology for the various series proposed, and creating corresponding S_N and G_N time series with realistic uncertainties. Once the new/revised time series have been developed, they will need to be independently reproduced and evaluated using benchmarks and proxy series. Certain methods may work better in data sparse environments, so composite methodologies may be required. This will take time.

We estimate that new databases will be available/released by early 2023, with the key reconstruction methods brought to maturity and corresponding series created by the end of that year. At that point, an evaluation team chaired by the SILSO Director, will select next versions of S_N and G_N for sanction by an International Astronomical Union (IAU) reviewing body, with formal release targeted for conjunction with the IAU General Assembly in 2024. Even with the release of S_N(3.0) and a consensus G_N(3.0), it is possible that the two series may not be complete reconstructions for years before 1750, given the broader uncertainties and more complex and indirect validations required for these early years. However, values with appropriate uncertainties will be provided for these early years for both series back to 1610, to include the lever arm of the Maunder Minimum. The new series will mark the next step in a now-permanent improvement and quality-insurance process. The new series will be continuously monitored by comparison with a basket of high-quality observers, as well as with proxies and benchmarks. As new data, new knowledge, and new mathematical tools continue to emerge, on a regular basis follow-on versions will be released at intervals of 3 to 10 years, when enough material has accumulated to warrant robust and substantial modification to the series. The goal is to provide the scientific community with a unique and trusted reference that summarizes our best knowledge about the long-term evolution of the solar activity, as traced by sunspots, and a reliable link to cosmogenic nuclide data for years before 1610.

Author contributions F. Clette and E.W. Cliver coordinated all contributions to this review article, and cared for the final global editing. All authors contributed contents to the different sections of this review, often focusing on the parts related to their own work. T. Chatzistergos produced several figures gathering and comparing different data series (Figures 2, 10, 12, 13, 14, 19, 20). In accordance with their special role during the ISSI Team sessions, M. Owens, A. Pevtsov, G. Kopp, D. Pesnell and L. van Driel-Gesztelyi acted as experts and observers from a wider scientific community, and provided a broader view of the present and future orientations of the S_N and G_N reconstruction work, in relation with the needs of current research in solar physics and related disciplines (primarily Sections 6 and 7). All authors iteratively reviewed the manuscript in the course of its rather long construction.

Declarations

Competing interests The authors declare no competing interests.

References

Aparicio, A.J.P., Lefèvre, L., Gallego, M.C., et al.: 2018, A sunspot catalog for the period 1952–1986 from observations made at the Madrid Astronomical Observatory. *Solar Phys.* **293**, 164. DOI.

Arlt, R.: 2008, Digitization of sunspot drawings by Staudacher in 1749–1796. *Solar Phys.* **247**, 399. DOI.

Arlt, R.: 2018, Sunspot observations by Pehr Wargentin in Uppsala in 1747. *Astron. Nachr.* **339**, 647. DOI.

Arlt, R., Vaquero, J.M.: 2020, Historical sunspot records. *Living Rev. Solar Phys.* **17**, 1. DOI.

Arlt, R., Leussu, R., Giese, N., Mursula, K., Usoskin, I.G.: 2013, Sunspot positions and sizes for 1825–1867 from the observations by Samuel Heinrich Schwabe. *Mon. Not. Roy. Astron. Soc.* **433**, 3165. DOI.

Arlt, R., Senthamizh Pavai, V., Schmiel, C., Spada, F.: 2016, Sunspot positions, areas, and group tilt angles for 1611–1631 from observations by Christoph Scheiner. *Astron. Astrophys.* **595**, A104. DOI.

Asvestari, E., Usoskin, I.G.: 2016, An empirical model of heliospheric cosmic ray modulation on long-term time scale. *J. Space Weather Space Clim.* **6**, A15. DOI.

Asvestari, E., Usoskin, I.G., Kovaltsov, G.A., Owens, M.J., Krivova, N.A., Rubinetti, S., Taricco, C.: 2017, Assessment of different sunspot number series using the cosmogenic isotope ^{44}Ti in meteorites. *Mon. Not. Roy. Astron. Soc.* **467**, 1608. DOI.

Baker, D.N., Balstad, R., Bodeau, J.M., et al.: 2008, *Severe Space Weather Events—Understanding Societal and Economic Impacts*, National Academies Press, Washington.

Beer, J., McCracken, K., von Steiger, R.: 2012, *Cosmogenic Radionuclides: Theory and Applications in the Terrestrial and Space Environments, Physics of Earth and Space Environments*, Springer, Berlin. ISBN 978-3-642-14650-3.

Bhattacharya, S., Teague, E.T.H., Fay, S., Lefèvre, L., Jansen, M., Clette, F.: 2021, A modern reconstruction of Richard Carrington's Observations (1853–1861). *Solar Phys.* **296**, 118. DOI.

Bhattacharya, S., Lefèvre, L., Hayakawa, H., Jansen, M., Clette, F.: 2023, Scale transfer in 1849: Heinrich Schwabe to Rudolf Wolf. *Solar Phys.* **298**, 12. DOI. ADS.

Brehm, N., Bayliss, A., Christl, M., et al.: 2021, Eleven-year solar cycles over the last millennium revealed by radiocarbon in tree rings. *Nat. Geosci.* **14**, 10. DOI.

Caballero-Lopez, R.A., Moraal, H.: 2004, Limitations of the force field equation to describe cosmic ray modulation. *J. Geophys. Res.* **109**, A01101. DOI.

Cameron, R.H., Schüssler, M.: 2019, Solar activity: periodicities beyond 11 years are consistent with random forcing. *Astron. Astrophys.* **625**, A28. DOI.

Cannon, P., Angling, M., Barclay, L., et al.: 2013, *Extreme Space Weather: Impacts on Engineered Systems and Infrastructure*, Roy. Acad. Eng, London.

Carrasco, V.M.S., Gallego, M.C., Vaquero, J.M.: 2020, Number of sunspot groups from the Galileo-Scheiner controversy revisited. *Mon. Not. Roy. Astron. Soc.* **496**, 2482. DOI.

Carrasco, V.M.S., Vaquero, J.M., Gallego, M.C.: 2021, A forgotten sunspot record during the Maunder Minimum (Jean Charles Gallet, 1677). *Publ. Astron. Soc. Japan* **73**, 747. DOI.

Carrasco, V.M.S., García-Romero, J.M., Vaquero, J.M., Rodríguez, P.G., Foukal, P., Gallego, M.C., Lefèvre, L.: 2018a, The umbra-penumbra area ratio of sunspots during the Maunder Minimum. *Astrophys. J.* **865**, 88. DOI.

Carrasco, V.M.S., Vaquero, J.M., Arlt, R., Gallego, M.C.: 2018b, Sunspot observations made by Hallaschka during the Dalton Minimum. *Solar Phys.* **293**, 102. DOI.

Carrasco, V.M.S., Vaquero, J.M., Gallego, M.C., Lourenço, A., Barata, T., Fernandes, J.M.: 2018c, Sunspot catalogue of the Observatory of the University of Coimbra (1929 – 1941). *Solar Phys.* **293**, 153. DOI.

Carrasco, V.M.S., Gallego, M.C., Villalba Álvarez, J., Vaquero, J.M.: 2019a, Sunspot observations by Charles Malapert during the period 1618 – 1626: a key data set to understand solar activity before the Maunder minimum. *Mon. Not. Roy. Astron. Soc.* **488**, 3884. DOI.

Carrasco, V.M.S., Vaquero, J.M., Gallego, M.C., et al.: 2019b, Sunspot characteristics at the onset of the Maunder minimum based on the observations of Hevelius. *Astrophys. J.* **886**, 18. DOI.

Carrasco, V.M.S., Vaquero, J.M., Gallego, M.C., Villalba Álvarez, J., Hayakawa, H.: 2019c, Two debatable cases for the reconstruction of the solar activity around the Maunder Minimum: Malapert and Derham. *Mon. Not. Roy. Astron. Soc. Lett.* **485**, L57. DOI.

Carrasco, V.M.S., Bertolin, C., Domínguez-Castro, F., de Ferri, L., Gallego, M.C., Vaquero, J.M.: 2020a, Sunspot records by Antonio Colla just after the Dalton Minimum. *Solar Phys.* **295**, 112. DOI.

Carrasco, V.M.S., Gallego, M.C., Arlt, R., Vaquero, J.M.: 2020b, Revisiting the amplitude of solar cycle 9: the case of sunspot observations by W.C. Bond. *Solar Phys.* **295**, 127. DOI.

Carrasco, V.M.S., Gallego, M.C., Villalba Álvarez, J., Vaquero, J.M., Hayakawa, H.: 2021c, Analyses of Early Sunspot Records by Jean Tarde (1615 – 1617) and Jan Smogulecki (1621 – 1625). *Solar Phys.* **296**, 170. DOI.

Carrasco, V.M.S., Hayakawa, H., Kuroyanagi, C., Gallego, M.C., Vaquero, J.M.: 2021d, Strong evidence of low levels of solar activity during the Maunder Minimum. *Mon. Not. Roy. Astron. Soc.* **504**, 5199. DOI.

Carrasco, V.M.S., Nogales, J.M., Vaquero, J.M., Chatzistergos, T, Ermolli, I.: 2021e, A note on the sunspot and prominence records made by Angelo Secchi during the period 1871 – 1875. *J. Space Weather Space Clim.* **11**, 51. DOI.

Carrasco, V.M.S., Pevtsov, A.A., Nogales, J.M., Vaquero, J.M.: 2021f, The sunspot drawing collection of the National Solar Observatory at Sacramento Peak (1947 – 2004). *Solar Phys.* **296**, 3. DOI.

Carrasco, V.M.S., Llera, J., Aparicio, A.J.P., Gallego, M.C., Vaquero, J.M.: 2022a, Relationship between the sunspot number and active day fraction: an application for the Maunder Minimum. *Astrophys. J.* **933**, 26. DOI.

Carrasco, V.M.S., Muñoz-Jaramillo, A., Gallego, M.C., Vaquero, J.M.: 2022b, Revisiting Christoph Scheiner's sunspot records: a new perspective on solar activity of the early telescopic era. *Astrophys. J.* **927**, 193. DOI.

Carrington, R.C.: 1858, On the distribution of the solar spots in latitudes since the beginning of the year 1854, with a map. *Mon. Not. Roy. Astron. Soc.* **19**, 1. DOI.

Carrington, R.C.: 1863, *Observations of the Spots on the Sun: From November 9, 1853, to March 24, 1861, Made at Redhill*. Williams and Norgate, London.

Casas, R., Vaquero, J.M.: 2014, The sunspot catalogues of Carrington, Peters and de la Rue: quality control and machine-readable versions. *Solar Phys.* **289**, 79. DOI.

Charbonneau, P.: 2020, Dynamo models of the solar cycle. *Living Rev. Solar Phys.* **17**, 4. DOI.

Chatzistergos, T.: 2022, Is there a link between the length of the solar cycle and Earth's temperature? *Atti Accad. Naz. Lincei, Rend. Cl. Sci. Fis. Nat.* DOI.

Chatzistergos, T.: 2017, Analysis of historical solar observations and long-term changes in solar irradiance. PhD Thesis (Uni-edition), ISBN 978-3-944072-55-5.

Chatzistergos, T., Usoskin, I.G., Kovaltsov, G.A., Krivova, N.A., Solanki, S.K.: 2017, New reconstruction of the sunspot group numbers since 1739 using direct calibration and "backbone" methods. *Astron. Astrophys.* **602**, A69. DOI.

Chatzistergos, T., Ermolli, I., Krivova, N.A., et al.: 2020, Analysis of full-disc Ca II K spectroheliograms. III. Plage area composite series covering 1892 – 2019. *Astron. Astrophys.* **639**, A88. DOI.

Chatzistergos, T., Ermolli, I., Krivova, N.A., Barata, T., Carvalho, S., Malherbe, J.-M.: 2022a, Scrutinizing the relationship between plage areas and sunspot areas and numbers. *Astron. Astrophys.* **667**, A167. DOI.

Chatzistergos, T., Krivova, N.A., Solanki, S.K., Ermolli, I.: 2022b, Full-disc Ca II K observations – a window to past solar magnetism. *Front. Astron. Space Sci.*, 9. DOI.

Chatzistergos, T., Krivova, N.A., Yeo, K.L.: 2023, *Long-term changes in solar activity and irradiance*. eprint, arXiv.

Clette, F.: 2021, Is the F10.7cm – sunspot number relation linear and stable? *J. Space Weather Space Clim.* **11**, 2. DOI.

Clette, F., Lefèvre, L.: 2016, The new sunspot number: assembling all corrections. *Solar Phys.* **291**, 2629. DOI.

Clette, F., Berghmans, D., Vanlommel, P., Van der Linden, R.A.M., Koeckelenbergh, A., Wauters, L.: 2007, From the Wolf number to the international sunspot index: 25 years of SIDC. *Adv. Space Res.* **40**, 919. DOI.

Clette, F., Svalgaard, L., Vaquero, J.M., Cliver, E.W.: 2014, Revisiting the sunspot number. A 400-year perspective on the solar cycle. *Space Sci. Rev.* **186**, 35. DOI.

Clette, F., Cliver, E.W., Lefèvre, L., Svalgaard, L., Vaquero, J.M.: 2015, Revision of the sunspot number(s). *Space Weather* **13**, 529. DOI.

Clette, F., Cliver, E.W., Lefèvre, L., Svalgaard, L., Vaquero, J.M., Leibacher, J.W.: 2016a, Preface to topical issue: recalibration of the sunspot number. *Solar Phys.* **291**, 2479. DOI.

Clette, F., Lefèvre, L., Cagnotti, M., Cortesi, S., Bulling, A.: 2016b, The revised Brussels-Locarno sunspot number (1981–2015). *Solar Phys.* **291**, 2733. DOI.

Clette, F., Lefèvre, L., Bechet, S., Ramelli, R., Cagnotti, M.: 2021, Reconstruction of the sunspot number source database and the 1947 Zürich discontinuity. *Solar Phys.* **296**, 137. DOI.

Cliver, E.W.: 2016, Comparison of new and old sunspot number time series. *Solar Phys.* **291**, 2891. DOI.

Cliver, E.W.: 2017, Sunspot number recalibration: 2017. The 1840–1920 anomaly in the observer normalization factors of the group sunspot number. *J. Space Weather Space Clim.* **7**, A12. DOI.

Cliver, E.W., Clette, F., Svalgaard, L.: 2013a, Recalibrating the sunspot number (SSN): the SSN workshops. *Cent. Eur. Astrophys. Bull.* **37**, 401.

Cliver, E.W., Herbst, K.: 2018, Evolution of the sunspot number and solar wind B time series. *Space Sci. Rev.* **214**, 56. DOI.

Cliver, E.W., Ling, A.G.: 2016, The discontinuity circa 1885 in the group sunspot number. *Solar Phys.* **291**, 2763. DOI.

Cliver, E.W., Richardson, I.G., Ling, A.G.: 2013b, Solar drivers of 11-yr and long-term cosmic ray modulation. *Space Sci. Rev.* **176**, 3. DOI.

Cliver, E.W., Clette, F., Svalgaard, L., Vaquero, J.M.: 2015, Recalibrating the sunspot number (SN): the 3rd and 4th SN workshops. *Cent. Eur. Astrophys. Bull.* **39**, 1.

Coddington, O., Lean, J., Pilewskie, P., et al.: 2019, Solar irradiance variability: comparisons of models and measurements. *Earth Space Sci.* **6**, 2525. DOI.

Cortesi, S., Cagnotti, M., Bianda, M., Ramelli, R., Manna, A.: 2016, Sunspot observations and counting at Specola Solare Ticinese in Locarno since 1957. *Solar Phys.* **291**, 3075. DOI.

Covington, A.E.: 1947, Micro-wave solar noise observations during the partial eclipse of November 23, 1946. *Nature* **159**, 405.

Covington, A.E., Medd, W.J.: 1954, Variations of the daily level of the 10.7-centimetre solar emission. *J. Roy. Astron. Soc. Can.* **48**, 136.

Dempster, A.P., Laird, N.M., Rubin, D.B.: 1977, Maximum likelihood from incomplete data via the EM algorithm. *J. Roy. Stat. Soc. B* **39**, 1.

Derham, W.: 1710, Observations upon the spots that have been upon the Sun, from the Year 1703 to 1711. With a letter of Mr. Crabtrie, in the year 1640, upon the same subject. *Philos Trans Ser I* **27**, 270.

Dudok de Wit, T., Lefèvre, L., Clette, F.: 2016, Uncertainties in the sunspot numbers: estimation and implications. *Solar Phys.* **291**, 2709. DOI. ADS.

Dudok de Wit, T., Kopp, G., Shapiro, A., Witzke, V., Kretzschmar, M.: 2018, Response of solar irradiance to sunspot-area variations. *Astrophys. J.* **853**, 197. DOI.

Eddy, J.A.: 1976, The Maunder minimum. *Science* **192**, 1189. DOI.

Ellis, W.: 1880, On the relation between the diurnal range of magnetic declination and horizontal force, as observed at the Royal Observatory, Greenwich, during the Years 1841 to 1877, and the period of solar spot frequency. *Philos. Trans. R. Soc. Lond. Ser. I* **171**, 541. ADS.

Ellis, W.: 1898, On the relation between the diurnal range of magnetic declination and horizontal force and the period of solar spot frequency. *Philos. Trans. R. Soc. Lond. Ser. I* **63**, 64. ADS.

Ermolli, I., Ferrucci, M.: 2021, The legacy of Angelo Secchi at the forefront of solar physics research. In: Chinnici, I., Consolmagno, G. (eds.) *Angelo Secchi and Nineteenth Century Science. Historical & Cultural Astronomy*, Springer, Cham. DOI.

Erwin, E.H., Coffey, H.E., Denig, W.F., Willis, D.M., Henwood, R., Wild, M.N.: 2013, The Greenwich photoheliographic results (1874–1976): initial corrections to the printed publications. *Solar Phys.* **288**, 157. DOI.

Ettmüller, M.E.: 1693, *De maculis in sole visis*. Vitebergae, Literis Christiani Kreusigii.

Feynman, J., Ruzmaikin, A.: 2011, The Sun's strange behavior: Maunder Minimum or Gleissberg Cycle? *Solar Phys.* **272**, 351. DOI.

Fligge, M., Solanki, S.K.: 1998, Long-term behavior of emission from solar faculae: steps towards a robust index. *Astron. Astrophys.* **332**, 1082.

Foukal, P.: 1996, The behavior of solar magnetic plages measured from Mt. Wilson observations between 1915 – 1984. *Geophys. Res. Lett.* **23**, 2169. DOI.

Frenkel, E.: 1913, *PhD Thesis. Publikationen der Sternwarte des Eidg. Polytechnikums zu Zürich V*, Friedrich Schulthess, Zürich.

Friedli, T.K.: 2009, *Die Wolfsche Reihe der Sonnenfleckenrelativzahlen. Verbesserte Likelihood Ratio Tests zur Homogenitätsprüfung in strukturellen Zustandsraummodellen*, Südwestdeutscher Verlag für Hochschulschriften, Saarbrücken.

Friedli, T.K.: 2016, Sunspot observations of Rudolf Wolf from 1849 – 1893. *Solar Phys.* **291**, 2505. DOI.

Friedli, T.K.: 2020, Recalculation of the Wolf series from 1877 to 1893. *Solar Phys.* **295**, 72. DOI.

Fujiyama, M., Hayakawa, H., Iju, T., et al.: 2019, Revisiting Kunitomo's sunspot drawings during 1835 – 1836 in Japan. *Solar Phys.* **294**, 43. DOI.

Gautier, J.-A.: 1852, Notice sur quelques recherches récentes, astronomiques et physiques, relative aux apparences que présente le corps du solei. In: *Bibliothèque Universelle de Genève, Archives des Sciences Physiques et Naturelles* **20**, Ferd. Ramboz et Comp, Genève, 177.

Gelman, A., Carlin, J.B., Stern, H.S., Rubin, D.B.: 2013, *Bayesian Data Analysis*, Chapman & Hall, London.

Gleissberg, W.: 1965, The eighty-year solar cycle in auroral frequency numbers. *J. Br. Astron. Assoc.* **75**, 227.

Hale, G.E.: 1908, On the probable existence of a magnetic field in sun-spots. *Astrophys. J.* **28**, 315. DOI.

Hapgood, M., Angling, M.J., Attrill, G., et al.: 2021, Development of space weather reasonable worst case scenarios for the UK national risk assessment. *Space Weather* **19**(4), e2020SW002593. DOI. ADS.

Hayakawa, H., Besser, B.P., Iju, T.: 2020, Thaddäus Derfflinger's sunspot observations during 1802 – 1824: a primary reference to understand the Dalton Minimum. *Astrophys. J.* **890**, 98. DOI.

Hayakawa, H., Ebihara, Y., Vaquero, J.M., et al.: 2018a, A great space weather event in February 1730. *Astron. Astrophys.* **616**, A177. DOI.

Hayakawa, H., Iwahashi, K., Fujiyama, M., et al.: 2018b, Sunspot drawings by Japanese official astronomers in 1749 – 1750. *Publ. Astron. Soc. Japan* **70**, 63. DOI.

Hayakawa, H., Iwahashi, K., Tamazawa, H., Toriumi, S., Shibata, K.: 2018c, Iwahashi Zenbei's sunspot drawings in 1793 in Japan. *Solar Phys.* **293**, 8. DOI.

Hayakawa, H., Ebihara, Y., Willis, D.M., et al.: 2019, Temporal and spatial evolutions of a large sunspot group and great auroral storms around the Carrington event in 1859. *Space Weather* **17**, 1553. DOI.

Hayakawa, H., Clette, F., Horiuchi, T., Iju, T., Knipp, D.J., Liu, H., Nakajima, T.: 2020a, Sunspot observations by Hisako Koyama: 1945 – 1996. *Mon. Not. Roy. Astron. Soc.* **492**, 4513. DOI.

Hayakawa, H., Iju, T., Kuroyanagi, C., Carrasco, V.M.S., Besser, B.P., Uneme, S., Imada, S.: 2021b, Johann Christoph Müller's sunspot observations in 1719 – 1720: snapshots of the immediate aftermath of the Maunder Minimum. *Solar Phys.* **296**, 154. DOI.

Hayakawa, H., Iju, T., Murata, K., Besser, B.P.: 2021c, Daniel Mögling's sunspot observations in 1626 – 1629: a manuscript reference for the solar activity before the Maunder Minimum. *Astrophys. J.* **909**, 194. DOI.

Hayakawa, H., Iju, T., Uneme, S., Besser, B.P., Kosaka, S., Imada, S.: 2021d, Reanalyses of the sunspot observations of Fogelius and Siverus: two "Long-Term" observers during the Maunder Minimum. *Mon. Not. Roy. Astron. Soc.* **506**, 650. DOI.

Hayakawa, H., Kuroyanagi, C., Carrasco, V.M.S., Uneme, S., Besser, B.P., Sôma, M., Imada, S.: 2021e, Sunspot observations at the Eimmart Observatory and its neighbourhood during the Late Maunder Minimum (1681 – 1718). *Astrophys. J.* **909**, 166. DOI.

Hayakawa, H., Lockwood, M., Owens, M.J., Sôma, M., Besser, B.P., van Driel, L.: 2021f, Graphical evidence for the solar coronal structure during the Maunder Minimum: comparative study of the total eclipse drawings in 1706 and 1715. *J. Space Weather Space Clim.* **11**, 1. DOI.

Hayakawa, H., Uneme, S., Besser, B.P., Iju, T., Imada, S.: 2021g, Stephan Prantner's sunspot observations during the Dalton Minimum. *Astrophys. J.* **919**, 1. DOI.

Hayakawa, H., Hattori, K., Soma, M., Iju, T., Besser, B.P., Kosaka, S.: 2022a, An overview of sunspot observations in 1727 – 1748. *Astrophys. J.* **941**, 151. DOI. ADS.

Hayakawa, H., Suzuki, D., Mathieu, S., Lefèvre, L., Takuma, H., Hier, E.: 2022b, Sunspot observations at Kawaguchi Science Museum: 1972 – 2013. *Geosci. Data J.*. DOI.

Hevelius, J.: 1647 *Selenographia: Sive Lunae*. Danzig, Hünefeld .

Hey, J.S.: 1946, Solar radiations in the 4 – 6 metre radio wave-length band. *Nature* **157**, 47.

Hossfield, C.H.: 2002, A history of the Zürich and American relative sunspot number indices. *J. Amer. Assoc. Var. Star Obs.* **31**, 48.

Hoyt, D.V., Schatten, K.H.: 1998a, Group sunspot numbers: a new solar activity reconstruction. *Solar Phys.* **179**, 189. DOI.

Hoyt, D.V., Schatten, K.H.: 1998b, Group sunspot numbers: a new solar activity reconstruction. *Solar Phys.* **181**, 491. DOI.

Hoyt, D.V., Schatten, K.H., Nesme-Ribes, E.: 1994, The one hundredth year of Rudolf Wolf's death: do we have the correct reconstruction of solar activity? *Geophys. Res. Lett.* **21**, 2067. DOI.

Jørgensen, C.S., Karoff, C., Senthamizh Pavai, V., Arlt, R.: 2019, Christian Horrebow's sunspot observations – I. Life and published writings. *Solar Phys.* **294**, 77. DOI.

Karachik, N.V., Pevtsov, A.A., Nagovitsyn, Y.A.: 2019, The effect of telescope aperture, scattered light and human vision on early measurements of sunspot and group numbers. *Mon. Not. Roy. Astron. Soc.* **488**, 3804. DOI.

Karoff, C., Inceoglu, F., Knudsen, M.F., Olsen, J., Fogtmann-Schulz, A.: 2015, The lost sunspot cycle: new support from 10Be measurements. *Astron. Astrophys.* **575**, A77. DOI.

Karoff, C., Jørgensen, C.S., Senthamizh Pavai, V., Arlt, R.: 2019, Christian Horrebow's sunspot observations – II. Construction of a record of sunspot positions. *Solar Phys.* **294**, 78. DOI.

Kendall, M.G.: 1945, The treatment of ties in ranking problems. *Biometrika* **33**, 239.

Knipp, D., Liu, H., Hayakawa, H.: 2017, Ms. Hisako Koyama: from amateur astronomer to long-term solar observer. *Space Weather* **15**, 1215. DOI.

Kopecký, M., Růžičková-Topolová, B., Kuklin, G.V.: 1980, On the relative inhomogeneity of long-term series of sunspot indices. *Bull. Astron. Inst. Czechoslov.* **31**, 267.

Kopp, G.: 2016, Magnitudes and timescales of total solar irradiance variability. *J. Space Weather Space Clim.* **6**, A30. DOI.

Kopp, G., Krivova, N., Wu, C.J., Lean, J.: 2016, The impact of the revised sunspot record on solar irradiance reconstructions. *Solar Phys.* **291**, 2951. DOI.

Kovaltsov, G.A., Mishev, A., Usoskin, I.G.: 2012, A new model of cosmogenic production of radiocarbon ^{14}C in the atmosphere. *Earth Planet. Sci. Lett.* **337**, 114. DOI.

Kovaltsov, G.A., Usoskin, I.G., Mursula, K.: 2004, An upper limit on sunspot activity during the Maunder Minimum. *Solar Phys.* **224**, 95. DOI.

Koyama, H.: 1985, *Observations of Sunspots 1947 – 1984*, Kawade Shobo Shinsha, Tokyo.

Krivova, N.A., Balmaceda, L., Solanki, S.K.: 2007, Reconstruction of solar total irradiance since 1700 from the surface magnetic flux. *Astron. Astrophys.* **467**, 335. DOI.

Krivova, N.A., Solanki, S.K., Beer, J.: 2002, Was one sunspot cycle in the 18th century really lost? *Astron. Astrophys.* **396**, 235. DOI.

Krivova, N.A., Solanki, S.K., Hofer, B., Wu, C.-J., Usoskin, I.G., Cameron, R.: 2021, Modelling the evolution of the Sun's open and total magnetic flux. *Astron. Astrophys.* **650**, A70. DOI.

Kuriyan, P.P., Muralidharan, V., Sampath, S.: 1982, Solar activity with respect to Ca-plages. *Indian J. Radio Space Phys.* **11**, 229.

Lepshokov, D.Kh., Tlatov, A.G., Vasil'eva, V.V.: 2012, Reconstruction of sunspot characteristics for 1853 – 1879. *Geomagn. Aeron.* **52**, 843. DOI.

Leussu, R., Usoskin, I.G., Senthamizh Pavai, V., Diercke, A., Arlt, R., Denker, C., Mursula, K.: 2017, Wings of the butterfly: sunspot groups for 1826 – 2015. *Astron. Astrophys.* **599**, A131. DOI.

Little, R.J.A., Rubin, D.B.: 2002, *Statistical Analysis with Missing Data*, 2nd edn. Wiley series in probability and statistics, New York. Wiley.

Lockwood, M.: 2013, Reconstruction and prediction of variations in the open solar magnetic flux and interplanetary conditions. *Living Rev. Solar Phys.* **10**, 4. DOI.

Lockwood, M., Owens, M.J., Barnard, L.: 2014a, Centennial variations in sunspot number, open solar flux, and streamer belt width: 1. Correction of the sunspot number record since 1874. *J. Geophys. Res.* **119**, 5172. DOI.

Lockwood, M., Owens, M.J., Barnard, L.: 2014b, Centennial variations in sunspot number, open solar flux, and streamer belt width: 2. Comparison with the geomagnetic data. *J. Geophys. Res.* **119**, 5183. DOI.

Lockwood, M., Barnard, L., Nevanlinna, H., Owens, M.J., Harrison, R.G., Rouillard, A.P., Davis, C.J.: 2013, Reconstruction of geomagnetic activity and near-Earth interplanetary conditions over the past 167 yr – part 2: a new reconstruction of the interplanetary magnetic field. *Ann. Geophys.* **31**, 1979. DOI.

Lockwood, M., Owens, M.J., Barnard, L.A., Usoskin, I.G.: 2016, An assessment of sunspot number data composites over 1845 – 2014. *Astrophys. J.* **824**, 54. DOI.

Lourenço, A., Carvalho, S., Barata, T., Garcia, A., Carrasco, V., Peixinho, N.: 2019, Solar observations at the Coimbra Astronomical Observatory. *Open Astron.* **28**, 165. DOI.

Mathieu, S., von Sachs, R., Ritter, C., Delouille, V., Lefèvre, L.: 2019, Uncertainty quantification in sunspot counts. *Astrophys. J.* **886**, 7. DOI.

Mathieu, S., Lefèvre, L. von Sachs, R., Delouille, V., Ritter, C., Clette, F.: 2023, Nonparametric monitoring of sunspot number observations. *J. Qual. Technol.* **55**, 104. DOI.

Maunder, E.W.: 1894, A prolonged sunspot minimum. *Knowledge* **17**, 173.

Maunder, E.W.: 1904, Note on the distribution of sun-spots in heliographic latitude, 1874 – 1902. *Mon. Not. Roy. Astron. Soc.* **64**, 747.

Maunder, E.W.: 1922, The prolonged sunspot minimum, 1645 – 1715. *J. Br. Astron. Assoc.* **32**, 140.

McKinnon, J.A.: 1987, Sunspot numbers: 1610 – 1985 based on the Sunspot-Activity in the Years 1610 – 1960. Report UAG-95. WDC A for Solar-Terrestrial Physics, Boulder.

Muñoz-Jaramillo, A., Vaquero, J.M.: 2019, Visualization of the challenges and limitations of the long-term sunspot number record. *Nat. Astron.* **3**, 205. DOI.

Muscheler, R., Adolphi, F., Herbst, K., Nilsson, A.: 2016, The revised sunspot record in comparison to cosmogenic radionuclide-based solar activity reconstructions. *Solar Phys.* **291**, 3025. DOI. ADS.

Neuhäuser, R., Arlt, R., Richter, S.: 2018, Reconstructed sunspot positions in the Maunder minimum based on the correspondence of Gottfried Kirch. *Astron. Nachr.* **339**, 219. DOI.

Nogales, J.M., Carrasco, V.M.S., Arlt, R., Domínguez-Castro, F., Vaquero, J.M.: 2020, Sunspot observations by Barnaba Oriani (1778 – 1779). *Solar Phys.* **295**, 71. DOI.

Nusinov, A.A.: 2006, Ionosphere as a natural detector for investigations of solar EUV flux variations. *Adv. Space Res.* **37**, 426. DOI.

Owens, B.: 2013, Long-term research: slow science. *Nature* **495**, 300. DOI.

Owens, M.J., Lockwood, M.: 2012, Cyclic loss of open solar flux since 1868: the link to heliospheric current sheet tilt and implications for the Maunder Minimum. *J. Geophys. Res.* **117**, A04102. DOI.

Owens, M.J., McCracken, K.G., Lockwood, M., Barnard, L.: 2015, The heliospheric Hale cycle over the last 300 years and its implications for a "lost" late 18th century solar cycle. *J. Space Weather Space Clim.* **5**, A30. DOI.

Owens, M.J., Cliver, E., McCracken, K.G., et al.: 2016, Near-Earth heliospheric magnetic field intensity since 1750: 1. Sunspot and geomagnetic reconstructions. *J. Geophys. Res.* **121**, 6048. DOI.

Pawsey, J.L., Payne-Scott, R., McCready, L.L.: 1946, Radio-frequency energy from the Sun. *Nature* **157**, 158.

Pesnell, W.D., Thompson, B.J., Chamberlin, P.C.: 2012, The Solar Dynamics Observatory (SDO). *Solar Phys.* **275**, 3. DOI.

Petrovay, K.: 2020, Solar cycle prediction. *Living Rev. Solar Phys.* **17**, 2. DOI.

Poluianov, S.V., Kovaltsov, G.A., Mishev, A.L., Usoskin, I.G.: 2016, Production of cosmogenic isotopes ^{7}Be, ^{10}Be, ^{14}C, ^{22}Na, and ^{36}Cl in the atmosphere: altitudinal profiles of yield functions. *J. Geophys. Res.* **121**, 8125. DOI.

Potgieter, M.S.: 2013, Solar modulation of cosmic rays. *Living Rev. Solar Phys.* **10**, 3. DOI.

Preminger, D.G., Walton, S.R.: 2006, Historical solar variability derived from sunspot areas using a FIR model. *Geophys. Res. Lett.* **33**, L23108. DOI.

Pulkkinen, T.: 2007, Space weather: terrestrial perspective. *Living Rev. Solar Phys.* **4**, 1. DOI.

Ramelli, R., Cagnotti, M., Cortesi, S., Bianda, M., Manna, A.: 2018, Sunspot data collection of Specola Solare Ticinese in Locarno. In: Banerjee, D., Jiang, J., Kusano, K., Solanki, S. (eds.) *Long-Term Datasets for the Understanding of Solar and Stellar Magnetic Cycles*, *Proc. IAU Symp.* **340**, 129.

Ribes, J.C., Nesme-Ribes, E.: 1993, The solar sunspot cycle in the Maunder minimum AD1645 to AD1715. *Astron. Astrophys.* **276**, 549.

Riley, P., Lionello, R., Linker, J.A., et al.: 2015, Inferring the structure of the solar corona and inner heliosphere during the Maunder Minimum using global thermodynamic magnetohydrodynamic simulations. *Astrophys. J.* **802**, 105. DOI.

Rozanov, E., Dyer, C., Sukhodolov, T., Feinberg, A.: 2019, Possible impacts. In: Miyake, F., Usoskin, I., Poluianov, S. (eds.) *Extreme Solar Particle Storms*, IOP Publishing, Bristol, 8.

Rubin, D.B.: 1996, Multiple imputation after 18+ years. *J. Am. Stat. Assoc.* **91**, 473.

Scheiner, C.: 1851, *Prodromus pro sole mobili et terra stabili contra Academicum Florentinum Galilaeum a Galilaeis*.

Scheiner, C.: 1830, *Rosa Ursina*.

Scherrer, P.H., Schou, J., Bush, R.I., et al.: 2012, The Helioseismic and Magnetic Imager (HMI) investigation for the Solar Dynamics Observatory (SDO). *Solar Phys.* **275**, 207. DOI.

Schwabe, M.: 1844, Sonnenbeobachtungen im Jahre 1843. Von Herrn Hofrath Schwabe in Dessau. *Astron. Nachr.* **21**, 233. DOI. ADS.

Secchi, A.: 1875. *Le Soleil*. Gauthier-Villars, Paris. DOI.

Silverman, S.M., Hayakawa, H.: 2021, The Dalton Minimum and John Dalton's auroral observations. *J. Space Weather Space Clim.* **11**, 17. DOI.

Snowball, I., Muscheler, R.: 2007, Palaeomagnetic intensity data: an Achilles heel of solar activity reconstructions. *Holocene* **17**, 851. DOI.

Solanki, S.K., Krivova, N.A., Haigh, J.D.: 2013, Solar Irradiance Variability and Climate. *Annu. Rev. Astron. Astrophys.* **15**, 311. DOI.

Solanki, S.K., Schüssler, M., Fligge, M.: 2000, Evolution of the Sun's large-scale magnetic field since the Maunder Minimum. *Nature* **408**, 445. DOI.

Solanki, S.K., Schüssler, M., Fligge, M.: 2002, Secular variation of the Sun's magnetic flux. *Astron. Astrophys.* **383**, 706. DOI.

Solanki, S.K., Usoskin, I.G., Kromer, B., Schüssler, M., Beer, J.: 2004, Unusual activity of the Sun during recent decades compared to the previous 11,000 years. *Nature* **431**, 1084. DOI.

Southworth, G.C.: 1945, Microwave radiation from the Sun. *J. Franklin Inst.* **239**, 285.

Spörer, G.: 1880, Beobachtungen der Sonnenflecken vom Januar 1874 bis December 1879. *Publ. Astrophys. Obs. Potsdam* **2**, 1.

Spörer, F.W.G.: 1887, On the periodicity of sunspots since the year 1618, especially with respect to the heliographic latitude of the same, and reference to a significant disturbance of this periodicity during a long period. *Vierteljahrsschr. Astron. Ges. (Leipzig)* **22**, 323.

Spörer, F.W.G.: 1889, Sur les différences que présente l'hémisphère sud du Soleil. *Bull. Astron.* **6**, 60.

Svalgaard, L.: 2012, How well do we know the sunspot number? In: Mandrini, C.H., Webb, D.F. (eds.) *Comparative Magnetic Minima: Characterizing Quiet Times in the Sun and Stars*, *Proc. IAU Symp.* **286**, 27. DOI.

Svalgaard, L.: 2013, Solar activity - past, present, future. *J. Space Weather Space Clim.* **3**, A24. DOI.

Svalgaard, L.: 2016, Reconstruction of solar extreme ultraviolet flux 1740 – 2015. *Solar Phys.* **291**, 2981. DOI.

Svalgaard, L.: 2017, A recount of sunspot groups on Staudach's drawings. *Solar Phys.* **292**, 4. DOI.

Svalgaard, L.: 2020, *Several Populations of Sunspot Group Numbers – Resolving a Conundrum*. eprint, arXiv.

Svalgaard, L., Cagnotti, M., Cortesi, S.: 2017, The effect of sunspot weighting. *Solar Phys.* **292**, 34. DOI.

Svalgaard, L., Cliver, E.W.: 2005, The IDV index: its derivation and use in inferring long-term variations of the interplanetary magnetic field strength. *J. Geophys. Res.* **110**, A12103. DOI.

Svalgaard, L., Cliver, E.W.: 2010, Heliospheric magnetic field 1835 – 2009. *J. Geophys. Res.* **115**, A09111. DOI.

Svalgaard, L., Cliver, E.W., Le Sager, P.: 2003, Determination of interplanetary magnetic field strength, solar wind speed and EUV irradiance, 1890 – 2003. In: Wilson, A. (ed.) *Solar Variability as an Input to the Earth's Environment*, *ESA* **SP-535**, ESA, Noordwijk, 15. ISBN 92-9092-845-X.

Svalgaard, L., Cliver, E.W., Le Sager, P.: 2004, IHV: a new long-term geomagnetic index. *Adv. Space Res.* **34**, 436. DOI.

Svalgaard, L., Schatten, K.H.: 2016, Reconstruction of the sunspot group number: the Backbone method. *Solar Phys.* **291**, 2653. DOI.

Svalgaard, L., Schatten, K.H.: 2017, Assessment of the failure of active days fraction method of sunspot group number reconstructions. arXiv e-prints, arXiv. ADS.

Tapping, K.F.: 2013, The 10.7 cm solar radio flux (F10.7). *Space Weather* **11**, 394. DOI. ADS.

Taricco, C., Bhandari, N., Cane, D., Colombetti, P., Verma, N.: 2006, Galactic cosmic ray flux decline and periodicities in the interplanetary space during the last 3 centuries revealed by ^{44}Ti in meteorites. *J. Geophys. Res.* **111**, A08102. DOI.

Taricco, C., Sinha, N., Bhandari, N., Colombetti, P., Mancuso, S., Rubinetti, S., Barghini, D.: 2016, Early 18th century cosmic ray flux inferred from ^{44}Ti in Agen meteorite. *Astrophys. Space Sci.* **361**, 338. DOI.

Tingley, M.P., Craigmile, P.F., Haran, M., Li, B., Mannshardt, E., Rajartnam, B.: 2012, Piecing together the past: statistical insights into paleoclimatic reconstructions. *Quat. Sci. Rev.* **35**, 1. DOI.

Tlatov, A., Riehokainen, A., Tlatova, K.: 2019, The characteristic sizes of the sunspots and pores in solar cycle 24. *Solar Phys.* **294**, 45. DOI.

Usoskin, I.G.: 2017, A history of solar activity over millennia. *Living Rev. Solar Phys.* **14**, 3. DOI.

Usoskin, I.G., Kovaltsov, G.A.: 2008, Production of cosmogenic ^{7}Be isotope in the atmosphere: full 3-D modeling. *J. Geophys. Res.* **113**, D12107. DOI.

Usoskin, I.G., Kovaltsov, G.A., Chatzistergos, T.: 2016b, Dependence of the sunspot-group size on the level of solar activity and its influence on the calibration of solar observers. *Solar Phys.* **291**, 3793. DOI.

Usoskin, I., Kovaltsov, G., Kiviaho, W.: 2021, Robustness of solar-cycle empirical rules across different series including an updated active-day fraction (ADF) sunspot group series. *Solar Phys.* **296**, 13. DOI.

Usoskin, I.G., Mursula, K., Kovaltsov, G.A.: 2003, Reconstruction of monthly and yearly group sunspot numbers from sparse daily observations. *Solar Phys.* **218**, 295. DOI.

Usoskin, I.G., Solanki, S.K., Korte, M.: 2006, Solar activity reconstructed over the last 7000 years: the influence of geomagnetic field changes. *Geophys. Res. Lett.* **33**, L08103. DOI.

Usoskin, I.G., Solanki, S.K., Schüssler, M., Mursula, K., Alanko, K.: 2003, Millennium-scale sunspot number reconstruction: evidence for an unusually active sun since the 1940s. *Phys. Rev. Lett.* **91**, 211101. DOI.

Usoskin, I.G., Alanko-Huotari, K., Kovaltsov, G.A., Mursula, K.: 2005, Heliospheric modulation of cosmic rays: monthly reconstruction for 1951 – 2004. *J. Geophys. Res.* **110**, A12108. DOI.

Usoskin, I.G., Mursula, K., Arlt, R., Kovaltsov, G.A.: 2009, A solar cycle lost in 1793–1800: early sunspot observations resolve the old mystery. *Astrophys. J.* **700**, L154. DOI.

Usoskin, I.G., Arlt, R., Asvestari, E., et al.: 2015, The Maunder minimum (1645–1715) was indeed a grand minimum: a reassessment of multiple datasets. *Astron. Astrophys.* **581**, A95. DOI.

Usoskin, I.G., Kovaltsov, G.A., Lockwood, M., Mursula, K., Owens, M., Solanki, S.K.: 2016a, A new calibrated sunspot group series since 1749: statistics of active day fractions. *Solar Phys.* **291**, 2685. DOI.

Usoskin, I.G., Solanki, S.K., Krivova, N.A., Hofer, B., et al.: 2021b, Solar cyclic activity over the last millennium reconstructed from annual 14C data. *Astron. Astrophys.* **649**, A141. DOI.

Vaquero, J.M., Trigo, R.M.: 2015, Redefining the limit dates for the Maunder Minimum. *New Astron.* **34**, 120. DOI.

Vaquero, J.M., Gallego, M.C., Usoskin, I.G., Kovaltsov, G.A.: 2011, Revisited sunspot data: a new scenario for the onset of the Maunder Minimum. *Astrophys. J.* **731**, L24. DOI.

Vaquero, J.M., Kovaltsov, G.A., Usoskin, I.G., Carrasco, V.M.S., Gallego, M.C.: 2015, Level and length of cyclic solar activity during the Maunder Minimum as deduced from the active-day statistics. *Astron. Astrophys.* **577**, A71. DOI.

Vaquero, J.M., Svalgaard, L., Carrasco, V.M.S., et al.: 2016, A revised collection of sunspot group numbers. *Solar Phys.* **291**, 3061. DOI.

Vasyliunas, V.M., Kan, J.R., Siscoe, G.L., Akasofu, S.-I.: 1982, Scaling relations governing magnetospheric energy transfer. *Planet. Space Sci.* **30**, 359. DOI.

Velasco Herrera, V.M., Soon, W., Hoyt, D., Muraközy, J. (Group Sunspot Numbers): 2022, A new reconstruction of sunspot activity variations from historical sunspot records using algorithms from machine learning. *Solar Phys.* **297**, 1. DOI.

Vokhmyanin, M., Arlt, R., Zolotova, N.: 2020, Sunspot positions and areas from observations by Thomas Harriot. *Solar Phys.* **295**, 39. DOI.

Vokhmyanin, M., Arlt, R., Zolotova, N.: 2021, Sunspot positions and areas from observations by Cigoli, Galilei, Cologna, Scheiner, and Colonna in 1612–1614. *Solar Phys.* **296**, 4. DOI.

Vokhmyanin, M., Zolotova, N.: 2018, Sunspot positions and areas from observations by Pierre Gassendi. *Solar Phys.* **293**, 150. DOI. ADS.

Waldmeier, M.: 1938, Chromosphärische Eruptionen. I. *Z. Astrophys.* **16**, 276.

Waldmeier, M.: 1961, *The Sunspot-Activity in the Years 1610–1960*. Schulthess & Co., Swiss Federal Observatory, Zürich.

Waldmeier, M.: 1968, Die Beziehung zwischen der Sonnenflecken-relativ-zahl und der Gruppenzahl. *Astr. Mitteil. Eidgn. Sternw Zürich.*, No. 285.

Wang, Y.-M, Lean, J.L.: 2021, A new reconstruction of the Sun's magnetic field and total irradiance since 1700. *Astrophys. J.* **920**, 100. DOI.

Wang, Y.-M, Lean, J.L., Sheeley, N.R. Jr.: 2005, Modeling the Sun's magnetic field and irradiance since 1713. *Astrophys. J.* **625**, 522. DOI.

Wang, Y.-M, Sheeley, N.R. Jr.: 2003, On the fluctuating component of the Sun's large-scale magnetic field. *Astrophys. J.* **590**, 1111. DOI.

Webber, W.R., Higbie, P.R.: 2003, Production of cosmogenic Be nuclei in the Earth's atmosphere by cosmic rays: its dependence on solar modulation and the interstellar cosmic ray spectrum. *J. Geophys. Res.* **108**, 1355. DOI.

Webber, W.R., Higbie, P.R., McCracken, K.G.: 2007, Production of the cosmogenic isotopes ^{3}H, ^{7}Be, ^{10}Be, and ^{36}Cl in the Earth's atmosphere by solar and galactic cosmic rays. *J. Geophys. Res.* **112**, A10106. DOI.

Willamo, T., Usoskin, I.G., Kovaltsov, G.A.: 2018, A test of the active-day fraction method of sunspot group number calibration: dependence on the level of solar activity. *Solar Phys.* **293**, 69. DOI.

Willamo, T., Usoskin, I.G., Kovaltsov, G.A.: 2017, Updated sunspot group number reconstruction for 1749–1996 using the active day fraction method. *Astron. Astrophys.* **601**, A109. DOI.

Willis, D.M., Coffey, H.E., Henwood, R., Erwin, E.H., Hoyt, D.V., Wild, M.N., Denig, W.F.: 2013a, The Greenwich photo-heliographic results (1874–1976): summary of the observations, applications, datasets, definitions and errors. *Solar Phys.* **288**, 117. DOI.

Willis, D.M., Henwood, R., Wild, M.N., Coffey, H.E., Denig, W.F., Erwin, E.H., Hoyt, D.V.: 2013b, The Greenwich photo-heliographic results (1874–1976): procedures for checking and correcting the sunspot digital datasets. *Solar Phys.* **288**, 141. DOI.

Wolf, R.: 1851, Sonnenflecken Beobachtungen in der zweiten Hälfte des Jahres 1850. *Mitt. Nat.forsch. Ges. Bern* **207**, 89.

Wolf, R.: 1856, Beobachtungen der Sonnenflecken in den Jahren 1849–1855. *Astron. Mitt. Eidgenöss. Sternwarte Zür.* **1**, 3.

Wolf, R.: 1857, Mitteilungen über die Sonnenflecken. IV. *Astron. Mitt. Eidgenöss. Sternwarte Zür.* **1**, 51.

Wolf, J.R.: 1852, Entdeckung des Zusammenhanges zwischen den Declinationsvariationen der Magnetnadel und den Sonnenflecken. *Mitth. Nat.forsch. Gesell. Bern 224 – 264* **245**, 179.

Wolfer, A.: 1895, Astronomische Mittheilungen, LXXXVI. *Astron. Mitt. Eidgenöss. Sternwarte Zür.* **9**, 187.

Wolfer, A.: 1902, Revision of Wolf's sunspot relative numbers. *Pop. Astron.* **10**, 449.

Wolfer, A.: 1912, Unpublished manuscript. Wissenschaftshistorische Sammlungen der ETH Bibliothek. Handschrift Hs 1050, 234, Zürich.

Wu, C.J., Krivova, N.A., Solanki, S.K., Usoskin, I.G.: 2018a, Solar total and spectral irradiance reconstruction over the last 9000 years. *Astron. Astrophys.* **620**, A120. DOI.

Wu, C.J., Usoskin, I.G., Krivova, N., Kovaltsov, G.A., Baroni, M., Bard, E., Solanki, S.K.: 2018b, Solar activity over nine millennia: a consistent multi-proxy reconstruction. *Astron. Astrophys.* **615**, A93. DOI.

Yamazaki, Y., Maute, A.: 2017, Sq and EEJ—a review on the daily variation of the geomagnetic field caused by ionospheric dynamo currents. *Space Sci. Rev.* **206**, 299. DOI. ADS.

Yeo, K.L., Solanki, S.K., Krivova, N.: 2020, How faculae and network relate to sunspots, and the implications for solar and stellar brightness variations. *Astron. Astrophys.* **639**, A139. DOI.

Zolotova, N.V., Ponyavin, D.I.: 2011, Enigma of the solar cycle 4 still not resolved. *Astrophys. J.* **736**, 115. DOI.

Publisher's Note Springer Nature remains neutral with regard to jurisdictional claims in published maps and institutional affiliations.

Authors and Affiliations

F. Clette[1] (iD) **· L. Lefèvre[1]** (iD) **· T. Chatzistergos[2]** (iD) **· H. Hayakawa[3,4,5,6]** (iD) **· V.M.S. Carrasco[7]** (iD) **· R. Arlt[8] · E.W. Cliver[9]** (iD) **· T. Dudok de Wit[10,11]** (iD) **· T.K. Friedli[12]** (iD) **· N. Karachik[13] · G. Kopp[14] · M. Lockwood[15]** (iD) **· S. Mathieu[16]** (iD) **· A. Muñoz-Jaramillo[17]** (iD) **· M. Owens[15]** (iD) **· D. Pesnell[18]** (iD) **· A. Pevtsov[9]** (iD) **· L. Svalgaard[19]** (iD) **· I.G. Usoskin[20]** (iD) **· L. van Driel-Gesztelyi[21,22,23]** (iD) **· J.M. Vaquero[7]** (iD)

✉ T. Chatzistergos
chatzistergos@mps.mpg.de

1   World Data Center SILSO, Royal Observatory of Belgium, 3 avenue Circulaire, 1180, Brussels, Belgium

2   Max Planck Institute for Solar System Research, Justus-von-Liebig-weg 3, 37077 Göttingen, Germany

3   Institute for Space-Earth Environmental Research, Nagoya University, Nagoya, 4648601, Japan

4   Institute for Advanced Research, Nagoya University, Nagoya, 4648601, Japan

5   Space Physics and Operations Division, RAL Space, Science and Technology Facilities Council, Rutherford Appleton Laboratory, Harwell Oxford, Didcot, Oxfordshire, OX11 0QX, UK

6   Nishina Centre, Riken, Wako, 3510198, Japan

7   Departamento de Física, Universidad de Extremadura, E-06006, Badajoz, Spain

8   Leibniz-Institut f. Astrophysik Potsdam, An der Sternwarte 16, 14482, Potsdam, Germany

9   National Solar Observatory, 3665 Discovery Drive, 3rd Floor, Boulder, CO, 80303, USA

10   LPC2E, CNRS/CNES/University of Orléans, 45067 Orléans, France

11   International Space Science Institute, Hallerstrasse 6, 3012, Bern, Switzerland

12   Rudolf Wolf Society, Ahornweg 29, 3123, Belp, Switzerland

13   Ulugh Beg Astronomical Institute, Uzbekistan Academy of Sciences, 33 Astronomicheskaya str., 100052, Tashkent, Uzbekistan

14 Laboratory for Atmospheric and Space Physics, University of Colorado, 3665 Discovery Dr., Boulder, CO, 80303, USA

15 Department of Meteorology, University of Reading, Earley Gate, PO Box 243, Reading, RG6 6BB, UK

16 ISBA/LIDAM, UCLouvain, Pl. de l'Université 1, 1348, Ottignies-Louvain-la-Neuve, Belgium

17 Division of Solar System Science, Southwest Research Institute, Boulder, CO, USA

18 Code 671, NASA Goddard Space Flight Center, Greenbelt, MD, 20771, USA

19 Hansen Experimental Physics Lab, Stanford University, Stanford, CA, 94305, USA

20 Space Physics and Astronomy Research Unit and Sodankylä Geophysical Observatory, University of Oulu, 90014, Oulu, Finland

21 Mullard Space Science Laboratory, University College London, Holmbury St. Mary, Dorking, Surrey, RH5 6NT, UK

22 Observatoire de Paris, Université PSL, CNRS, Sorbonne Université, Univ. Paris Diderot, Sorbonne Paris Cité, 5 place Jules Janssen, F-92195, Meudon, France

23 Konkoly Observatory, Research Centre for Astronomy and Earth Sciences, Konkoly Thege út 15-17, H-1121, Budapest, Hungary